

Medical University of South Carolina

**MEDICA**

---

MUSC Theses and Dissertations

---

2018

## Nonalcoholic Steatohepatitis: Role of Gut Microbiota is Dependent on Lipopolysaccharide-Toll-like Receptor-4 Axis

S. M. Touhidul Islam

*Medical University of South Carolina*

Follow this and additional works at: <https://medica-musc.researchcommons.org/theses>

---

### Recommended Citation

Islam, S. M. Touhidul, "Nonalcoholic Steatohepatitis: Role of Gut Microbiota is Dependent on Lipopolysaccharide-Toll-like Receptor-4 Axis" (2018). *MUSC Theses and Dissertations*. 588. <https://medica-musc.researchcommons.org/theses/588>

This Dissertation is brought to you for free and open access by MEDICA. It has been accepted for inclusion in MUSC Theses and Dissertations by an authorized administrator of MEDICA. For more information, please contact [medica@musc.edu](mailto:medica@musc.edu).

**Nonalcoholic Steatohepatitis: Role of Gut Microbiota is Dependent on  
Lipopolysaccharide-Toll-like Receptor-4 Axis**

By

S.M. Touhidul Islam

A dissertation submitted to the faculty of the Medical University of South Carolina in  
partial fulfillment of the requirements for the degree of Doctor of Philosophy in the  
College of Graduate Studies.

Department of Microbiology and Immunology

2018

Approved by:

Chairman, Advisory Committee

---

Kenneth D. Chavin

---

Inderjit Singh

---

Michael G. Schmidt

---

Caroline Westwater

---

Stephen Tomlinson

This dissertation is dedicated to the beloved Imam Hussain Ibn Ali Ibn Abi Talib (PBUH)  
for his sacrifice for the sake of truth, justice, humanity, dignity, and freedom.

## **Acknowledgements**

This is a moment of great happiness for me to accomplish the writing of my Ph.D. dissertation. I am taking this opportunity to express my gratitude to all who have shown their incredible support and cooperation during this long journey. Although the actual list would be lengthy, I have here only mentioned the name of some of those individuals who have made my graduate research and education successful. Without the help of these people, the entire process would not have been possible.

I would like to thank the 'College of Graduate Studies' of 'Medical University of South Carolina' for offering me the opportunity to carry on the Ph.D. in Biomedical Sciences. All the Faculty and staffs of the 'College of Graduate Studies' have been very supportive in whatever I needed from the very beginning of the program. I would particularly mention the cooperation I received from The Dean of the 'College of Graduate Studies', Dr. Paula Traktman, for doing the necessary paperwork for one year of 'Curricular Practical Training' at 'Case Western Reserve University' during the fourth year of my Ph.D. studies. I am very grateful to the Department of Microbiology and Immunology for accepting me as a graduate student. I am very thankful to the Faculty members of this department for their intellectual guidance especially in the meetings of the journal club and the seminar series. I have a special gratitude to the Graduate Program Director of the Department of Microbiology and Immunology, Dr. Bei Liu, for her valuable suggestions regarding any academic issue I had during the past four years.

I would like to express my humble gratitude to my committee members. I acknowledge their thoughtful contributions in the committee meetings to make my project scientifically more solid. They were always eager to listen to my ideas about how the

design of experiments can shape the project into a better one and make it successful. I have a very special thankfulness to Dr. Michael Schmidt for his vast contribution in reviewing my manuscripts and dissertation. His thoughtful comments, corrections, and suggestions had not only helped me to finish my dissertation successfully, but also trained me with the art of scientific writing for future. I also thank Dr. Caroline Westwater for collaborating with Dr. Chavin's lab by taking care of the germ free mice. I appreciate her quick response to any need regarding the use of her lab equipment during the process of moving Dr. Chavin's lab to Case Western Reserve University. I also thank Dr. Stephen Tomlinson for being on my committee and providing insightful suggestions.

I am very grateful to my co-supervisor Dr. Inderjit Singh for allowing me in his lab. His depth of knowledge, insightful questions, curiosity, and passion for research was really inspiring. One of the specific aims of my research proposal on the 'functional alteration of peroxisomes' came from his idea which might open a completely new avenue in NASH research. I have learned how to critically think and raise scientific questions from conversations in the journal club and data presentation meetings in Dr. Singh's lab. I am very grateful to all the members of Dr. Singh's lab for their cooperation in a very agreeable manner. Dr. Mushfiquddin Khan deserves special mention. I was always welcome to discuss him my research, career plan and any related academic issue. I am also thankful to Dr. Seung Choi for his technical supports for performing some experiments in Dr. Singh's lab.

I would also like to mention my family in this acknowledgement list to whom I am indebted. I have a very special gratitude to my parents for their endless support to go through this long way of my academic life. I thank my brothers and sister-in-laws for their

continuous moral support. I am also grateful to my angelic nephew and nieces for being the source of peace during the stressful moments.

Finally, most of my gratefulness goes to my mentor Dr. Kenneth D. Chavin. I am thankful to him from the bottom of my heart for taking me as his student and giving me the opportunity to pursue research on a very exciting project. It would not be possible to travel through this long way without his intellectual guidance and support. It was really incredible that he managed time for the lab, especially for me to get update on my research progress, from his extremely tied-up schedule for clinical responsibilities. He allowed me to pursue anything I found interesting. I could share any academic and personal issue with him in a very frank manner. He provided an environment that was very helpful to develop myself academically, professionally and personally. It is worth mentioning that I received every kind of cooperation from him during my stay in my co-supervisor's lab at MUSC while Dr. Chavin was in his new station at Case Western Reserve University. This acknowledgement would remain incomplete if I do not express my gratitude to the members of Dr. Chavin's lab. I worked with some wonderful colleagues in his lab both at MUSC and Case Western Reserve University. I am especially thankful to Dr. Arun Palanisamy for his contribution in idea formulation, experiment designing, and manuscript preparation. I am also thankful to Dr. Gabriel Chedister, Kathy Haines, Julie Lench, Suhanti Banerjee, and Julia Gaspare-Pruchnicki for their technical cooperation in performing experiments. They offered me a very friendly and scientific atmosphere that pave the way to accomplish my research under Dr. Chavin's supervision.

S.M. TOUHIDUL ISLAM. Nonalcoholic Steatohepatitis: Role of Gut Microbiota is Dependent on Lipopolysaccharide-Toll like Receptor-4 Axis. (Under the direction of KENNETH D. CHAVIN)

### **Abstract**

Hepatic steatosis is the hepatic manifestation of metabolic syndrome which is increasingly becoming a health problem worldwide, especially in the western hemisphere. Hepatic steatosis is benign, but long standing hepatic steatosis can lead to non-alcoholic steatohepatitis (NASH). NASH is a form of nonalcoholic fatty liver disease where excessive fat accumulation in the liver leads to chronic inflammation of a patient without any history of alcohol abuse. However, the mechanism underlying the progression of hepatic steatosis to NASH is unclear. Role of gut microbiota in metabolic syndrome has long been reported. Here, we hypothesized that gut microbiota plays an important role in the modulation of NASH through the involvement of lipopolysaccharide (LPS)-toll-like receptor-4 (TLR-4) pathway in dietary fat mediated hepatic steatosis. To test this hypothesis, germ free or broad-spectrum antibiotics-treated mice were fed high fat diet, which resulted in decreased level of inflammation in their fatty liver compared to the specific pathogen free control mice. This result demonstrated the involvement of gut microbiota in mediating NASH. To address the role of LPS-TLR-4 pathway, broad spectrum antibiotics-treated mice fed high fat diet were injected i.p. with low dose LPS, resulting in an increased level of inflammation in the liver which was decreased upon the co-treatment with TAK-242, an inhibitor of TLR-4. To investigate the role of TLR-4-expressing kupffer cells in mediating NASH, wild-type kupffer cells in the liver of wild-type mice were replaced with TLR-4 KO kupffer cells by bone marrow transplantation, which

resulted in a decreased level of inflammation in liver upon NASH induction. It was also investigated whether the peroxisomal anti-oxidative function is altered in the livers of mice fed high fat diet in a TLR-4 dependent manner. Indeed, the level and function of catalase, the principal antioxidative enzyme in peroxisomes, was decreased in mice fed high fat diet, which was reversed in TLR-4 KO mice fed high fat diet. This individual piece of data demonstrated the role of TLR-4 pathway in modulating NASH through the alteration of peroxisomal anti-oxidative function. In conclusion, this project established the role of gut microbiota in modulating NASH which is dependent on LPS-TLR-4 pathway.

## Table of contents

<b>Chapter</b>	<b>Heading</b>	<b>Page</b>
	Acknowledgements	iii
	Abstracts	v
	List of abbreviations	xii
	List of figures	xiv
	List of tables	xvi
<b>Chapter 1</b>		1
<b>An Overview of Nonalcoholic Steatohepatitis and Gut Microbiota</b>		1
	Epidemiology of NAFLD and NASH	2
	Risk of progression of NASH to end stage liver diseases	2
	From metabolic syndrome to NASH	3
	A 'Two-hit hypothesis' to explain the pathogenesis of NASH	7
	Pro-inflammatory mediators of NASH	7
	Gut microbiota and their contribution to human health	9
	Dynamic composition of gut microbiota and metabolic syndrome	10
	Gut microbiota bridges gut-liver axis	11
	Gut microbiota induces pro-inflammatory pathways through the interaction with toll-like receptors	12
	Potential role of low grade chronic endotoxemia in metabolic syndrome	13
	TLR-4 pathway is essential in the modulation of metabolic syndrome	17
	Potential role of LPS-TLR-4 axis in NASH	17
<b>Chapter 2</b>		18
<b>Materials and Methods</b>		18
	Animal experiment	19
	Partial hepatectomy	20
	Treatment with broad-spectrum antibiotic, LPS and TLR-4 inhibitor	21
	Bone marrow transplantation and depletion of kupffer cells	23
	ALT and AST assays	25
	Endotoxin assays	25
	Liver histology and immunohistochemical staining	26
	Quantitative real time reverse transcriptase polymerase chain reaction (RT-PCR)	28
	Western blot analysis	29
	Catalase activity assay	31
	16S rRNA analyses	31
	Isolation of kupffer cells and flow cytometric analyses	32
	Statistical analyses	33
<b>Chapter 3</b>		34

<b>Dietary Model of NASH: Pathology of NASH Develops at a Higher Level in Animals Fed a Diet Rich in Saturated Fats</b>	<b>34</b>
Summary	35
Introduction	36
Results	39
Both LD and MD led to the development of hepatic steatosis at week 16 and 32, while MD showed a non-significant higher trend than LD	39
Both LD and MD led to the development of chronic inflammation in the fatty liver, while MD displayed a non-significant higher trend than LD at week 16 and 32	39
Mice fed LD or MD both showed an indication of fibrosis in the fatty liver, yet feeding with MD showed a higher level of expression of TGF- $\beta$ than feeding with LD	43
Discussion	45
<b>Chapter 4</b>	<b>48</b>
<b>High Fat Diet-mediated Nonalcoholic Steatohepatitis Impairs Hepatic Regeneration Following Partial Hepatectomy</b>	<b>48</b>
Summary	49
Introduction	50
Results	51
Mice fed LD and MD led to the development of NASH in both resected and regenerated livers	51
Both LD or MD caused damage in resected and regenerated livers	51
NASH-affected livers of mice fed MD or LD demonstrated impaired regeneration following partial hepatectomy (PHx)	54
Discussion	57
<b>Chapter 5</b>	<b>59</b>
<b>Gut Microbiota Plays a Critical Role in Nonalcoholic Steatohepatitis</b>	<b>59</b>
Summary	60
Introduction	61
Results	63
GF mice developed less steatosis in their livers compared to the SPF mice	63
Steatotic livers in GF mice were resistant to NASH	63
GF mice fed MD had decreased level of collagen accumulation in their livers compared to the SPF mice fed MD	68
Broad spectrum antibiotics-treated mice fed MD showed similar levels of steatosis, but had a decreased level of NASH compared to the control mice fed MD	70
Conventionalization of GF mice fed MD resulted in increased level of NASH	75

Composition of gut microbial community was altered in mice fed MD	80
Discussion	83
<b>Chapter 6</b>	86
<b>Role of Gut Microbiota in Causing NASH is Dependent on LPS-TLR-4-Kupffer Cell Axis</b>	86
Summary	87
Introduction	88
Results	89
Diminishing of gut microbiota resulted in reduced concentration of serum endotoxin which was restored upon LPS injection	89
LPS injection resulted in increased level of NASH in broad spectrum antibiotics-treated mice fed MD	89
Administration of TLR-4 inhibitor (TAK-242) blunted the effect of injection of low dose LPS resulting in decreased level of NASH	91
TLR-4 has an obvious role in the modulation of NASH in mice fed MD	96
TLR-4-expressing kupffer cells play a crucial role in mediating NASH in mice fed MD	100
Reconstituted kupffer cells were derived from the transplanted bone marrow	107
Discussion	109
<b>Chapter 7</b>	111
<b>Peroxisomal Structural and Anti-oxidative Function is Compromised in NASH in a TLR-4 Dependent Manner</b>	111
Summary	112
Introduction	113
Results	116
Peroxisomal structure is altered in the livers of mice fed MD in a TLR-4 dependent manner	116
Catalase level and function are altered in the livers of mice fed MD in a TLR-4 dependent manner	116
Discussion	121
<b>Chapter 8</b>	124
<b>Conclusions and Overall Discussion</b>	124
Study of NASH in mice fed high fat diet represents a clinically relevant model	125
Gut microbiota spans gut-liver axis in causing NASH	127
Gut microbial community is altered in NASH	128
Altered gut permeability facilitates the elevation of circulating endotoxin level	129
LPS-TLR-4 pathway plays an essential role in mediating NASH	130

TLR-4 pathway is a promising target for therapeutic intervention against NASH and ischemia/reperfusion injury in liver transplantation	
Therapeutic interference of LPS-TLR-4 pathway may improve hepatic regeneration following partial hepatectomy in steatotic liver	131
Why peroxisomes are important in controlling oxidative stress	133
Peroxisomal anti-oxidative function is impaired in NASH	134
Intervention of TLR-4 pathway can improve peroxisomal anti-oxidative function	135

<b>References</b>	<b>137</b>
-------------------	------------

## List of abbreviations

ATM	Adipose Tissue Macrophage
AFLD	Fatty Liver Disease
ALD	Alcoholic Steatohepatitis
ALT	Alanine Transaminase
AST	Aspartate Transaminase
$\alpha$ -SMA	$\alpha$ -Smooth Muscle Actin
BrdU	5-romo-2'-deoxyuridine
ChREBP	Carbohydrate Response Element Binding Protein
CCL-2	C-C Motif Chemokine Ligand-2
CD	Control Diet
Col-1a	Collagen-1a
DAPI	4',6-diamidino-2-phenylindole
$\Delta\Delta$ Ct	Delta Delta Threshold Cycles
ER	Endoplasmic Reticulum
ECM	Extracellular Matrices
Fc	Fragment Crystallizable
FFA	Free Fatty Acid
FFPE	Formalin Fixed Paraffin Embedded
FOXO1	Forkhead Box Protein O1
GF	Germ Free
GMR	Gut Microbiota Re-constituted
Gy	Gray
HCV	Hepatitis C Virus
HBV	Hepatitis B Virus
HIV	human immunodeficiency virus
H <sub>2</sub> O <sub>2</sub>	Hydrogen Peroxide
HPRT	Hypoxanthine-guanine Phosphoribosyl Transferase
HSCs	Hepatic Stellate Cells
HSP	Heat Shock Protein
IL-1 $\beta$	Interleukin-1beta
i.p.	Intraperitoneal
i.v.	Intravenous
LAL	Limulus Amebocyte Lysate
LD	Lard-based Unsaturated High Fat Diet
LRR	Leucine Rich Repeats
MAMPs	Microbe Associated Molecular Patterns
MAPK	Mitogen-Activated Protein Kinase
MD	Milk-based Saturated High Fat Diet

mTORC2	mTOR Complex 2
NAFLD	Nonalcoholic Fatty Liver Disease
NASH	Nonalcoholic Steatohepatitis
NFκB	Nuclear Factor Kappa-light-chain-enhancer of Activated B Cells
OCT	Optimum Cutting Temperature
PDGF	Platelet Derived Growth Factor
PDK1	3-Phosphoinositide-Dependent Kinase-1
PHx	Partial Hepatectomy
P13K	Phosphoinositide 3-Kinase
PMP70	Peroxisomal Membrane Protein 70
PNPLA3	Patatin-like Phospholipase Domain-containing 3
PPAR-α	Peroxisome Proliferator-activated Receptor-α
PPAR-α	Peroxisome Proliferator-activated Receptor-γ
PTEN	Phosphatase and Tensin Homologue
RIPA	Radioimmunoprecipitation Assay Buffer
ROS	Reactive Oxygen Species
SLE	Systemic Lupus Erythematosus
SNP	Single Nucleotide Polymorphism
SPF	Specific Pathogen Free
SREBP-1c	Sterol Regulatory Element Binding Protein-1c
STAT3	Signal Transducer and Activator of Transcription 3
T2DM	Type-2 Diabetes Mellitus
TCA	Tri-Carboxylic Acid
TG	Triglyceride
TGF-β	Transforming Growth Factor-beta
TIR	Toll/Interleukin-1 Receptor
TLRs	Toll-like Receptors
TLR-4	Toll-like Receptor-4
TNF-α	Tumor Necrosis Factor
UPR	Unfolded Protein Response
VEGF	Vascular Endothelial Growth Factor
WHO	World Health Organization
WT	Wild-type

## List of figures

<b>Figure</b>	<b>Title</b>	<b>Page</b>
Figure 1.1	Role of metabolic syndrome in the development of nonalcoholic fatty liver disease	6
Figure 1.2	Role of free fatty acids in the production of reactive oxygen species	8
Figure 2.1	Diagrammatic representation of hepatic regeneration experiment	22
Figure 2.2	Diagrammatic representation of antibiotic/LPS/TAK-242 treatment and kupffer cell reconstitution experiment	24
Figure 3.1	Consumption of unsaturated or saturated high fat diet led to hepatic steatosis both at week 16 and 32	40
Figure 3.2	Feeding with unsaturated or saturated high fat diet led to the development of NASH both at week 16 and 32	42
Figure 3.3	Mice fed unsaturated or saturated high fat diet showed the indication of fibrosis both at week 16 and 32	44
Figure 4.1	Unsaturated or saturated high fat diet led to the development of NASH in both resected and regenerated livers	52
Figure 4.2	Unsaturated or saturated high fat diet resulted in liver damage in both resected and regenerated livers	53
Figure 4.3	Hepatic regeneration following partial hepatectomy was impaired in mice fed unsaturated or saturated high fat diet.	56
Figure 5.1	Germ free mice fed high fat diet developed less hepatic steatosis compared to the specific pathogen free mice	65
Figure 5.2	Germ free mice fed high fat diet showed lower levels of NASH-indicative markers in their livers compared to the specific pathogen free mice fed high fat diet	67
Figure 5.3	Germ free mice fed high fat diet showed decreased level of collagen accumulation in their livers compared to the specific pathogen free mice	69
Figure 5.4	Broad spectrum antibiotic-treated mice fed high fat diet developed similar level of hepatic steatosis compared to the control mice	70
Figure 5.5	Broad spectrum antibiotic-treated mice fed high fat diet showed decreased levels of NASH-indicative markers compared to the control mice fed high fat diet	73
Figure 5.6	Broad spectrum antibiotic-treated mice fed high fat diet showed decreased level of collagen accumulation in their livers compared to the control mice fed high fat diet	74
Figure 5.7	Reconstitution of gut microbiota in germ free mice fed high fat diet did not make any difference in the hepatic steatosis	76
Figure 5.8	Reconstitution of gut microbiota in germ free mice fed high fat diet showed elevated levels of NASH-indicative markers in their steatotic livers	78
Figure 5.9	Reconstitution of gut microbiota in germ free mice fed high fat diet resulted in increased collagen accumulation in their steatotic livers	79

Figure 5.10	Composition of gut microbiota changed in mice fed high fat diet	81
Figure 5.11	Principal component analysis resulted in different clustering of mice fed high fat diet	82
Figure 6.1	Diminishing of gut microbiota resulted in reduced concentration of endotoxin in portal serum and feces	90
Figure 6.2	Injection of LPS or TLR-4 inhibitor in broad spectrum antibiotics-treated mice fed high fat diet did not alter hepatic steatosis	92
Figure 6.3	Injection of low dose LPS in broad spectrum antibiotics-treated mice fed high fat diet resulted in increased level of NASH which was reversed upon administration of TLR-4 inhibitor	94
Figure 6.4	Injection of low dose LPS in broad spectrum antibiotics-treated mice fed high fat diet resulted in increased accumulation of collagen which was reversed upon administration of TLR-4 inhibitor	95
Figure 6.7	TLR-4 KO mice fed high fat diet displayed similar level of hepatic steatosis as compared to the wild-type mice fed high fat diet	97
Figure 6.8	TLR-4 KO mice fed high fat diet exhibited decreased level of NASH which remained unchanged upon injection of low dose LPS	99
Figure 6.9	TLR-4 KO mice fed high fat diet displayed decreased level of collagen accumulation in their livers which remained unchanged upon injection of low dose LPS	101
Figure 6.10	TLR-4-expressing kupffer cells are involved in the accumulation of fat in mice fed high fat diet	102
Figure 6.11	TLR-4-expressing kupffer cells play crucial role in mediating NASH in mice fed high fat diet	105
Figure 6.12	TLR-4-expressing kupffer cells play an important role in collagen accumulation in the livers of mice fed high fat diet	106
Figure 6.13	Reconstituted kupffer cells in the livers of bone marrow recipient mice are derived from the transplanted cells	108
Figure 7.1	Fluorescence immunohistochemistry of peroxisomal membrane protein 70 in liver sections displayed a reduced level of fluorescence intensity in mice fed milk-based high fat diet in a TLR-4 dependent manner	118
Figure 7.2	Fluorescence immunohistochemistry of catalase in liver sections displayed a reduced level of fluorescence intensity in mice fed milk-based high fat diet in a TLR-4 dependent manner	119
Figure 7.3	Catalase level and activity are decreased in the livers of mice fed milk-based high fat diet which is dependent on TLR-4	120

## List of Tables

<b>Table</b>	<b>Title</b>	<b>Page</b>
Table 1	List of Toll-like receptors and their microbial/non-microbial ligands	14
Table 2.1	List of probes used for RT-PCR	30
Table 2.2	List of antibodies used for immunoblot analyses	30
Table 2.3	List of antibodies used for flow cytometric analyses	33

# Chapter 1

An Overview of Nonalcoholic Steatohepatitis and Gut Microbiota

Nonalcoholic fatty liver disease (NAFLD) is defined as a condition with excessive fat accumulation and related complications in the liver of patients without any record of alcoholism [1]. Fat accumulation in the liver can also result from alcohol abuse which is called alcoholic fatty liver disease (AFLD) [2, 3]. NAFLD is an umbrella term which encompasses simple steatosis to nonalcoholic steatohepatitis (NASH) [4]. Hepatic steatosis refers to the normal accumulation of fat in the liver without or with minor inflammation. Hepatic steatosis is benign, but long standing steatosis can lead to the development of NASH which is the advanced stage of NAFLD showing clear indication of chronic inflammation in the fatty liver [5, 6].

### **Epidemiology of NAFLD and NASH**

NAFLD is a rapidly expanding health problem throughout the world. Currently, its global incidence is approximately 25% [7]. Variations in the incidence rate for NAFLD vary across the globe; the prevalence rate in Asia ranges from 5% to 18% and in Western countries from 20% to 30% [8]. Of the individuals with NAFLD, approximately 7% to 30% meet the clinical criteria for NASH [9]. Here in the USA, the prevalence rate for NAFLD is 30%, with 25% of them satisfying the clinical definition of NASH. Thus, an overall incidence rate for NASH within the US population is approximately 3-8% [10-13].

### **Risk of progression of NASH to end stage liver diseases**

A major concern for individuals with NASH is the likelihood of their progression to end stage liver diseases, that will ultimately require transplantation [14]. The potential of NASH to progress into fibrosis and hepatocellular carcinoma is recognized. Alarming, it has been projected that NASH is going to become the leading cause of liver related

morbidity and mortality [15-18]. Although the patients with NASH are at greater risk, individuals with simple steatosis and mild inflammation can also progress to fibrosis and hepatocellular carcinoma [4, 5, 19-21]. Hepatic fibrosis is defined as an excessive deposition of extracellular matrices, especially collagen, within the liver. While hepatic fibrosis results in only minor clinical complications and/or hepatocyte dysfunction, it is considered a predictor that the patient has a greater risk of developing cirrhosis [22]. Hepatocellular carcinoma is considered the fifth most common cancer and third leading cause of cancer-related death in the United States [23]. Hepatitis C virus, alcohol-related liver diseases, and hepatitis B virus have been implicated as the three leading causes of hepatocellular carcinoma in the western world [24]. A role for NASH in this demographic has been underestimated. However, an increasing prevalence of NASH-related hepatocellular carcinoma predicts that NASH is going to become the leading cause of hepatocellular carcinoma in the Western countries in near future [10, 24]. Given the epidemiological data with respect to NASH and its role in end stage liver diseases, approaches to curb the transition from NAFLD to NASH is paramount if we wish to improve the morbidity and mortality of patients afflicted with a steatotic liver.

### **From metabolic syndrome to NASH**

The etiology of NASH is closely associated with metabolic syndrome [1, 4]. According to the World Health Organization, metabolic syndrome is a condition characterized by multiple metabolic abnormalities including obesity, insulin resistance and type-2 diabetes mellitus [25]. Diet and a sedentary life style have been implicated in the development of metabolic syndrome. In the latter half of the 20<sup>th</sup> century with the emergence of a sedentary 'corporate professional life-style' and 'fast food culture'

(containing high fat, carbohydrate, and calories), Westerners are now considered to have a greater risk for developing metabolic syndrome than the people in developing countries where manual labor is still the norm for the bulk of the population [26-28].

Obesity is strongly associated with an increased risk of developing NAFLD. Prevalence rate of NAFLD increases with an increase in body mass index [29, 30]. Incident rates of hepatic steatosis and NASH have been observed to occur respectively at 95% and 20% in obese patients [9]. Fat deposition in the liver is directly correlated with the accumulation of visceral adipose tissue. Mesenteric fat, a specific type of visceral adipose tissue, is drained into the liver through portal circulation, leading to the deposition of fat droplets causing hepatic steatosis [31, 32].

Insulin resistance is a common condition observed in individuals with metabolic syndrome. Insulin resistance results in impaired glucose uptake and disposal, an increase in *de novo* synthesis of fatty acids, and an inadequate level of free fatty acid oxidation [33, 34]. Therefore, insulin resistance leads to the increased level of free fatty acids, adding to the accumulation of fat in the liver [35].

As a mechanism, insulin action on the liver is coordinated between hepatocytes and adipose tissue. In hepatocytes under a normal condition, insulin signaling pathways result in a decreased expression of gluconeogenic enzymes, an inactivation of glycogen synthase kinase 3 $\beta$  resulting in an activation of glycogen synthase, and improved rates of glycolysis and mitochondrial oxidative phosphorylation. A decrease in the expression of gluconeogenic enzymes and activation of glycogen synthase results in reduced free glucose formation. Reduced level of free glucose indirectly inhibits the *de novo* synthesis of fat by limiting the availability of precursor compounds [36, 37].

In adipose tissues under a normal condition, insulin signaling suppresses lipolysis which in turn decreases the supply of free fatty acids and glycerol into the liver resulting in a reduced formation of fat droplets. A reduced supply of glycerol into the liver inhibits gluconeogenesis through the reduced conversion of glycerol to glucose [38-40].

In contrast to the insulin signaling in a normal condition, insulin resistance constrains hepatic glycogen synthesis leading to an excess of free glucose. Insulin resistance in adipose tissue impedes insulin-mediated suppression of lipolysis leading to increased delivery of free fatty acids and glycerol into the liver [36, 41-45]. Insulin resistance in the liver leads to an elevated level of free glucose. Elevated level of free glucose is correlated with altered adipose lipid metabolism resulting in an increased supply of free fatty acids and glycerol [46-50]. Therefore, insulin resistance mediates a complex, reciprocal form of feedback between adipose tissue and the liver leading to hepatic steatosis.

Type-2 diabetes mellitus (T2DM) is the most studied metabolic disorder with an occurrence of insulin resistance and inability of pancreatic beta cells to produce sufficient insulin to address the phenomenon of insulin resistance, [51]. The prevalence of NAFLD has been linked to T2DM. In one study, it was reported that the prevalence of NAFLD in obese patients with T2DM was 70% higher than in obese patients without T2DM [52]. These data taken collectively suggest that a close association exists between metabolic syndrome and NAFLD [53]. Obesity, insulin resistance and T2DM are interrelated in causing NAFLD, while insulin resistance plays the pivotal role in this inter-connection (Fig. 1.1).

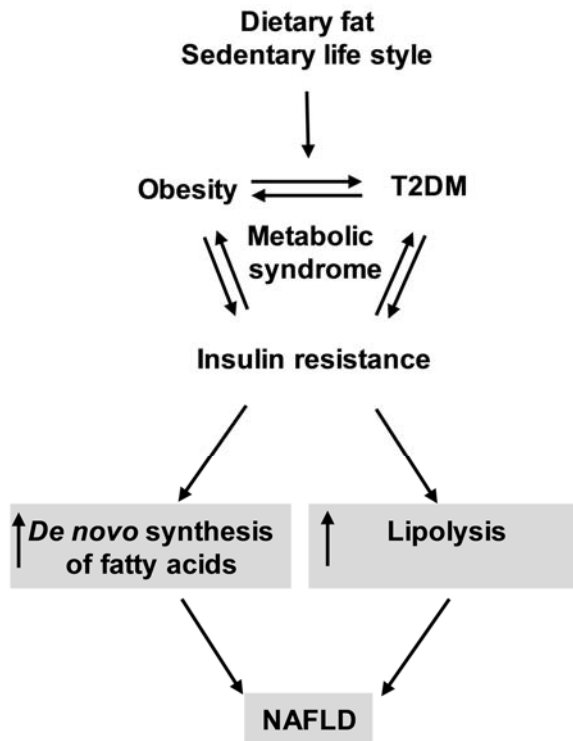


**Figure 1.1. Role of metabolic syndrome in the development of nonalcoholic fatty liver disease.**

Excessive consumption of fat in concert with a sedentary lifestyle result in metabolic syndrome as manifested by obesity, insulin resistance and type-2 diabetes mellitus. Insulin resistance plays the pivotal role of metabolic syndrome in causing an increased level of free fatty acids in the liver through their *de novo* synthesis in hepatocytes and enhanced adipose lipolysis resulting in nonalcoholic fatty liver disease.

## **A 'Two-hit hypothesis' to explain the pathogenesis of NASH**

The pathogenesis of NASH has yet to be fully elucidated. Currently, it is explained by a 'two-hit hypothesis' originally proposed by Day and James [54]. According to this hypothesis, the first hit results from the accumulation of excessive fat leading to 'hepatic steatosis'. A liver is considered steatotic if it contains more than 5% to 10% fat [55]. Hepatic steatosis is phenotypically unremarkable, but a long-term steatosis can result in the second hit caused by oxidative stress, dyslipidemia, mitochondrial dysfunction, an altered cytokine milieu, immune infiltrations, and endoplasmic reticulum stress [56]. Subsequent to the second hit, the transition of the steatotic liver occurs from being pathologically benign to a state where the organ is chronically inflamed [56].

## **Pro-inflammatory mediators of NASH**

Oxidative stress, endoplasmic reticulum stress and hepatocyte apoptosis are considered key pro-inflammatory mediators of NASH [56]. The concentration of free fatty acids within hepatocytes is low in the normal condition. An increased influx of free fatty acids into the hepatocytes initiates chronic inflammation within the liver. This increased influx of free fatty acids can result from 1) the consumption of a diet rich in carbohydrates or fat, 2) the lipolysis of stored fat, or 3) the *de novo* synthesis of fatty acids [56-58]. Such an increase in the availability of free fatty acids within the hepatocytes results in an increased fatty acid oxidation in mitochondrial and extra-mitochondrial sites leading to the over-production of reactive oxygen species (ROS). An excess production of ROS creates an imbalance with antioxidants, which in turn leads to oxidative stress and mitochondrial dysfunction [59, 60] (Fig. 1.2).

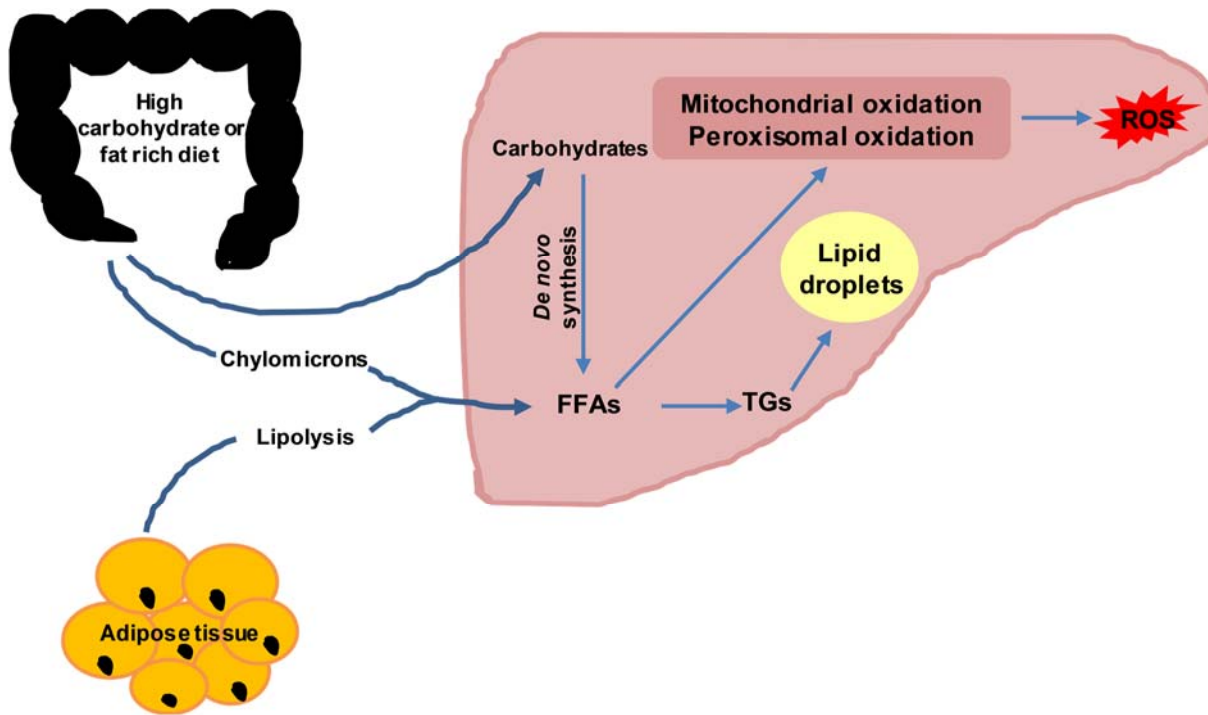


**Figure 1.2. Role of free fatty acids in the production of reactive oxygen species.** Free fatty acids can be directly transported into the liver from diet via chylomicrons. Free fatty acids can also be delivered from the lipolysis of adipose tissues. They can also be synthesized *de novo* from diet-derived carbohydrates. Free fatty acids are incorporated into triglycerides which are then accumulated into lipid droplets leading to hepatic steatosis. Excess free fatty acids undergo fatty acid oxidation in mitochondrial and extra-mitochondrial sites especially peroxisomes. Increased fatty acid oxidation in hepatocytes leads to the elevated level of reactive oxygen species resulting in oxidative stress which is the key initiator of steatohepatitis.

The presence of excess free fatty acids within hepatocytes can also lead to an overload of lipids in the endoplasmic reticulum (ER), resulting in ER dysfunction. ER dysfunction results in the accumulation of unfolded and/or misfolded proteins manifested as ER stress [61]. Mitochondrial dysfunction and ER stress culminate in the apoptosis of hepatocytes, leading to the activation of hepatic innate cells and pro-inflammatory immune infiltrates [59-62].

### **Gut microbiota and their contribution to human health**

In addition to the consequences associated with free fatty acid-mediated oxidative and ER stress, the role of other endogenous and exogenous mediators of NASH are of interest. One area receiving significant attention is the role that gut microbiota plays in the onset of NASH, but further investigation is required to have a better picture on the mechanistic role of gut microbiota in mediating NASH. Bacterial cells living inside and outside the human body outnumber the host eukaryotic cells [63]. The majority of these microbes reside within the gastrointestinal tract due to favorable growth conditions and the continuous influx of nutrients. It has been estimated that the total number of microbes harbored in the gastrointestinal tract collectively make up to 100 trillion microbes which is ten-fold higher than the human cells [64]. The unique gastro-intestinal niche confers increased fitness and stability to the microbes through their continuous communication and interactions with the host [65]. A tremendous number of studies have suggested that the gut microbiota plays a critical role in the control and onset of human health and disease. For instance, gut microbiota has an essential role in energy homeostasis and nutrient recovery from ingested diets. The microbial genes from the collective microbial community provide unique enzymes required for specific biochemical pathways [66, 67].

These enzymes have essential roles in the metabolism of xenobiotics, undigested carbohydrates and the biosynthesis of vitamins and cofactors essential to the host [67, 68]. Significantly, the gut microbiota generates short chain fatty acids that are used as an energy source by the gut epithelial cells. These short chain fatty acids have an important role in regulating gut motility and inflammation [69-71]. The gut microbiota also serve an important role in providing a barrier to pathogens through competitive exclusion and production of antimicrobial substances [67, 72-74].

Additionally, the gut microbiota has an essential role in the development of the immune system of the host. It has been reported that there are an abnormal number of immune cells and perturbations to the cytokine milieu in the lymphoid organs of germ free mice [67, 75]. Depletion of gut microbiota in mice has been shown to result in the depression of immunity and an abnormally reduced immune infiltrates in the gut [76]. Due to a direct communication between the liver and gut, it is assumed that gut microbiota may be responsible for the maintenance of intestinal health, which in turn may have an impact on the overall function of the liver.

### **Dynamic composition of gut microbiota and metabolic syndrome**

Compositional changes to the gut microbiota have been observed secondary to environmental, immunological, dietary and/or nutritional alteration experienced by the host. Such compositional changes have been associated with various host pathologies, including metabolic syndrome [77-83]. Our understanding of the factors affecting the composition of gut microbial community and how such changes can alter the risk of metabolic disease in mammals was first attributed to studies conducted by Jeffrey Gordon

and his group [84-86]. They showed that changes to the gut microbiota are secondary to diet-induced obesity in mice. These changes significantly influence energy harvest from diet, its utilization, and storage [86-88]. Apart from these studies in animal models, changes to the gut microbiota in obese humans have been reported by Ley and colleagues [89]. They showed that the proportions of Bacteroidetes to Firmicutes was decreased in the gut of obese patients as compared to the lean controls. In concert with obesity, dysbiosis was also observed in the metabolic syndrome manifested by T2D. Reduced proportions of the phylum Firmicutes and class Clostridia in concert with higher proportions of beta-proteobacteria were observed in patients with T2D compared to healthy individuals [79]. Positive correlations have occurred with the concentration of glucose observed in human plasma and the ratio of Bacteroidetes to Firmicutes as well as the ratio of Bacteroides-Prevotella group to *Clostridium coccooides-Eubacterium rectale* group [79]. These data suggest a potential association of T2D with compositional changes to the microbial community within the human gut. Due to the close relationship between metabolic syndrome and NASH, similar changes to the composition of gut microbiota are anticipated in patients with NASH.

### **Gut microbiota bridges gut-liver axis**

The term 'gut-liver axis' was first proposed by Volta and colleagues in 1978 [90]. Since then, a substantial number of studies have evaluated the association between the gut and liver in concert with human health and diseases [91]. In a healthy state, the gut epithelial layer selectively allows the entry of nutrients, ions and water across the gut epithelial boundary while simultaneously excluding deleterious compounds and microbes. The gut microbiota serves to protect the epithelial layer from pathogens through

competitive exclusion and production of pathogen specific antimicrobials. In addition to providing a protective layer to exclude pathogens, the gut microbiota serves an important role in maintaining a healthy epithelial barrier. The gut microbiota generates acetate, propionate and butyrate which contribute to maintain a tight epithelial barrier [92-94]. Consequently, any change to the gut microbiota that alters the delicate balance to epithelial nutrients may potentially compromise epithelial integrity, resulting in a condition termed leaky gut [95]. During this abnormal circumstance, the gut epithelial layer will demonstrate an impaired ability to regulate the entry of waste and other toxic components into the circulation. A leaky gut has been observed in patients with NAFLD [95, 96]. All gut-derived components crossing the epithelial barrier are drained into the liver through portal circulation. Therefore, a leaky gut poses a potential threat to the liver by increasing the supply of pro-inflammatory gut microbes-derived compounds into an organ that is already susceptible to inflammation secondary to an excessive accumulation of fat [97, 98].

### **Gut microbiota induces pro-inflammatory pathways through the interaction with toll-like receptors**

Toll-like receptors are pattern recognition molecules expressed by a variety of professional and non-professional immune cells. Toll receptor was originally identified in *Drosophila melanogaster* as a molecule essential to determine the dorsal-ventral axis orientation during embryogenesis [99]. Subsequently, human homologues were discovered and named Toll-like receptors (TLRs) [100, 101]. The intracellular domains of TLRs have similarity to the interleukin-1-receptor (IL-1R) known as Toll/Interleukin-1

receptor (TIR) domain. The function of TIR domain is to recruit adaptor molecules that in turn pass the signal upon the binding of ligands to the TLRs.

TLRs recognize microbe associated molecular patterns (MAMPs) and are responsible for the induction of pro-inflammatory responses. In addition to microbial components, TLRs can also recognize endogenous ligands known as danger associated molecular patterns released from damaged tissue, infected tissue or dead cells. Upon the binding of ligand to the extracellular domain of TLRs, adaptor molecules are recruited to the cytoplasmic TIR domain resulting in a sequential activation of intracellular signaling molecules called signal transduction. The consequence of signal transduction is the activation of transcription factor nuclear factor kappa-light-chain-enhancer of activated B cells (NF- $\kappa$ B), which results in an expression of pro-inflammatory mediators such as cytokines and chemokines. In addition to activating the NF- $\kappa$ B pathway, mitogen activated protein kinase cascades are also activated by the TLR-ligand interaction [100, 102, 103]. TLRs were initially considered only to induce anti-pathogen inflammatory responses, but growing body of evidence indicates that activated TLRs are the underlying cause for a number chronic inflammatory diseases (Table 1) [100, 103-112].

### **Potential role of low grade chronic endotoxemia in metabolic syndrome**

The gut microbiota contains both Gram-positive and Gram-negative bacteria. Lipopolysaccharide (LPS), also known as endotoxin, is a major outer membrane constituent of Gram-negative bacteria. LPS is continuously produced and shed from

**Table 1.** List of Toll-like receptors and their microbial/non-microbial ligands

TLRs	Microbe-derived ligands		Nonmicrobial ligands	Diseases
	Ligands	Sources		
TLR-1/2/6	Triacyl lipopeptides	Bacteria	Fatty acids	Atherosclerosis
	Peptidoglycans	Gram-positive bacteria	Hyaluronan fragments	Inflammatory bowel disease
	Phenol soluble modulin	<i>Staphylococcus aureus</i>	HMGB-1	Asthma
	Glycolipids	<i>Treponema maltophilum</i>	HSPs	Rheumatoid arthritis
	Atypical LPS	Non-entero bacteria		
	Phospholipomannan	<i>Candida albicans</i>		
	LPG	<i>Leishmania major</i>		
	Tc52	<i>Trypanosoma cruzi</i>		
	Diacyl lipopeptides	<i>Mycoplasma</i>		
	Lipoteichoic acid	Gram-positive bacteria		
	Zymosan	<i>Saccharomyces cerevisiae</i>		
	GPI anchor	<i>Trypanosoma cruzi</i>		
	Envelope protein	Measles virus		
	Human cytomegalovirus			
	herpes simplex virus type I			
TLR-3	dsRNA	Viral dsRNA	Synthetic dsRNA (Poly(I:C))	Type 1 diabetes
TLR-4	LPS	Gram-negative bacteria	Fatty acids	Rheumatoid arthritis Atherosclerosis
	Mannan	<i>Saccharomyces cerevisiae</i>	Hyaluronan fragments	Multiple sclerosis
		<i>Candida albicans</i>	HMGB-1	Asthma
	Glucuronoxylomannan	<i>Cryptococcus neoformans</i>	HSPs	Rheumatoid arthritis
	F protein	Respiratory syncytial virus	Fibronectin fragments	
	Envelope protein	Mouse mammary tumor virus		

TLR-5	Flagellin	Flagellated bacteria		Inflammatory bowel disease
TLR-7/8	ssRNA		Synthetic imidazoquinoline derivatives	Systemic lupus erythematosus Type 1 diabetes
TLR-9	CpG DNA	Bacteria	Immune complexes/dsDNA	Systemic lupus erythematosus Type 1 diabetes
		Virus	HMGB-1	
	Genomic DNA	<i>Babesia bovis</i>		Multiple sclerosis
		<i>Trypanosoma cruzi</i>		Inflammatory bowel disease Rheumatoid arthritis
		<i>Trypanosoma brucei</i>		
Hemozoin	<i>Plasmodium falciparum</i>			
TLR-11	Not determined	Uropathogenic bacteria		
	Profilin-like protein	<i>Trypanosoma gondii</i>		
	CpG DNA	Virus		

bacteria either through their lysis or growth [113, 114]. Although the presence of LPS is restricted to the intestinal lumen [115], small amounts of LPS can pass through the epithelial barrier and enter the circulation in healthy individuals [116]. While the presence of LPS in circulation is normal, an increased concentration can result in chronic endotoxemia. Thus, the role of an increased concentration of gut-derived LPS in blood circulation is an important topic of investigation in relation to chronic inflammatory diseases, in particular, the metabolic syndrome.

Inflammatory responses associated with acute endotoxemia, secondary to sepsis, have revealed alterations to lipid metabolism [117, 118]. A lethal or sub-lethal dose of endotoxin in mice leads to increased adipose lipolysis resulting in an elevated concentration of circulating free fatty acids [119-121]. Despite an increased level of circulating free fatty acids, fat accumulation in the liver is prevented due to the autophagy induced by a lethal dose of endotoxin [120]. In contrast to acute endotoxemia, our understanding of the pro-inflammatory consequences associated with a low concentration of circulating LPS and its impact on lipid metabolism is still unclear. Recently, Cani and colleagues have observed that a low concentration of endotoxin is increased in obese (ob/ob) mice and in lean mice fed a high fat diet. They have shown that a chronic elevation to the concentration of endotoxin through the infusion of low grade LPS results in fat deposition in adipose tissue, which is in direct conflict to observations associated with the animals exposed to acute endotoxemia [122, 123]. Moreover, plasma levels of LPS have been reported to increase in patients with abdominal obesity compared to the healthy controls, which is in line with the observations associated with mice exposed to chronic endotoxemia [124].

## **TLR-4 pathway is essential in the modulation of metabolic syndrome**

LPS interacts with TLR-4 upon binding to CD14 to induce inflammation [125]. Cani and colleagues have shown that CD14 knockout mice are partially protected from a high fat diet-induced increase in adipose tissue and body weight [122, 123]. This study suggested a role for the TLR-4 pathway in metabolic derangements in high fat diet-mediated obesity in mice [123]. The TLR-4 pathway has also been linked to metabolic syndrome in human patients. Creely et al. have shown that the expression level of TLR-4 is higher in obese and in type-2 diabetes patients compared to healthy individuals [126].

## **Potential role of LPS-TLR-4 axis in NASH**

In human, the liver is the first organ to encounter LPS delivered from the gut microbial community. TLR-4 expressing Kupffer cells are a major and well characterized target of LPS in the liver to execute the subsequent pro-inflammatory events [127, 128]. In comparison to healthy individuals, a slightly elevated level of serum endotoxin was reported in NASH patients which led to investigations examining the potential role of low dose LPS in driving inflammation in NASH in experimental models [129-132]. Indeed, injection of subclinical dose of LPS in mice fed high fat diet or obese mice (ob/ob) resulted in exacerbated hepatic inflammation indicating the role of chronic endotoxemia in causing NASH [133]. Based on these reports, a comprehensive study to investigate the role of LPS-TLR-4 axis in causing chronic inflammation in the fatty liver is needed. Therefore, in this project, we attempted to establish the role of gut-derived LPS-TLR-4 pathway as an actual risk factor to sustain a chronic inflammation during the pathogenesis of NASH. We also attempted to employ the LPS-TLR-4 pathway as a potential target for therapeutic intervention to stop the progression of NASH.

# Chapter 2

## Materials and Methods

Our initial objective was to investigate the global involvement of gut microbiota in causing NASH. This objective was experimentally addressed by using specific pathogen free and germ free mice. We also conducted gut microbiota reconstitution (conventionalization) experiment to test whether the restoration of gut microbiota in germ free mice through fecal transfer from normal mice could impact the level of NASH. We then intended to assess the role of LPS-TLR-4 pathway in mediating NASH by using wild-type and TLR-4 KO mice individually treated with broad-spectrum antibiotics, LPS, or TLR-4 inhibitor. Bone marrow transplantation experiment was performed to investigate the role of TLR-4-expressing kupffer cells in the modulation of NASH. Following euthanization, tissue samples were collected for subsequent analyses. In this chapter, different experimental steps and methods used in this project have been described with detailed information in a reproducible manner.

### **Animal experiments**

Six-week-old male wild-type C57BL/6 mice were purchased from Jackson Laboratories and maintained under specific pathogen free conditions. Six-week-old germ free male C57BL/6 mice were bred and housed in flexible plastic gnotobiotic isolators following a strict 12 h light cycle at the gnotobiotic animal research facility of the Medical University of South Carolina. Six-week-old toll-like receptor knock out (TLR-4 KO) C57BL/6 male mice were purchased from Jackson Laboratories and maintained under specific pathogen free conditions. After two weeks of equilibration on normal chow, the now eight-week-old mice were placed either on an isocaloric control diet ((CD), TD.08810, 10% kcal from fat), a lard-based high fat diet ((LD), TD.06414, 60% kcal from fat, 63% unsaturated) or a milk-based high fat diet ((MD), TD.09766, 60% kcal from fat, 61%

saturated), purchased from Harlan Laboratories (IN, USA). Mice were housed at 22 °C with 12 h light/dark cycle, fed special diets for 8, 16 or 32 weeks *ad libitum* and weighed each week. After 8, 16, or 32-weeks of feeding, they were euthanized whereupon the liver were harvested and blood samples were collected. Whole livers were weighed with portions of them processed for the isolation of total RNA and subsequent analysis for specific proteins. The remaining fraction of the liver was fixed in 10% neutral buffered formalin (Starplex Scientific Inc., Ontario, Canada) for 24 h at room temperature, with its subsequent embedding into paraffin, sectioning, and histological/immunohistochemical staining. All of the animal studies were reviewed and approved by the Medical University of South Carolina's Institutional Animal Care and Use Committee (IACUC).

For conventionalization (restoration of normal gut flora) experiment, gut microbiota was reconstituted in six-week old germ free mice fed CD or MD by fecal transplantation from specific pathogen free wild-type donor mice. Stool from donor mice were diluted in saline (0.1g/mL) and gavaged into germ free animals on a weekly basis for a period of 16 weeks (200 µL per animal). The remaining stool solution was placed on the fur of the animals. Part of soiled bedding was collected from the cages of stool donors and placed into the cages of the conventionalized/recipient animals on the same weekly schedule.

### **Partial hepatectomy**

Partial hepatectomy experiment was performed to investigate the role of dietary fat-mediated NASH on hepatic regeneration. After 16 weeks of continuous feeding with CD, LD or MD, C57BL/6 mice were anesthetized with isoflurane and subjected to a mid-ventral laparotomy with approximately 70% of liver resection (left lateral and median lobes hereafter referred to as resected lobes) [134]. Animals from individual diet interventional

and control group were sacrificed 2 or 7 days post-hepatectomy. One hour prior to sacrifice, a single dose of 5-bromo-2'-deoxyuridine (BrdU, Sigma-Aldrich, MO, USA) was injected intraperitoneally at a dose of 50 mg/kg animal weight using a vehicle of 0.2% pyrogen free phosphate buffered saline (Fig. 2.1). At the time of sacrifice, animals were anesthetized with isoflurane and total blood was harvested from the right ventricle of the heart. The remaining lobes of the liver, hereafter referred to as regenerated lobes, were harvested. Both of the resected and regenerated lobes of the livers were weighed and were processed for RNA, protein and histological analyses.

### **Treatment with broad-spectrum antibiotic, LPS and TLR-4 inhibitor**

It was intended to investigate the role of LPS in causing NASH as a sole gut-derived molecule present in the circulation. To ensure that chronic inflammation was not induced by any gut-derived component other than LPS, gut microbiota was diminished by the treatment of broad spectrum antibiotics followed by the chronic administration of low dose LPS. Broad spectrum antibiotics-treated and LPS-injected mice were administered with TLR-4 inhibitor to demonstrate the role of TLR-4 pathway in causing NASH. To accomplish this experiment, specific pathogen free, C57BL/6 mice fed CD or MD for 16 weeks were treated with ampicillin (1 g/l: Sigma-Aldrich, USA), neomycin sulfate (1 g/l: Sigma-Aldrich, USA), metronidazole (1 g/l: Sigma-Aldrich, USA) and vancomycin (500 mg/l: Sigma Aldrich, USA) ad libitum through the drinking water. During the last four weeks of antibiotic treatment, the mice were injected intraperitoneally daily with 0.25 mg/kg body weight LPS (O55:B5, Sigma Aldrich, USA) or vehicle (0.9% saline). During LPS injection, mice were also injected intraperitoneally three times per week with 3 mg/kg body weight TAK-242 (Sigma Aldrich, USA) or vehicle (1% DMSO (Sigma Aldrich, USA)).

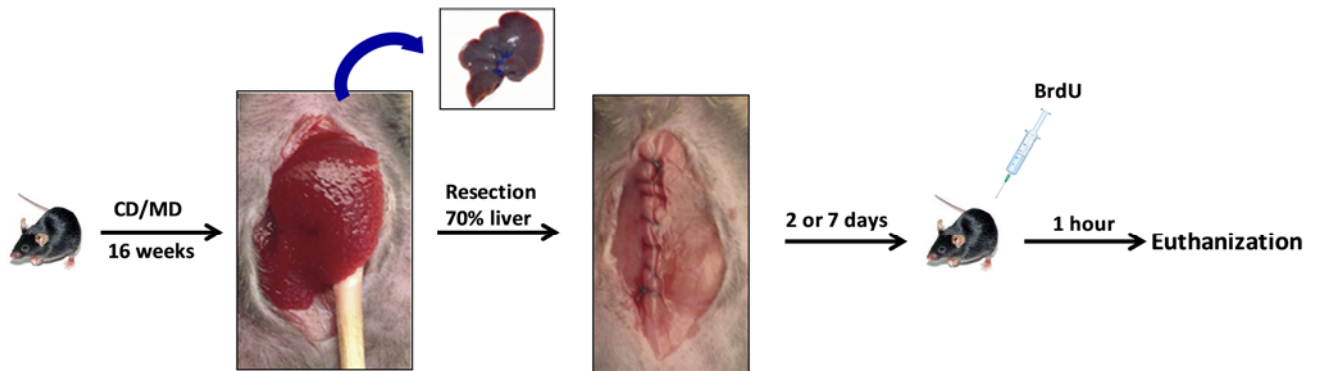


**Figure 2.1. Diagrammatic representation of hepatic regeneration experiment.** Mice fed control diet or milk-based high fat diet for 16 weeks were subjected to partial hepatectomy. After 2 or 7-days of partial hepatectomy, mice were injected with BrdU one hour prior euthanization. CD and MD indicate control diet and milk-based high fat diet, respectively.

TLR-4 KO mice fed CD or MD were injected with LPS using same protocol as mentioned above (Figure 2.2A).

### **Bone marrow transplantation and depletion of kupffer cells**

To investigate the role of TLR-4-expressing kupffer cells in mediating NASH, an experiment was designed where kupffer cells in the livers of wild-type mice were reconstituted with TLR-4 KO cells and kupffer cells in the livers of TLR-4 KO mice were reconstituted with wild-type cells. To accomplish this experiment,  $8 \times 10^6$  bone marrow cells, obtained from wild-type or TLR-4 KO mice, were injected into tail vein of lethally irradiated (11 Gy) TLR-4 KO or wild-type mice respectively. After 2 weeks of bone marrow transplantation, mice were injected intravenously just once with 200  $\mu$ l of 5 mg/mL of liposomal chlodronate (Encapsula NanoSciences, USA). Injection of chlodronate depleted the former kupffer cells resident in the liver and served to create an available niche for the transplanted bone marrow-derived monocytes to settle as new kupffer cells. After 10 weeks of chlodronate injection (during this 10 weeks mice were on regular chow provided by the animal facility), both the wild-type and TLR-4 KO mice were fed CD or MD for 16 weeks (Figure 2.2B) [135].

A question was raised whether the engrafted hematopoietic cells-derived monocytes were actually settled as kupffer cells in the livers. Following experiment was performed to answer this question using CD45.1 (donor) and CD45.2 (recipient) congenic mice.  $8 \times 10^6$  bone marrow cells isolated from CD45.1 donor mice were intravenously injected into lethally irradiated (11 Gy) congenic CD45.2 recipient mice. Following 2 weeks after bone marrow cell injection, mice were injected intravenously just once with

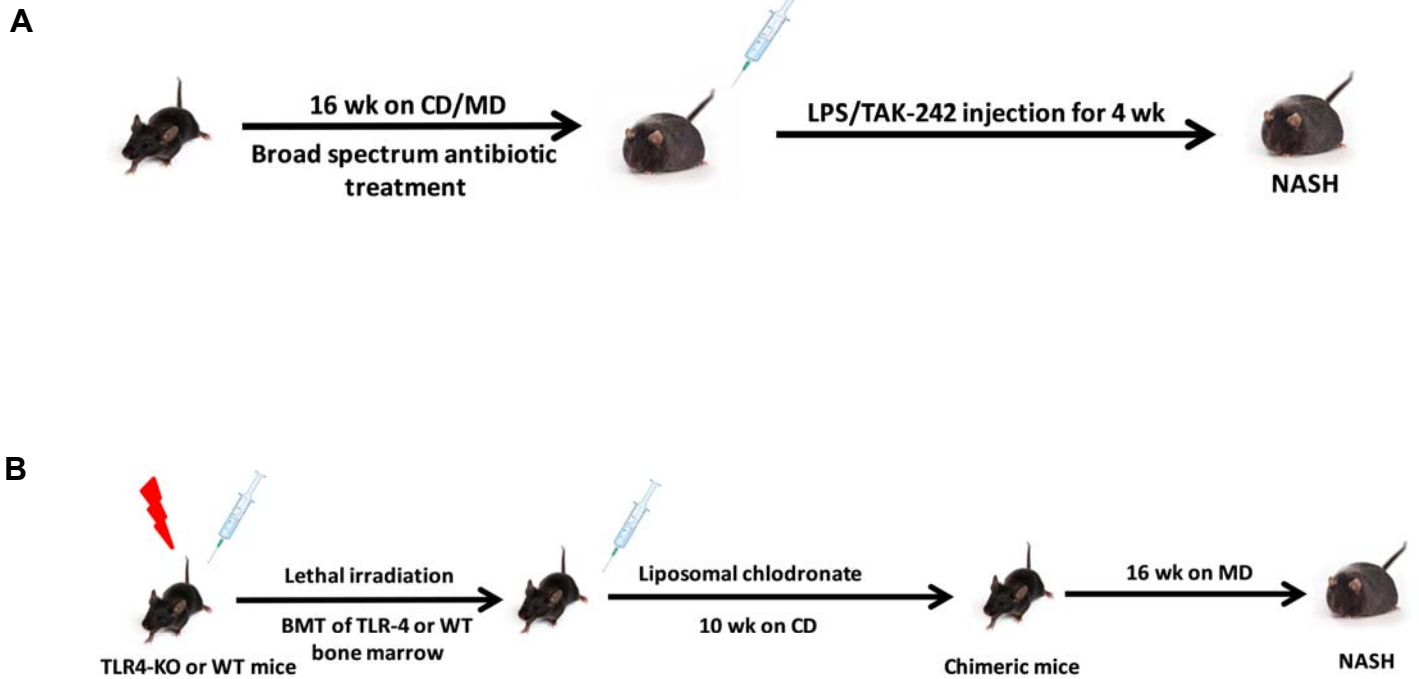


**Figure 2.2. Diagrammatic representation of (A) antibiotic/LPS/TAK-242 treatment and (B) kupffer cell reconstitution experiment. (A)** Broad spectrum antibiotics-treated mice fed CD or MD for 16 weeks were injected with LPS or administered with TAK-242 for last 4 weeks of experiment. **(B)** Lethally irradiated TLR-4 KO or wild-type mice were transplanted with bone marrow isolated from wild-type or TLR-4 KO mice. After 2 weeks of bone marrow transplantation, mice were injected with liposomal chlodronate. Following 10 weeks of liposomal chlodronate injection, mice were fed control diet or milk-based high fat diet for 16 weeks. CD and MD indicate control diet and milk-based high fat diet, respectively.

chlodronate (200  $\mu$ l of 5 mg/mL). After 10 weeks of chlodronate injection, non-parenchymal cells were isolated from the livers of chimeric and control mice and used for flow cytometric analyses.

### **ALT and AST assays**

Presence of alanine aminotransferase (ALT) and aspartate aminotransferase (AST) in the serum was determined as an indicator of NASH. After the collection of whole blood through heart puncture, it was allowed to clot by leaving undisturbed at room temperature for 15–30 min. The clot was removed by centrifuging at 1,000–2,000x g for 10 minutes at 4°C. Following centrifugation, the transparent yellowish liquid component (serum) was immediately transferred into a clean polypropylene microcentrifuge tube and stored at -20 °C [136]. Serum was assessed for the presence of ALT and AST using standard kit protocols provided by the manufacturer (BioVision Inc., USA).

### **Endotoxin assays**

In order to assess the concentration of circulating endotoxin, serum was collected from the portal blood following the protocol used for serum collection from the whole blood [136]. Portal serum was used to determine the concentration of LPS using the Pierce Limulus Amebocyte Lysate (LAL) chromogenic endotoxin assay kit following standard protocol provided by the manufacturer (Thermo Scientific, USA).

In order to assess the concentration of endotoxin resident in the fecal material of the animals, 20 mg of fecal matter was collected from the cecum of each animal whereupon it was placed into 50 mL PBS within a pyrogen-free tube. The material was then sonicated at 20 KHz for 1 h on ice. Subsequent to sonication, the resulting material

was centrifuged at  $400 \times g$  for 15 min. The upper 30 mL of the sonicate was collected, sterilized by filtration through a 0.45- $\mu\text{m}$  filter, re-filtered through a 0.22- $\mu\text{m}$  filter, and inactivated for 10 min at 70°C [137]. The LPS concentration present in the filtered sonicate was determined using the Pierce Limulus Amebocyte Lysate (LAL) chromogenic endotoxin assay kit following standard protocol provided by the manufacturer (ThermoFisher Scientific, USA).

### **Liver histology and immunohistochemical staining**

In order to assess the histopathological status of NAFLD, formalin fixed and paraffin-embedded (FFPE) tissues were evaluated. The 5  $\mu\text{m}$  FFPE sections were stained with Hematoxylin and Eosin (Richard-Allan Scientific® Histology/Cytology Reagents, ThermoFisher Scientific, USA) using the standard protocol provided by the manufacturer. Slides were assessed for the extent to which each liver sample met the criteria for NAFLD. This evaluation was performed by an experienced liver pathologist using an established semi-quantitative schema [138-140]. In brief, NAFLD activity was determined from the sum of the total steatosis observed, the extent with which lobular inflammation was present and the level of hepatocellular ballooning. Levels of steatosis were scored as a percent area of the field occupied by the empty spots secondary to the release of fat droplets as a consequence of ethanol wash during the paraffin embedding. Lobular inflammation was scored from the level of cellular infiltration and hepatocellular ballooning was scored from the number of enlarged hepatocytes with rarefied cytoplasm that achieved a size greater than 1.5 to 2 times the diameter of a normal cell [138-140].

In order to visualize the deposition of fat within the liver, liver tissues were embedded in optimal cutting temperature (O.C.T) compound. The 5  $\mu\text{m}$  O.C.T sections

were stained with oil red O (Sigma-Aldrich, USA) using the standard protocol provided by the manufacturer [141]. Oil red O-stained O.C.T sections were visualized and imaged using ZEISS Axiovert 200M inverted microscope equipped with a digital camera (20x magnification).

In order to assess the level of collagen accumulation, 5  $\mu$ m FFPE liver sections were stained with picrosirius red. Briefly, FFPE sections were deparaffinized in xylene, whereupon they were rehydrated by serially soaking in 100%, 95%, 90% and 0% ethanol and then incubated in a solution of 0.1% Sirius red (Direct red 80, Sigma-Aldrich, USA) and 1.3% saturated picric acid (Sigma-Aldrich, USA) for 1 hour. Subsequent to staining, the sections were washed using a 0.5% acetic acid solution, whereupon they were dehydrated by serially soaking in 0%, 90%, 95% and 100% ethanol and xylene. Picrosirius red-stained sections were imaged using ZEISS Axiovert 200M inverted microscope equipped with a digital camera (20x magnification).

Hepatocyte nuclear staining for BrdU was performed by using BrdU immunohistochemistry kit essentially as described by the manufacturer (abcam, USA). BrdU-incorporated hepatocytes were counted in high-power field of light microscope using 20x magnification and expressed as a percentage of total hepatocytes (both BrdU stained and non-stained).

The number of neutrophils present in each FFPE section was determined by staining the sections with Leder stain (Naphthol AS-D chloroacetate esterase, Sigma-Aldrich, USA). The number of infiltrating neutrophils was determined by counting the number of Leder-positive cells encountered in each high-power field (20x magnification) from each section evaluated.

The number of macrophages present in each FFPE section was determined by immunostaining for F-4/80. FFPE sections were incubated in 0.3% H<sub>2</sub>O<sub>2</sub> for 30 min to quench the activity of endogenous peroxidase followed by an incubation with primary antibody (rat anti-mouse F4/80, clone BM8, Biolegend, USA) and secondary antibody using Vectastain ABC kit (Vector Laboratories, USA) following the standard protocols provided by the manufacturers. The percentage of macrophage infiltration was determined as the number of positively stained macrophages against the total number of cells present in each high power field (20x magnification) per section [142].

In order to do fluorescence immunohistochemistry, FFPE sections were boiled in sodium citrate buffer (10 mM sodium citrate, 0.05% Tween 20, pH 6.0) for 30 min for antigen retrieval followed by the blocking with 5% BAS for 30 min at room temperature, overnight incubation with the primary antibody at 4°C, 1.5 hour incubation with secondary antibody, and DAPI staining following standard protocol (abcam, USA).

### **Quantitative real time reverse transcriptase polymerase chain reaction (RT-PCR)**

Expression levels of different NASH-indicative genes were determined by using RT-PCR. Total RNA was isolated from 20-50 mg liver tissue using Trizol (Ambion, USA) according to the manufacturer's instructions. The concentration of RNA recovered was determined by Nanodrop Spectrophotometer (ThermoFisher Scientific, USA). The quality of RNA was assured by determining the ratio of absorbance at 260 nm and 280 nm. A ratio of absorbance at 260 nm and 280 nm higher than 2.0 confirmed the purity of RNA samples [143]. The concentrations of RNA between samples were equalized through dilution using sterile, RNase free water.

RT-PCR was accomplished by taking 500 ng of RNA, subjecting it to reverse transcription with subsequent amplification of the DNA template using LightCycler 480 instrument (Roche, USA) using the TaqMan Fast Virus 1-step PCR master mix (Applied Biosystems, USA) and TaqMan-FAM-MGB primers/probes (Applied Biosystems, USA) in a final reaction volume of 20  $\mu$ L using the following thermocycling profile. 1) Reverse transcription at 50°C for 5 min; 2) inactivation of the reverse transcriptase by exposing the reaction to 95°C for 20 sec; and 3) amplification of newly transcribed DNA template with 40 successive cycles at 60°C for 30 seconds followed by denaturation at 95°C. Gene-specific probe information are provided in Table 2.1. The expression level of a given gene was calculated as a fold difference in relative to the normalized expression level housekeeping gene HPRT1 using the comparative  $\Delta\Delta$ Ct method [144].

### **Western blot analysis**

Differences in the expression level of different NASH-associated proteins in the liver were assessed by using Western blot analysis. In order to prepare tissue homogenate, 50 mg of liver tissue was homogenized in 200  $\mu$ L of RIPA buffer (25 mM Tris-HCl, 150 mM NaCl, 1% Triton X-100, 1% sodium deoxycholate, 0.1% SDS and 5% mammalian proteinase inhibitor) (Sigma-Aldrich, USA) [145]. Protein concentration in the tissue homogenate was determined by following the instruction of BCA assay kit (Pierce, USA). Then, 5  $\mu$ g of protein samples were run on 4-12% NuPage polyacrylamide gels (Life Technologies, USA) and transferred to nitrocellulose membrane (ThermoFisher Scientific, USA). After blocking with TBS-T (Sigma-Aldrich, USA) containing 5% milk for 30 min, blots were incubated overnight at 4°C with the primary antibody diluted in TBS-T containing 5% milk [146]. The blots were then washed with TBS-T, incubated with

peroxidase-conjugated secondary antibody diluted in TBS-T containing 5% milk for 1.5 hr at room temperature (information about the antibodies used in Western blot analysis are provided in Table 2.2). After 3×5 min washing with TBS-T, blots were

**Table 2.1.** List of probes used for RT-PCR

<b>Probe</b>	<b>Gene bank address</b>	<b>Company</b>
HPRT	Mm00446968_m1	ThermoFisher
TNF- $\alpha$	Mm00443258_m1	ThermoFisher
IL-1 $\beta$	Mm00434228_m1	ThermoFisher
CCL-2	Mm00441242_m1	ThermoFisher
TGF- $\beta$	Mm00441724_m1	ThermoFisher
$\alpha$ -SMA	Mm01546133_m1	ThermoFisher
Col-1a	Mm00801666_g1	ThermoFisher

**Table 2.2.** List of antibodies used for immunoblot and immunofluorescence staining

<b>Antibody</b>	<b>Dilution</b>	<b>Company</b>	<b>Clone/RRID</b>
Rabbit anti-PARP Ab	1:1000	Cell Signaling	46D11
Goat anti-rabbit HRP-linked secondary Ab	1:2000	Cell Signaling	7074S
Mouse anti-catalase monoclonal Ab	1:4000	ThermoFisher	12C2DB9
Mouse anti-GAPDH Ab	1:4000	Ambion	6C5
Goat anti-mouse HRP-linked secondary Ab	1:4000	ThermoFisher	AB_2533947
Alexa Fluor 488 Goat anti-Rabbit IgG	1:1000	Invirogen	AB_143165
Rabbit polyclonal to Catalase	1:500	abcam	ab16731
Rabbit polyclonal to PMP70	1:500	abcam	ab3421

incubated with freshly prepared SuperSignal West Femto Maximum Sensitivity Substrate (Thermo Scientific, USA) for 1-5 min and imaged using luminescent image analyzer (Image Quant LAS 4000, GE Healthcare Life Sciences, PA, USA). Densitometry analyses were performed using Image J software (National Institutes of Health, USA).

### **Catalase activity assay**

Catalase activity present in liver homogenates was assessed in order to provide an approximation of the alteration to peroxisomal anti-oxidative function. 50 mg tissue homogenates were prepared and used for catalase activity assay using standard protocol of catalase activity colorimetric/fluorometric assay kit (BioVison Inc., USA).

### **16S rRNA analyses**

To investigate the impact of change of diet on gut microbiota, diet-conversion experiment was performed. In this experiment, six-week-old mice were fed milk diet (MD) for 16 weeks. Then, the diet was switched from MD to control diet (CD) for another 16 weeks. Following euthanization, mice abdomen was opened and stool pellets were collected from the severed distal ileum using blade and tweezers. Collected stool was snap frozen and stored at -80°C. Analysis of the 16S bacterial DNA from was carried out at the Microbiome Core Facility of the University of North Carolina. DNA was extracted from samples using the Epicentre® MasterPure Complete DNA Purification Kit (Illumina, Inc.) and bacterial DNA was amplified and sequenced by the Illumina MiSeq system. 16S rDNA amplicons was purified and quantified on an Invitrogen Qubit system and assessed on an Agilent Bioanalyzer. Following quality filtering, sequences was de-multiplexed and trimmed using QIIME open source software (<http://qiime.org>). Downstream alignment of

QIIME processed sequences; identification of open taxonomic units (OTUs), clustering, and phylogenetic analysis was conducted using the Phylosift open source software package (<http://phylosift.wordpress.com>). Statistical analyses of community diversity within and amongst experimental groups included Principal Components Analysis, Squash Clustering, and Kantorovich-Rubinstein distance (akin to weighed UniFrac).

### **Isolation of kupffer cells and flow cytometric analyses**

In order to do the flow cytometric analysis, kupffer cells were isolated from the liver using the following protocol [147, 148]. Livers were perfused with 5 ml Hank's balanced salt solution (HBSS), followed by 12 ml digestion buffer (HBSS containing 0.5 mg/ml type VI collagenase (Sigma-Aldrich) and 10 mg/ml DNase I (Roche)). The livers were removed, minced and incubated in digestion buffer at 37°C for 20 min with subsequent passage through a 40 mm cell strainer. Parenchymal cells were removed by low speed centrifugation at 50xg for 2 min. The supernatant enriched in non-parenchymal cells was centrifuged at 800xg for 30 min through a 25% (v/v) percoll gradient at room temperature with no brake. The pellets of the gradient containing kupffer cells were washed and used for flow cytometric staining.  $0.5-5 \times 10^6$  cells in 200  $\mu$ l stain buffer plus Fc blocker (1:50) in FACS tubes were incubated on ice for 20 min. Then, surface marker-specific conjugated antibodies or unconjugated primary antibodies (5  $\mu$ l/ $10^6$  cells) (Table 2.3) were added and incubated for 30 min on ice in the dark. Then, cells were washed and incubated with conjugated secondary antibodies (5  $\mu$ l/ $10^6$  cells) for 30 min on ice in the dark. After incubation, cells were again washed and treated with propidium iodide at the concentration of 1  $\mu$ g/ml. Then, the cells were run through LSR II flow cytometer (BD, Bioscience) and analyzed using FlowJo software (FlowJo LLC).

**Table 2.3.** List of antibodies used for flow cytometric analyses

<b>Antibodies</b>	<b>Target cells</b>	<b>Company</b>	<b>Clone</b>
Ly6G BV650	Granulocytes, Neutrophil, Eosinophil	BD Biosciences	1A8
SiglecF BV650	Granulocytes, Neutrophil, Eosinophil	BD Biosciences	E50-2440
Ly6C BV421	Monocytes	BD Biosciences	AL-21
F4/80-Biotin	Kupffer cells	Biolegend	BM8
CD45.1 PECy7	Donor cells	BD Biosciences	A20
CD45.2 PerCP-Cy5.5	Recipient cells	BD Biosciences	104
Streptavidin-QDot650	Kupffer cells	ThermoFisher	-
Fc blocker	Fc receptor blocker	BD Biosciences	2.4G2
Propidium iodide	Dead cells	ThermoFisher	-

### **Statistical analyses**

All values were expressed as mean  $\pm$  standard error of the mean. Statistical significance was chosen *a priori* as  $\alpha \leq 0.05$ . Two groups of data were analyzed using non-parametric statistics employing the Mann-Whitney U test to analyze single, unpaired comparisons of normally distributed data sets. Multiple groups of data were analyzed using nonparametric one way ANOVA. Statistical analyses were performed using GraphPad PRISM version 7.

# Chapter 3

Dietary Model of NASH: Pathology of NASH Develops at a Higher Level in Animals Fed a Diet Rich in Saturated Fats

## **Summary**

In order to study NASH, it is essential to have an animal model that faithfully mimics the pathology and symptoms of the disease observed in humans. Of the different NASH models available, those employing a high fat diet to facilitate the development of NASH better represent the symptoms and pathological indicators of NASH than those relying on genetic perturbation or other forms of dietary intervention. Both unsaturated and saturated fats result in hepatic steatosis followed by the development of NASH. However, their comparative role in triggering inflammation in the fatty liver is still unclear. Reports state that saturated fatty acids are more toxic than unsaturated fatty acids. Therefore, we hypothesized that mice fed a saturated high fat diet would manifest higher level of inflammation in the liver compared to mice fed an unsaturated high fat diet. To test this hypothesis, 6-8 week-old mice were fed three distinct diets: a low fat control diet ((CD), 10% calories from fat), a lard-based unsaturated high fat diet ((LD), 60% calories from unsaturated fat), and a milk-based saturated high fat diet ((MD), 60% calories from saturated fat). The mice were fed for a period of 8, 16 or 32 weeks in order to assess the time at which NASH was clinically more apparent. Serum and liver tissues were examined for inflammation-indicative markers, which demonstrated an elevated level of NASH in mice fed LD or MD compared to the mice fed CD at week 16 and 32. At week 8, none of the mice fed LD or MD developed significant level of NASH as compared to the mice fed CD. As a comparison between LD and MD, mice fed MD exhibited a higher trend of NASH than the mice fed LD at week 16 and 32. In conclusion, while both types of high fat diets can induce NASH in mice after 16 or 32 weeks of feeding, saturated high fat diet is more efficient in inducing inflammation than unsaturated high fat diet.

## **Introduction**

In order to develop a strategy for the successful management of NASH, we first need to understand the pathogenesis of the disease. To this end, it is essential to be able to follow the progression of disease in human patients or experimental models [149]. Although human patients are the first choice for studying NASH, it is subjected to some major limitations. Because of the long period of time, sometimes even decades, required to develop NASH in humans, and given the ethical restrictions of administering drugs to and collecting liver tissues from NASH patients, it is extremely important to have an experimental model faithfully mimicking NASH [150]. A suitable animal model of NASH can help researchers understand the pathology of NASH and test the effects of different therapeutic products [150, 151]. An appropriate animal model of NASH should correctly reflect the histological lesions (fat accumulation, immune infiltration, fibrosis) and pathophysiological indicators observed in human patients [151]. Currently both genetic and dietary models of NASH are available. Because none of these models perfectly mimics the histopathology or pathophysiology of NASH in humans, they are only useful for investigating certain aspects of the disease. Available genetic models of NASH are sterol regulatory element binding protein (SREBP)-1c transgenic mice, leptin deficient *ob/ob* mice, leptin receptor deficient *db/db* mice, phosphatase and tensin homologue deleted on chromosome 10 (PTEN) null mice, agouti gene mice, peroxisome proliferator-activated receptor- $\alpha$  (PPAR- $\alpha$ ) knockout mice, acyl-coenzyme A oxidase (AOX) null mice and methionine adenosyltransferase-1A (MAT-1A) null mice [53, 150, 151]. One major limitation of these genetic models of NASH is that none of the genetic perturbations are present in the human patients. Moreover, some of these models (*ob/ob* mice, *db/db* mice

and agouti mice) do not progress from steatosis to steatohepatitis spontaneously. They require an additional insult ( e.g. feeding with special diet) to induce steatohepatitis [150]. As compared to the genetic models, dietary models have a higher relevance to NASH in humans, because they develop the disease only through the consumption of special diets without the need for genetic alterations. Currently available such special diets are methionine choline deficient diet, diet containing cholesterol and cholate, fructose enriched diet, and high fat diet [150, 151]. An important limitation of these dietary models is that none of these diets represents regular human diet. A Combination of genetic perturbation and dietary challenge can also develop the histopathological and pathophysiological features of NASH [152-156]. Of these available genetic and dietary models, high fat diet-mediated NASH is clinically more relevant due to its similarity to the 'western diet' in having high fat content.

A typical 'Western diet' contains calories from both unsaturated and saturated fats [157]. A Pro-inflammatory role for saturated fats has been demonstrated in different diseases [158-163]. Diets containing high amount of saturated fats have been linked with coronary heart disease, insulin resistance, metabolic syndrome and diabetes [158]. Saturated high fat diet causes higher incidence of colitis in genetically susceptible mice compared to the polyunsaturated high fat diet [159]. Role of saturated fats in the progression of NAFLD has also been shown in numerous reports [160-163]. Saturated fats mediate NAFLD through the accumulation of elevated level of reactive oxygen species, endoplasmic reticulum stress and lipotoxicity [164]. Due to these pro-inflammatory roles of saturated fat over unsaturated fat, it was investigated in this study whether a milk-based saturated high fat diet (MD) is more efficient in inducing NASH

compared to the lard-based unsaturated high fat diet (LD). It was reported that feeding of mice with high fat diet for 8-12 weeks could induce NASH [133, 142], but no previous study had demonstrated the impact of different feeding periods on NASH development. Therefore, an important aspect of this study was to identify an optimum time (8, 16 or 32 weeks) for feeding mice so that the maximum level of inflammation in the fatty liver is ensured.

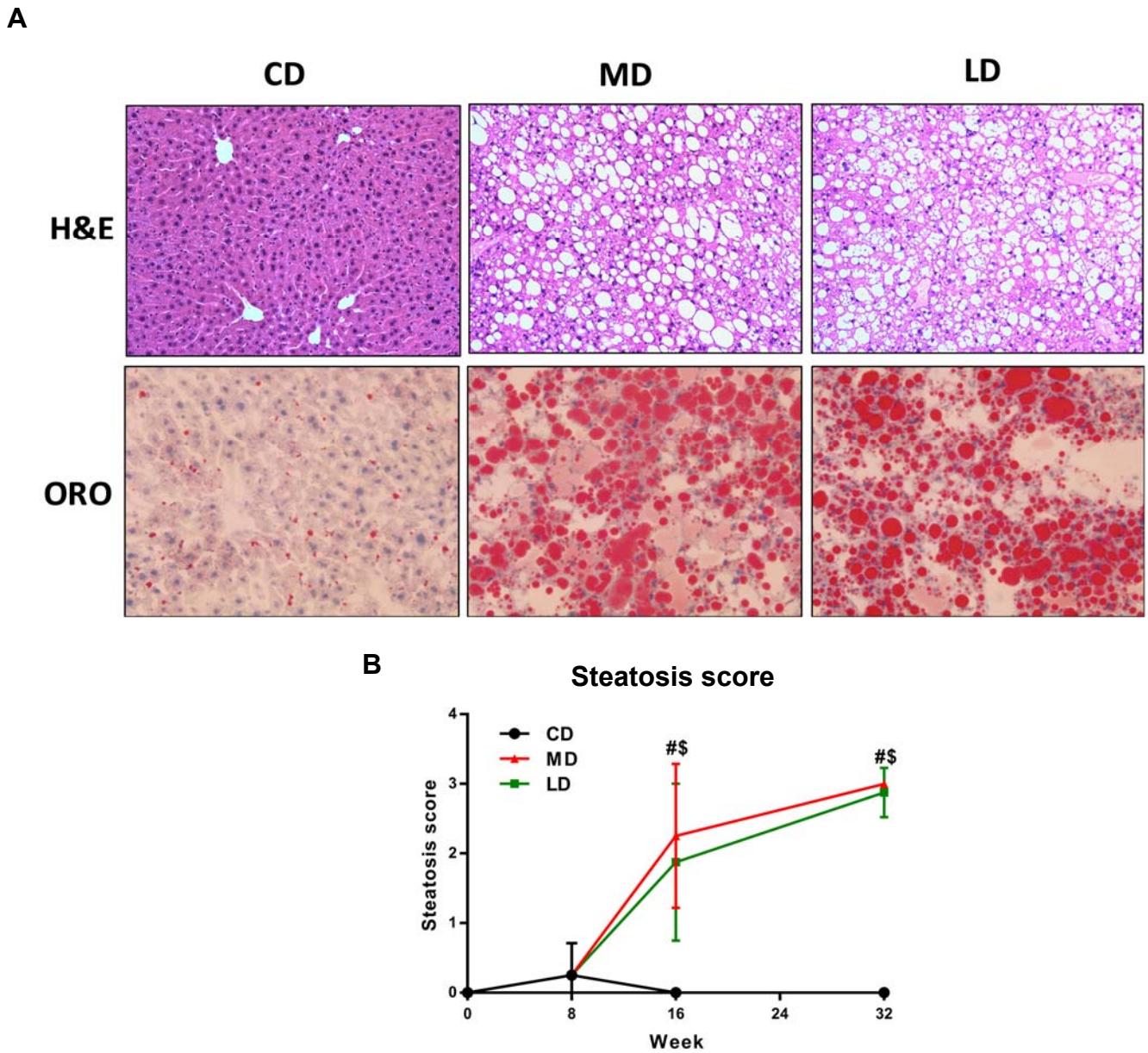
## **Results**

**Both LD and MD led to the development of hepatic steatosis at week 16 and 32, while MD showed a non-significant higher trend than LD**

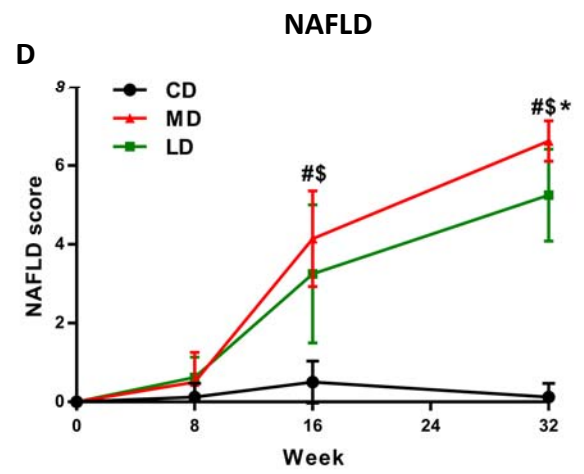
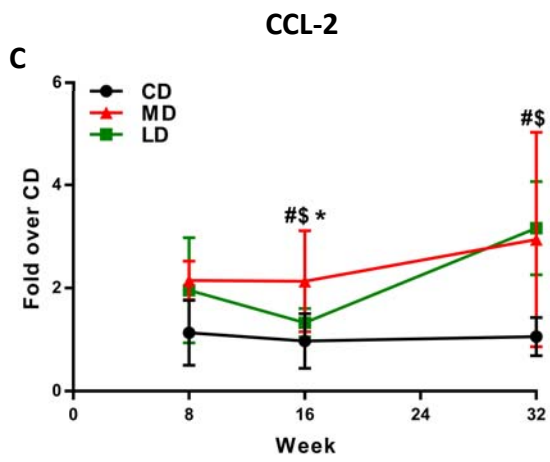
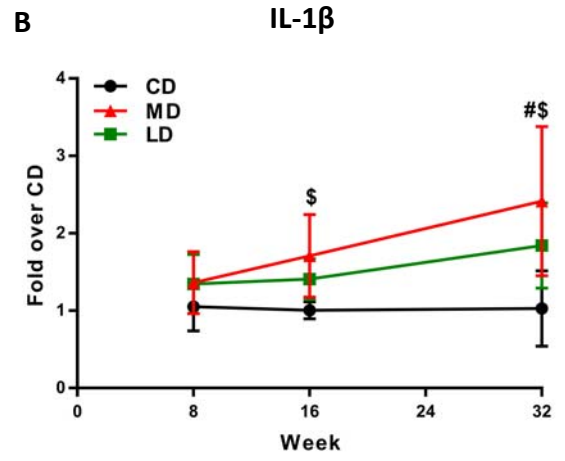
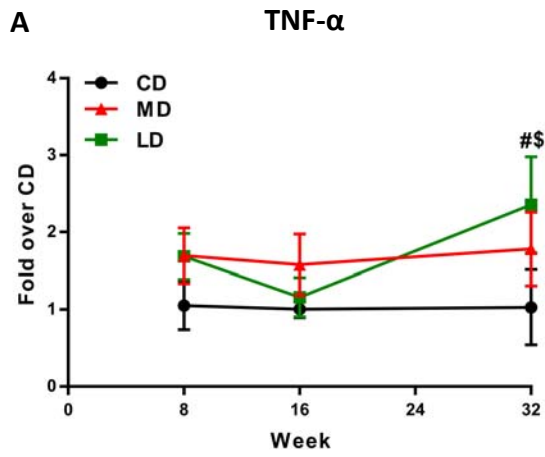
Both of the mice fed LD or MD led to the development of hepatic steatosis at week 16 and 32 (Figure 3.1). Representative images of H&E and ORO stained liver sections clearly displayed massive fat accumulation in the livers of mice fed LD or MD at week 16 (Figure 3.1A). Clinical scores of steatosis reflected higher levels of fat accumulation in the livers of mice fed LD or MD compared to the mice fed CD both at week 16 and 32 (Figure 3.1B). At week 8, there was only a higher trend of fat accumulation in the livers of mice LD or MD compared to the mice fed CD. When compared between LD and MD, mice fed MD showed higher trends of steatosis score compared to the mice fed LD at week 16 and 32.

**Both LD and MD led to the development of chronic inflammation in the fatty liver, while MD displayed a non-significant higher trend than LD at week 16 and 32**

Both of the mice fed LD or MD showed higher expression of TNF- $\alpha$ , IL-1 $\beta$  and CCL-2, higher levels of NAFLD score, higher infiltration of neutrophils and macrophages, and elevated serum activities of ALT and AST compared to the mice fed CD at week 16 and 32 (Figure 3.2A-H). At week 8, both of the mice fed LD or MD showed only higher trend of NASH indicators compared to the mice fed CD. When compared between LD and MD, mice fed MD showed higher trend of these NASH-indicative parameters compared to the mice fed LD at week 16 or 32.



**Figure 3.1. Consumption of unsaturated or saturated high fat diet led to hepatic steatosis both at week 16 and 32.** Mice fed either a lard-based unsaturated or milk-based saturated high fat diet for 16 or 32 weeks responded with fat accumulation in their livers as shown by the representative images of **(A)** H&E and ORO stained liver sections (at 16 weeks) and **(B)** clinical score of steatosis. CD, LD, and MD denote control diet, lard-based unsaturated and milk-based saturated high fat diet, respectively. # indicates significant difference between CD and LD when  $P < 0.05$ , \$ indicates significant difference between CD and MD when  $P < 0.05$ ; data are expressed as mean  $\pm$  SEM;  $n = 6-8$  (Man-Whitney test).



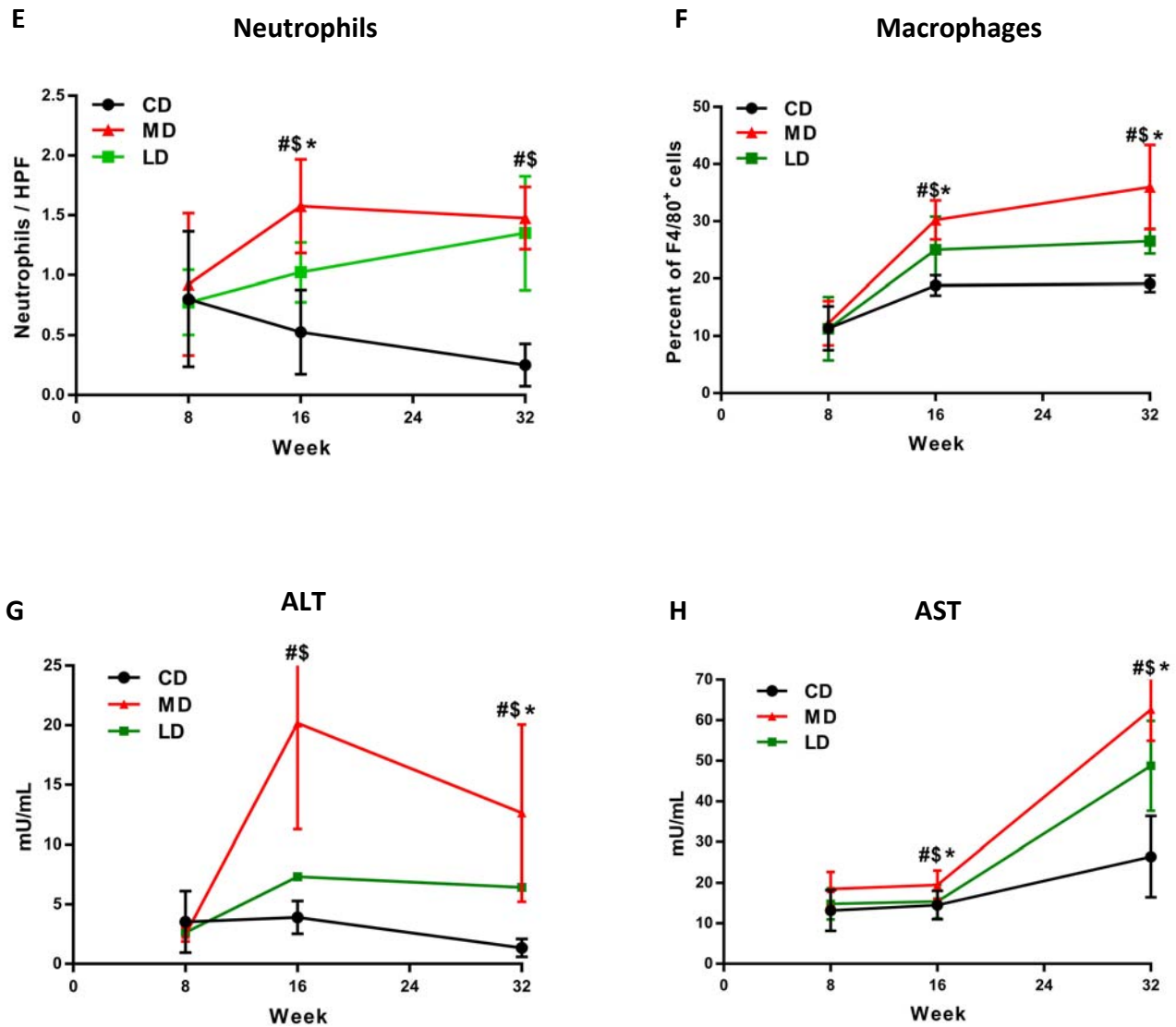


**Figure 3.2. Feeding with unsaturated or saturated high fat diet led to the development of NASH both at week 16 and 32.** Mice fed either a lard-based unsaturated or milk-based saturated high fat diet for 16 or 32 weeks resulted in the development of NASH as indicated by the higher expression of (A) TNF- $\alpha$ , (B) IL-1 $\beta$  and (C) CCL-2, (D) higher levels of NAFLD score, higher infiltration of (E) neutrophil and (F) macrophages and higher serum activities of (G) ALT and (H) AST. CD, LD, and MD denote control diet, lard-based unsaturated and milk-based saturated high fat diet, respectively. # indicates significant difference between CD and LD when  $P < 0.05$ , \$ indicates significant difference between CD and MD when  $P < 0.05$ , \* indicates significant difference between LD and MD when  $P < 0.05$ ; data are expressed as mean  $\pm$  SEM;  $n = 6-8$  (Man-Whitney test).

**Mice fed LD or MD both showed the indication of fibrosis in the fatty liver, yet feeding with MD showed a higher level of expression of TGF- $\beta$  than feeding with LD**

Mice fed LD or MD both showed higher levels of indicators of fibrosis in their livers compared to the mice fed CD. Representative images of picrosirius red stained liver sections of mice fed LD or MD at week 16 displayed higher levels of collagen accumulation compared to the mice fed CD (Figure 3.3A). Mice fed LD or MD showed higher levels of expression Col-1a and TGF- $\beta$  in their livers compared to the mice fed CD at week 16 and 32 (Figure 3.3B-C). Mice fed MD showed significantly higher level of expression of TGF- $\beta$  compared to the mice fed LD at week 16 (Figure 3.3B-C).

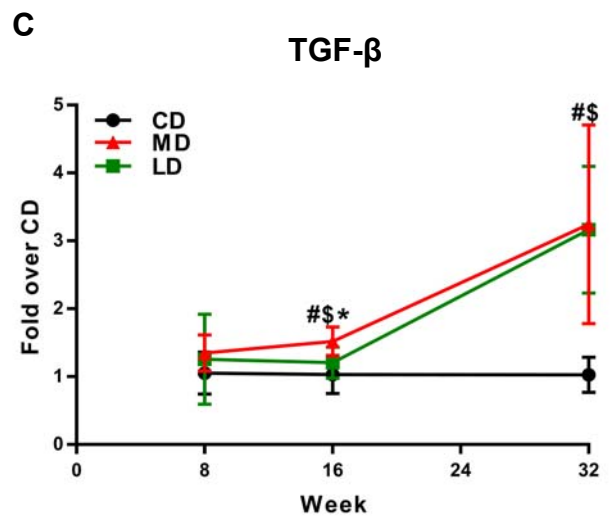
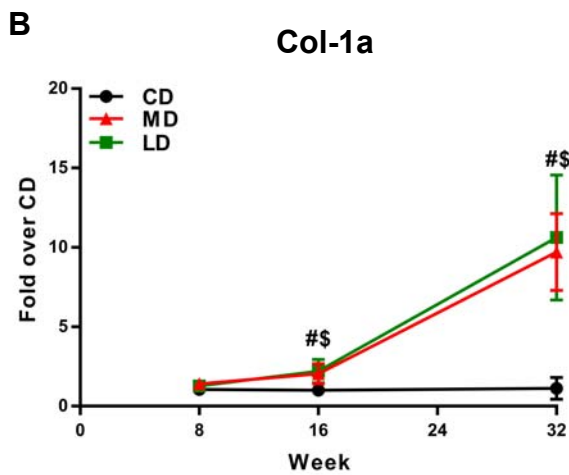
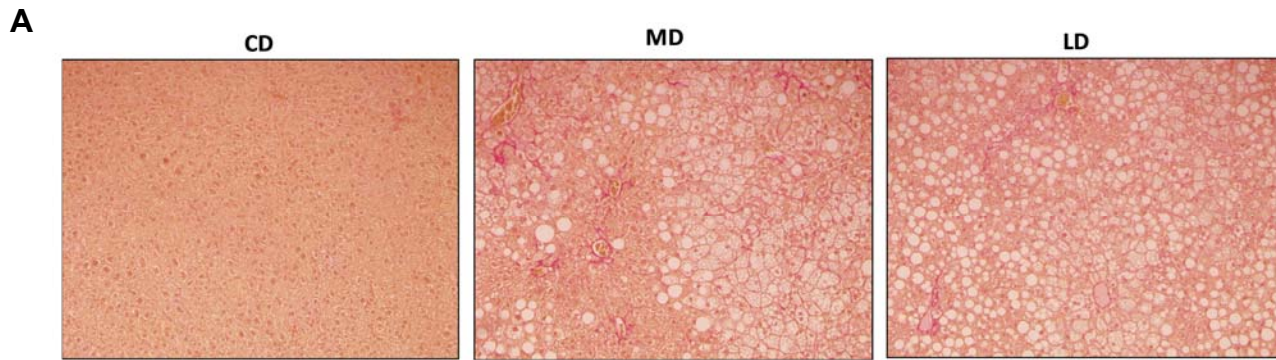


**Figure 3.3. Mice fed unsaturated or saturated high fat diet showed the indication of fibrosis both at week 16 and 32.** Mice fed either a lard-based unsaturated or milk-based saturated high fat diet for 16 or 32 weeks resulted in the accumulation of collagen in their livers as shown by the representative images of **(A)** picrosirius red stained liver sections (at 16 weeks) and higher levels of expression of **(B)** col-1a and **(C)** TGF- $\beta$ . CD, LD, and MD denote control diet, lard-based unsaturated and milk-based saturated high fat diet, respectively. # indicates significant difference between CD and LD when  $P < 0.05$ , \$ indicates significant difference between CD and MD when  $P < 0.05$ , \* indicates significant difference, between LD and MD when  $P < 0.05$ ; data are expressed as mean  $\pm$  SEM;  $n = 6-8$  (Man-Whitney test).

## **Discussion**

To investigate the pathogenesis of NASH, it is essential to have a model appropriately mimicking the disease in human. In compared to the genetic models, induction of NASH in obesogenic high fat diet-fed mice does not associate any genetic defects or pathological feature not observed in clinical paradigm of NASH [150, 165, 166]. Therefore, a high fat diet model is considered as the clinically most relevant model of NASH. Although high fat diets are widely used for NASH research, different pathological aspects of NASH in humans are poorly reflected in this model. For instance, fibrosis is a very common phenomenon in patients with NASH. Around 40% of NASH patients have advanced stages of fibrosis in their livers [167]. However, mice fed a high fat diet develop a very poor level of fibrosis, which is a major obstacle to study fibrosis in NASH using this model [168]. In the current study, mice fed a high fat diet for 16 or 32 weeks resulted in increased expression of col-1a and a pro-fibrotic cytokine TGF- $\beta$ , and higher accumulation of collagen indicating an a progression to fibrosis. Other indicators of NASH, e.g. higher expression of pro-inflammatory cytokines, immune infiltrations, and hepatocyte damage as reflected in higher serum ALT/AST level, were clearly manifested in mice fed either an unsaturated or saturated high fat diet.

When compared the mice fed LD and MD, we detected a higher trend (although statistically non-significant) of NASH-indicative markers in mice fed MD compared to the mice fed LD at week 16. Notably, differences between the mice fed LD and MD became less prominent at week 32. This might be due to the maximum impacts of either types of diets on NASH, resulting in a level of saturation. The higher level of inflammation in the livers of mice fed MD compared to the mice fed LD could be attributed to the higher

amount of saturated fatty acids in MD [164, 169]. Pro-inflammatory mechanisms of saturated fatty acids have been explained in different reports. Excess free fatty acids, released from the lipolysis of subcutaneous and visceral adipose tissues, enter the liver. Upon entering the liver, free fatty acids are disposed through  $\beta$ -oxidation, triglyceride, and phospholipid synthesis. Mitochondrial  $\beta$ -oxidation leads to the gradual break down of the fatty acids into two-carbon acetyl-coA which enters the tricarboxylic acid cycle. Excess free fatty acids can also be disposed by esterification into triglycerides and phospholipids. In the case of excess level of saturated free fatty acids, higher amounts of saturated fatty acids are channeled to the esterification of phospholipids than to the esterification of triglycerides or  $\beta$ -oxidation. Abnormal saturation of phospholipids can compromise the membrane fluidity of endoplasmic reticulum leading to impaired protein folding and trafficking which eventually results in endoplasmic reticulum stress through unfolded protein signaling pathway [164, 170-172].

In compared to unsaturated fatty acids, saturated fatty acids are used for the synthesis of toxic molecules. For instance, condensation of palmitate (16:0 saturated fatty acid) and serine leads to the synthesis of ceramide, a toxic lipid molecule [173, 174]. Accumulation of ceramides in mitochondrial membrane results in an increased permeability resulting in cytochrome c release, that eventually induces apoptosis [175]. Increased accumulation of ceramides in sphingolipid-rich lipid rafts of plasma membrane drives the coalescence of lipid rafts into larger platforms, which facilitate the apoptotic signaling by clustering membrane receptors and signaling molecules [176-179]. Saturated fatty acid-derived ceramide can also directly interact with the pro-enzyme cathepsin D and induce its autolytic cleavage releasing the active components of

cathepsin D, which mediates the cleavage and activation of pro-apoptotic Bcl-2 family member Bid [180, 181].

Another important difference between unsaturated and saturated fatty acids is that saturated fatty acids can induce inflammation through the direct interaction with, and activation of TLR-4 [182-184]. Saturated fatty acids are essential component of endotoxins. Human TLR-4 can sense only the endotoxins containing lipid-A portion acylated with six saturated fatty acids (usually 12-16 carbons in length). It has been shown that replacement of these saturated fatty acids with monounsaturated or polyunsaturated fatty acids halts the pro-inflammatory effects of lipopolysaccharides [184, 185]. From the inflammatory point of view, saturated fatty acids can also induce the expression of cyclooxygenase-2 through an NF- $\kappa$ B-dependent activation of macrophages [183]. Cyclooxygenase enzymes catalyze the synthesis of prostaglandins and thromboxanes, which are important mediators of different aspects of inflammation, e.g. vasodilation, leukocyte migration etc. [184, 186-188]. Therefore, it is possible that saturated fatty acids leads to the production of these mediators inducing pro-inflammatory immune infiltration in the fatty liver.

Both LD and MD contain unsaturated and saturated fatty acids of different lengths and saturation types/levels, but the levels of saturated fatty acids, particularly the toxic ones like palmitic, stearic, and lauric acids, are higher in MD compared to LD [184, 189-191]. Because of the higher pro-inflammatory roles of saturated fatty acids over unsaturated fatty acids, as reflected in the higher trends of NASH-indicative markers in mice fed MD versus the mice fed LD, we chose MD to induce NASH in mice for the experiments reported herein.

# Chapter 4

High Fat Diet-mediated Nonalcoholic Steatohepatitis Impairs Hepatic  
Regeneration Following Partial Hepatectomy

## **Summary**

Although surgical resection of part of the liver (partial hepatectomy) is a well-recognized treatment option for hepatocellular carcinoma, pre-existing pathological abnormalities originating from fat-rich diet mediated steatosis can alter the postoperative outcomes. Despite the well-established effect of NASH in liver, little is known about the impact of fat-rich diet on the ability of the liver to regenerate. In this study, we investigated the impact of both saturated and unsaturated fat-rich diet on liver regeneration following partial hepatectomy in C57BL/6 mice. Six week-old mice were fed control diet (CD), Lard-based unsaturated fat-rich diet (LD) or milk-based saturated fat-rich diet (MD) for 16 weeks. Partial hepatectomy (70% of the liver) was carried out at 16 weeks. At day 2 and at day 7 post partial hepatectomy, mice were injected with 5-bromo-2'-deoxyuridine (BrdU) i.p., one hour prior to euthanization to analyze hepatic regeneration. Samples were collected from the resected and regenerated liver and examined for inflammation-indicative markers and histological analyses. Mice fed LD or MD exhibited higher nonalcoholic fatty liver disease (NAFLD) score, levels of inflammatory cytokines, and infiltration of neutrophil and macrophage in both resected and regenerated livers compared to mice fed CD. Mice fed LD or MD resulted in decreased BrdU incorporation in their resected and regenerated livers compared to the mice fed CD. Our study demonstrated the impaired hepatic regeneration post partial hepatectomy of mice fed LD or MD compared to that of mice fed CD. Importantly, mice fed MD demonstrated reduced regeneration compared to the mice fed LD. Collectively, this study illustrates the significance of fat and type of fat type in impairing hepatic regeneration following partial hepatectomy.

## **Introduction**

The liver has a unique ability to regenerate, even when mature, following a toxic insult or partial hepatectomy (PHx) [192, 193]. In spite of its substantial metabolic role, the liver is a quiescent organ in terms of hepatocyte proliferation. Although hepatocytes undergo a very low rate of proliferation under normal conditions, they can reach a dramatically high proliferation rate within the acinar architecture of the remnant liver following a surgical resection leading to total recovery of the organ within 2-6 weeks [194]. As a result of this ability to regenerate, surgical resection is often considered a viable treatment option for end stage liver diseases including liver cirrhosis or hepatocellular carcinoma [195, 196]. Although surgical resection of part of the liver (PHx) is considered a viable treatment option for patients with end-stage liver diseases, post-resection regeneration capacity is of major concern. Therefore, it is important to have a clear understanding of the effect that pre-existing steatosis or NASH have on the hepatic regeneration following PHx.

Although the role of a high fat diet in causing an impairment of hepatic regeneration following PHx in mice has been reported [142], it is still not clear how differently NASH, induced by either unsaturated or saturated high fat diet, may impact hepatic regeneration following PHx. This study assessed the ability of a lard-based unsaturated high fat diet (LD) and a milk-based, saturated fat rich diet (MD) in conferring an impairment to the livers of mice to regenerate following a PHx. The findings here may influence the decision to perform and/or post-operative management of patients being considered for PHx surgery.

## **Results**

### **Mice fed LD or MD led to the development of NASH in both resected and regenerated livers**

Levels of expression of TNF- $\alpha$ , IL-1 $\beta$ , TGF- $\beta$ , and CCL-2 were increased in both of the resected and regenerated livers of mice fed either LD or MD compared to the mice fed CD (Figure 4.1A-D). Hepatic infiltrations of neutrophils and F4/80<sup>+</sup> macrophages were increased in both of the resected and regenerated livers of mice fed either LD or MD compared to the mice fed CD (Figure 4.1E-F). Each of these NASH indicators clearly demonstrated the development of NASH in the resected and regenerated livers of mice fed LD or MD. Noticeably, resected and regenerated livers of mice fed the MD trended to exhibit higher levels of expression of inflammatory cytokines (Figure 4.1A-D) and infiltration of neutrophils and macrophages (Figure 4.1E-F) compared to the levels observed in mice fed the LD.

### **Both LD and MD caused damage in resected and regenerated livers**

Both of the resected and regenerated liver sections from mice fed either LD or MD displayed higher NAFLD scores compared to the mice fed CD (Figure 4.2A). Liver sections from the mice fed MD trended to have higher NAFLD scores compared to the mice fed LD (Figure 4.2A). Sera from mice fed LD or MD showed increased levels of ALT (Figure 4.2B) and AST (Figure 4.2C) both on day-2 or day-7 compared to the mice fed CD. This indicated higher levels of liver damage in the mice fed unsaturated or saturated high fat diets. When compared between the mice fed LD and MD, sera from

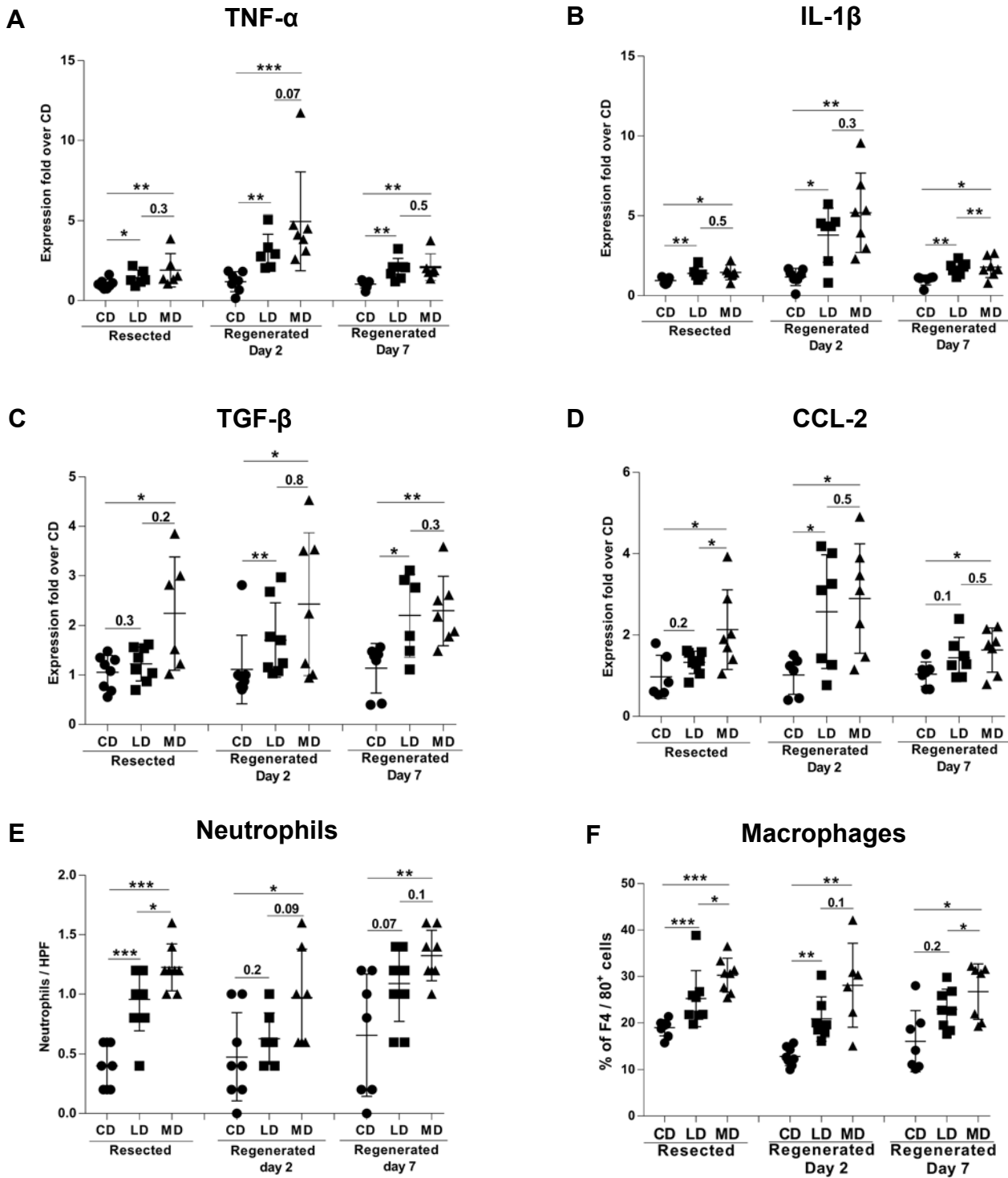


**Figure 4.1. Unsaturated or saturated high fat diet led to the development of NASH in both resected and regenerated livers.** Both of the lard-based unsaturated and milk-based saturated high fat diet resulted in the development of NASH as evidenced by increased expression of pro-inflammatory cytokines: **(A)** TNF- $\alpha$ , **(B)** IL-1 $\beta$ , **(C)** TGF- $\beta$  and **(D)** CCL-2; increased infiltration of **(E)** neutrophils and **(F)** macrophages. CD, LD, and MD denote control diet, lard-based unsaturated and milk-based saturated high fat diet, respectively. \*P<0.05, \*\*P<0.01, \*\*\*P<0.001 (Man-Whitney test); data are expressed as mean $\pm$ SEM; n=6-8.

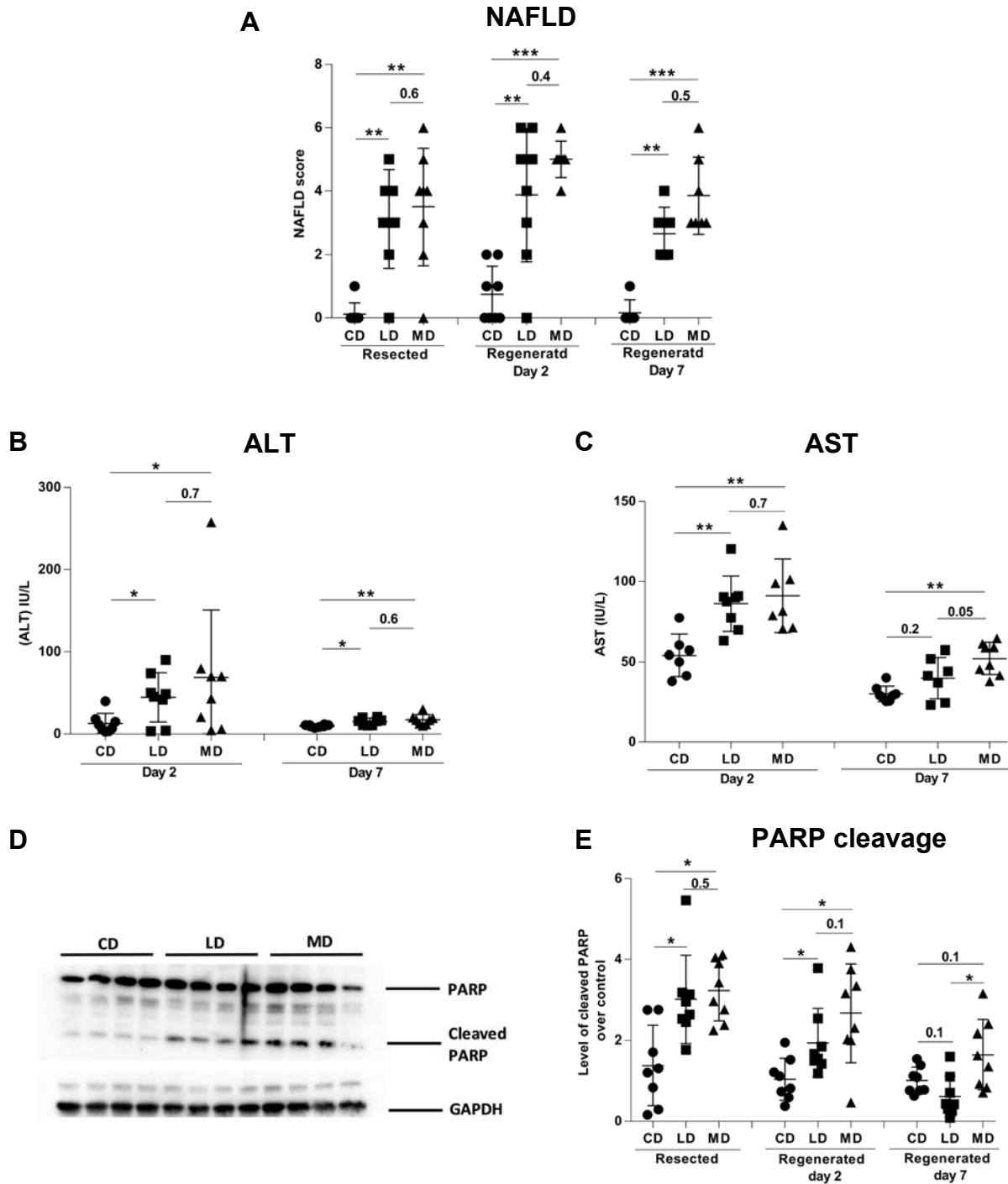


**Figure 4.2. Unsaturated or saturated high fat diet resulted in liver damage in both resected and regenerated livers.** Unsaturated or saturated high fat diet resulted in **(A)** higher NAFLD scores and elevated level of serum **(B)** ALT and **(C)** AST. **(D)** Western blot images demonstrated higher level of cleavage of poly ADP-ribose polymerase (PARP) in the livers of mice fed unsaturated or saturated high fat diet (shown regenerated day-2) **(E)** Densitometry analyses of immunoblots exhibited increased level of cleavage of PARP in resected and regenerated livers of mice fed unsaturated or saturated high fat diet. CD, LD, and MD denote control diet, lard-based unsaturated and milk-based saturated high fat diet, respectively. \* $P < 0.05$ , \*\* $P < 0.01$ , \*\*\* $P < 0.001$  (Man-Whitney test); data are expressed as mean  $\pm$  SEM;  $n = 6-8$ .

the mice fed MD showed a higher trend of ALT and AST levels both on day-2 and day-7 compared to the mice fed LD.

Apoptosis resulting from the NASH-mediated hepatic tissue injury was determined by comparing the level of cleaved poly ADP-ribose polymerase (PARP). Both resected and regenerated tissues on day-2 or day-7 from the mice fed MD showed an increased level of cleaved PARP compared to the mice fed CD (Figure 4.2D-E). Mice fed LD showed an increased level of cleaved PARP in the tissues from the resected and regenerated day-2 livers compared to the mice fed CD (Figure 4.2E). However, mice fed MD displayed a higher trend of PARP cleavage compared to the mice fed LD in both resected and regenerated livers on day-2 and day-7 (Figure 4.2E).

#### **NASH-affected livers of mice fed MD or LD demonstrated impaired regeneration following partial hepatectomy (PHx)**

Percentage of BrdU-incorporated hepatocytes was determined in regenerated liver sections on day-2 and day-7 in order to assess the effect of NASH on hepatic regeneration following partial hepatectomy. The percentage of BrdU-incorporated hepatocytes was 2.2 and 5.2 fold lower in the regenerated liver sections of mice fed LD or MD respectively compared to that of the regenerated liver sections of mice fed CD on day-2 (Figure 4.3A). These data demonstrate the impaired hepatic regeneration in mice fed fat-rich diet of either types compared to the mice fed control diet. Of note, percentage of BrdU-incorporated hepatocytes was 2.3-fold lower in mice fed MD compared to the mice fed LD. This observation was consistent with the higher trending indicators of NASH (Figure 2.1), hepatic damage (Figure 4.2A-C) and apoptosis (Figure 4.3D-E) in the livers of the mice fed MD when compared to the livers of mice fed LD. Because hepatic

regeneration following PHx reached the level of saturation by day-7 [197], no significant difference in BrdU incorporation was observed at day-7. However, the percentage of BrdU-incorporated hepatocytes trended to be lower in the livers of mice fed LD or MD compared to that incorporated into the livers of mice fed CD.

Regenerated liver output was measured as the ratio of regenerated liver-to-total body weight (Figure 4.3B) or regenerated liver-to-resected liver weight (Figure 4.3C). In either cases, ratios were lower in mice fed LD or MD compared to those of mice fed CD on day-7. Regenerated livers from the mice fed LD or MD showed a 1.3 and 1.2-fold reductions to regenerated liver-to-body weight ratios, respectively compared to the mice fed CD (Figure 4.3B). Regenerated livers from the mice fed LD or MD were found to have 1.7 and 1.6 fold reduction in their regenerated liver-to-resected liver weight ratio respectively compared to the mice fed control diet (Figure 4.3C). These data again corroborated the impaired regeneration of NASH-affected livers following PHx.

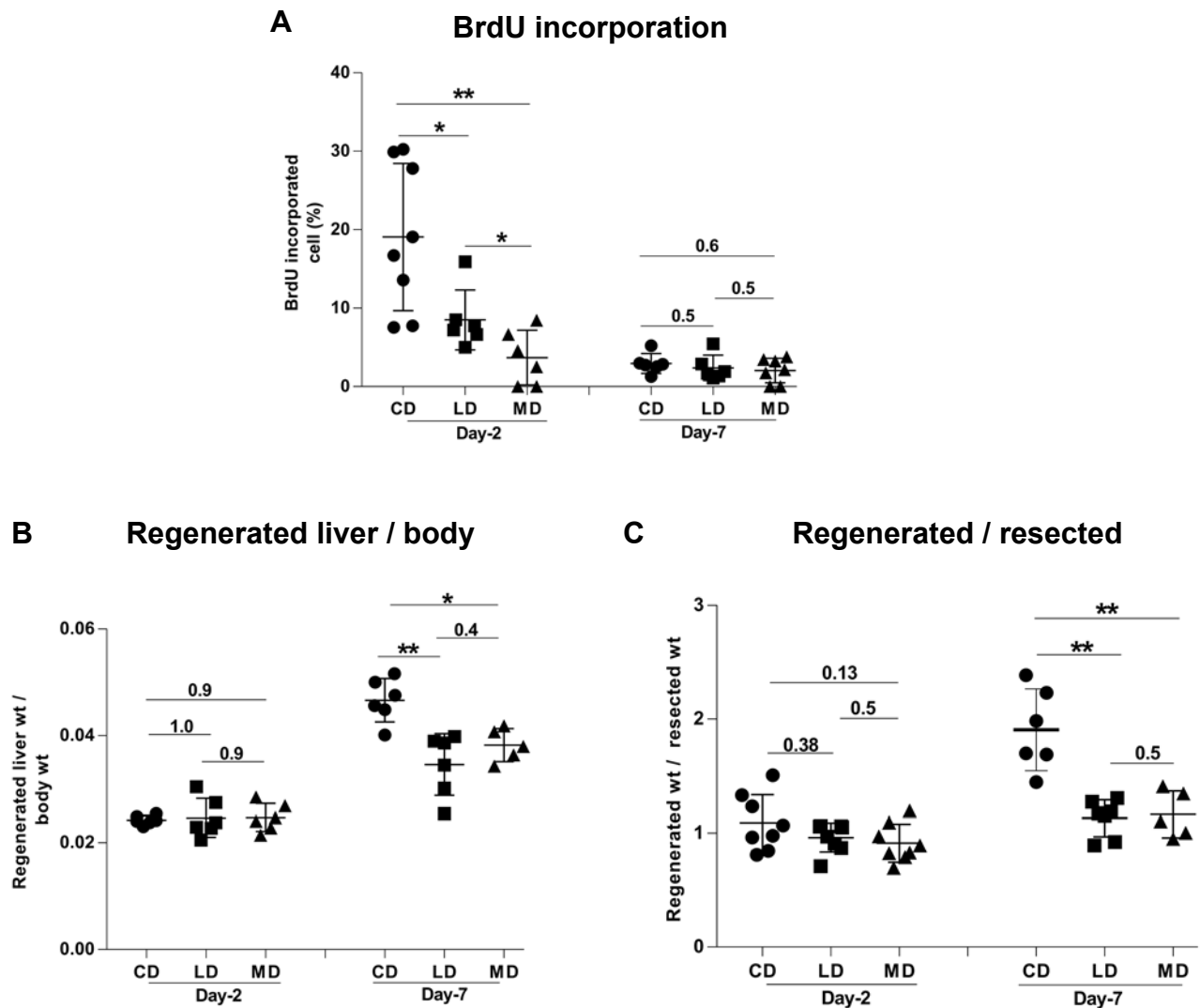


**Figure 4.3. Hepatic regeneration following partial hepatectomy was impaired in mice fed unsaturated or saturated high fat diet.** NASH induced through the consumption of high fat diets resulted in impaired regeneration of partially resected livers as evidenced by (A) reduced rates of BrdU incorporation in hepatocytes, decreased (B) regenerated liver/body ratio and (C) regenerated liver/resected liver ratio. CD, LD, and MD denote control diet, lard-based unsaturated and milk-based saturated high fat diet, respectively. \* $P < 0.05$ , \*\* $P < 0.01$  (Man-Whitney test); data are expressed as mean  $\pm$  SEM;  $n = 6-8$ .

## **Discussion**

NASH is presently the third most common cause of end stage liver diseases necessitating transplantation. If current trends continue, NASH is anticipated to surpass hepatitis C as the dominant cause of liver failure and will likely increase the rate of hepatocellular carcinoma (HCC) [23, 198]. Although liver transplantation has opened a new avenue for the treatment of HCC, the benefit of this treatment is limited mainly by shortage of available grafts and also long-term complications such as immunosuppression-related infections, risk of tumor progression etc. Therefore, PHx is still considered as the most viable treatment for HCC [199]. Because of the co-existence of NASH and HCC in a large number of patients [200, 201], it is important to investigate how the presence of NASH would affect hepatic regeneration in these patients following PHx. Absence of an appropriate animal model that effectively mimics the genesis of human NASH represents a barrier in being able to appreciate the consequences that NASH has on hepatic regeneration following surgical resection. However, amongst the currently available genetic and dietary models, dietary fat induced NASH is clinically more relevant. Previously, we have shown how employing a model requiring significant exposure to a fat-rich diet was sufficient to induce and then mimic the complex behavior associated with NASH that closely reflects what occurs in humans [163]. Our current data primarily demonstrates that long-standing hepatic steatosis in mice fed high fat diet leads to NASH and impairs hepatic regeneration following PHx. Comparison between the impacts of unsaturated and saturated dietary fat on hepatic regeneration was an additional aspect of this study. The data collected provided evidence for a trend towards higher levels of expression of pro-inflammatory cytokines, increases in NAFLD score, collagen

accumulation, serum ALT/AST levels and apoptosis in the livers of mice fed MD compared to the mice fed LD indicating an exacerbating role of a diet high in saturated fats in causing NASH. An exacerbation of impairment of hepatic regeneration following PHx in the fatty livers of mice fed MD was consistent with a higher trend of hepatic inflammation and hepatocyte damage compared to the mice fed LD. Such a higher trend of hepatic inflammation can be attributed to aggravated oxidative stress, lipotoxicity, and endoplasmic reticulum stress mediated by the saturated fat [164, 169]. In our study, concentration of serum endotoxin was found to trend higher in mice fed MD compared to the mice fed CD and LD (Chapter 5). Therefore, chronic endotoxemia might also be plausible in offering an explanation for higher inflammation in mice fed MD. Several NASH drugs are now under phase 3 clinical trials. Therefore, it would also be important to test if the treatment of mice with a drug that reverses NASH could improve hepatic regeneration post PHx. Treatment with such drug that suppresses NASH could make the surgical resection a more viable treatment option for end stage liver diseases.

# Chapter 5

Gut Microbiota Plays a Critical Role in Nonalcoholic Steatohepatitis

## **Summary**

Apart from fat accumulation, additional pro-inflammatory insults to the steatotic liver play an important role in the modulation of NASH. The role of gut microbiota has been reported in metabolic syndrome. As NAFLD is the hepatic manifestation of metabolic syndrome, it is important to investigate the role of gut microbiota in the progression of disease from the benign hepatic steatosis to the stage with chronic inflammation. Therefore, this part of our study investigated whether gut microbiota has any influence on the development of NASH. Three specific experiments were accomplished: First, individual groups of specific pathogen free (SPF) mice and germ free (GF) mice were fed a control diet (CD) or a milk based, saturated high fat diet (MD) for 8, 16 or 32 weeks. The resulting decrease in the levels of NASH-indicative markers in GF mice fed MD compared to the SPF mice fed MD indicated the role of gut microbiota in mediating NASH. Second, it was tested if the diminishing of gut microbiota could reduce the level of inflammation in the fatty livers of mice fed MD. In order to do that, individual groups of SPF mice fed CD or MD were treated with broad spectrum antibiotics through drinking water for 16 weeks. Treatment of mice fed MD with broad spectrum antibiotics resulted in a reduced level of NASH-indicative markers in their livers indicating the role of gut microbiota in modulating the dietary fat-mediated NASH. Third, conventionalization of GF mice fed MD by fecal transfer from SPF mice resulted in an increased level of inflammation. These three experiments clearly showed the generalized role of gut microbiota in causing NASH. In addition, 16S rRNA analysis resulted in alteration of relative abundance of specific phyla in mice fed MD, indicating their plausible role in mediating NASH.

## **Introduction**

Gut microbiota that dwell in the gastrointestinal tract consists of 100 trillion bacterial cells that weigh 1-2 kg in mass and possess 100-fold more unique genes than human genome [114, 202]. Gut microbiota play a crucial role in maintaining the normal human physiology and nutrition [65, 203]. Changes in gut microbiota have been shown to be associated with different metabolic and physiological disorders [86, 89, 122, 202, 204, 205]. The evidence supporting the contribution of gut-liver axis to the development of NASH has accumulated over the last twenty years [206]. NASH was first encountered as a complication of jejunio-ileal bypass surgery used for the treatment of morbid obesity [207, 208]. Furthermore, NASH was also reported in case of jejunal diverticulosis and intestinal bacterial overgrowth in human [209, 210]. Experimental evidence about the role of gut microbiota in mediating NASH in animal models is also growing. Initial clues came from the studies of Backhead and colleagues [85, 88]. They showed that germ free (GF) mice fed high fat diet gained less weight compared to the specific pathogen free (SPF) mice fed high fat diet. Conventionalization of GF mice through fecal transfer from SPF mice resulted in an increase in body fat content [88]. Other studies have shown that GF mice fed high fat diet are resistant to hepatic steatosis [211, 212]. One study reported that transfer of gut microbiota from steatotic mice to GF mice can promote the development of high fat diet-induced steatosis [211]. The pathogenic role of intestinal bacteria in causing NASH was also supported by the observation that administration of antibiotics can improve NASH in rat and human [213]. All of these studies suggested the role of gut microbiota in the pathogenesis of NASH. Therefore, in this chapter, comprehensive experiments were designed to demonstrate an obvious involvement of

gut microbiota in mediating high fat diet-induced NASH using both GF and broad spectrum antibiotics-treated mice. The role of gut microbiota in causing NASH was also investigated through the restoration of gut microbiota in GF mice fed milk-based high fat diet (MD). Any change to the population composition of gut microbes in mice fed high fat diet may reveal a taxa-specific role of gut microbiota in mediating NASH. Therefore, 16S rRNA analysis was performed to elucidate a plausible change in the composition of gut microbial community in mice fed MD.

## **Results**

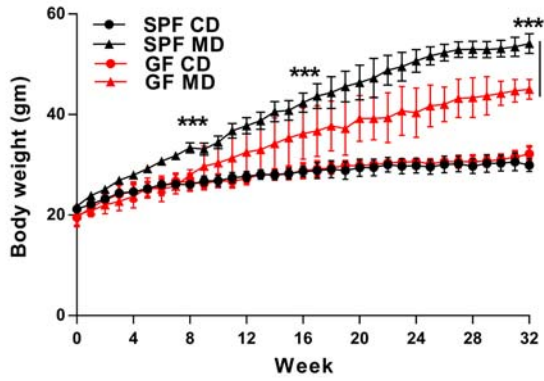
### **GF mice developed less steatosis in their livers compared to the SPF mice**

After feeding with MD, GF mice showed less body weight and percent of body weight increase compared to the SPF mice at week 8, 16 and 32 (Fig. 5.1A-B). GF mice fed MD showed reduced liver weight and liver-to-body weight ratio compared to the SPF mice fed MD at week 32 (Fig. 5.1C-D). H&E staining of the liver sections (Fig. 5.1E) and clinical scores of steatosis (Fig. 5.1F) displayed a lower trend of fat accumulation in the livers of GF mice fed MD compared to the SPF mice fed MD at week 16 and 32. These data indicate the role of gut microbiota in mediating hepatic steatosis.

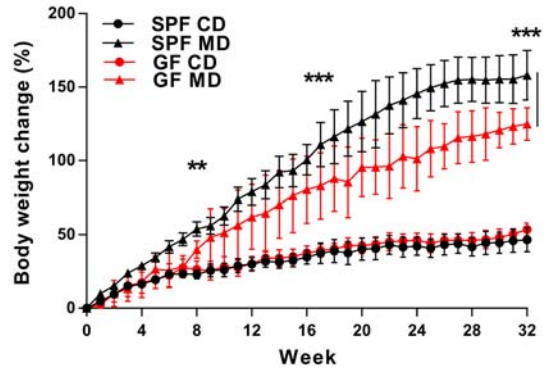
### **Steatotic livers in GF mice were resistant to NASH**

To investigate the development of inflammation in steatotic livers, levels of different NASH-indicative markers were analyzed. Expression levels of TNF- $\alpha$ , IL-1 $\beta$ , CCL-2 and TGF- $\beta$  (Fig. 5.2A-D) and infiltration of neutrophils and macrophages (Fig. 5.2E-F) in the livers of GF mice fed MD failed to show any increase compared to the GF mice fed CD at any time point. On the other hand, SPF mice fed MD showed significant increases of expression of TNF- $\alpha$ , IL-1 $\beta$ , CCL-2 and TGF- $\beta$  (Fig. 5.2A-D) and infiltration of neutrophils and macrophages (Fig. 5.2E-F) compared to the GF mice fed MD at week 16 and 32. Although there was an increase of NAFLD score in GF mice fed MD compared to the GF mice fed CD at week 16 and 32 (Fig. 5.2G), it was significantly lower (approximately 1.3 to 2-fold) than the SPF mice fed MD. These data demonstrate that the steatotic livers in GF mice fed MD are protected from NASH, thus indicating the role of gut microbiota in the progression of NASH from the normal steatosis to an inflammatory stage.

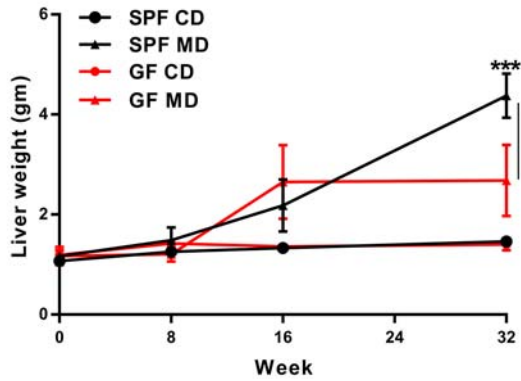
**A** Body weight



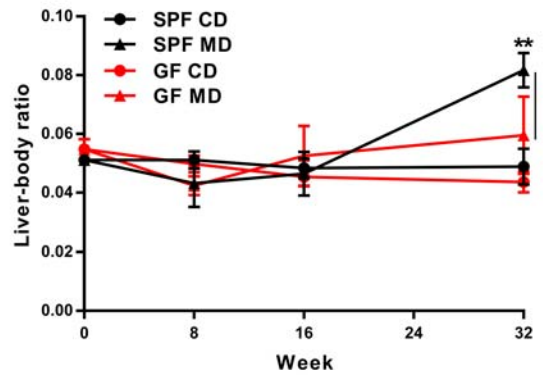
**B** Body weight change

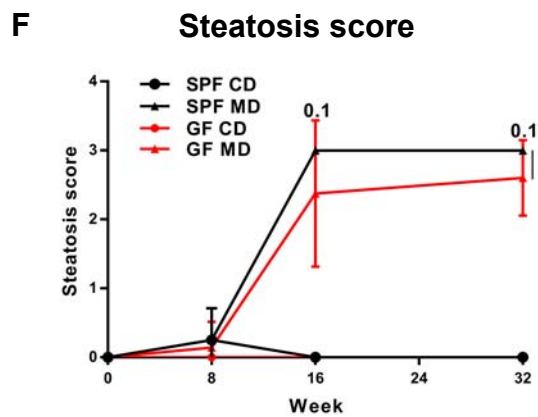
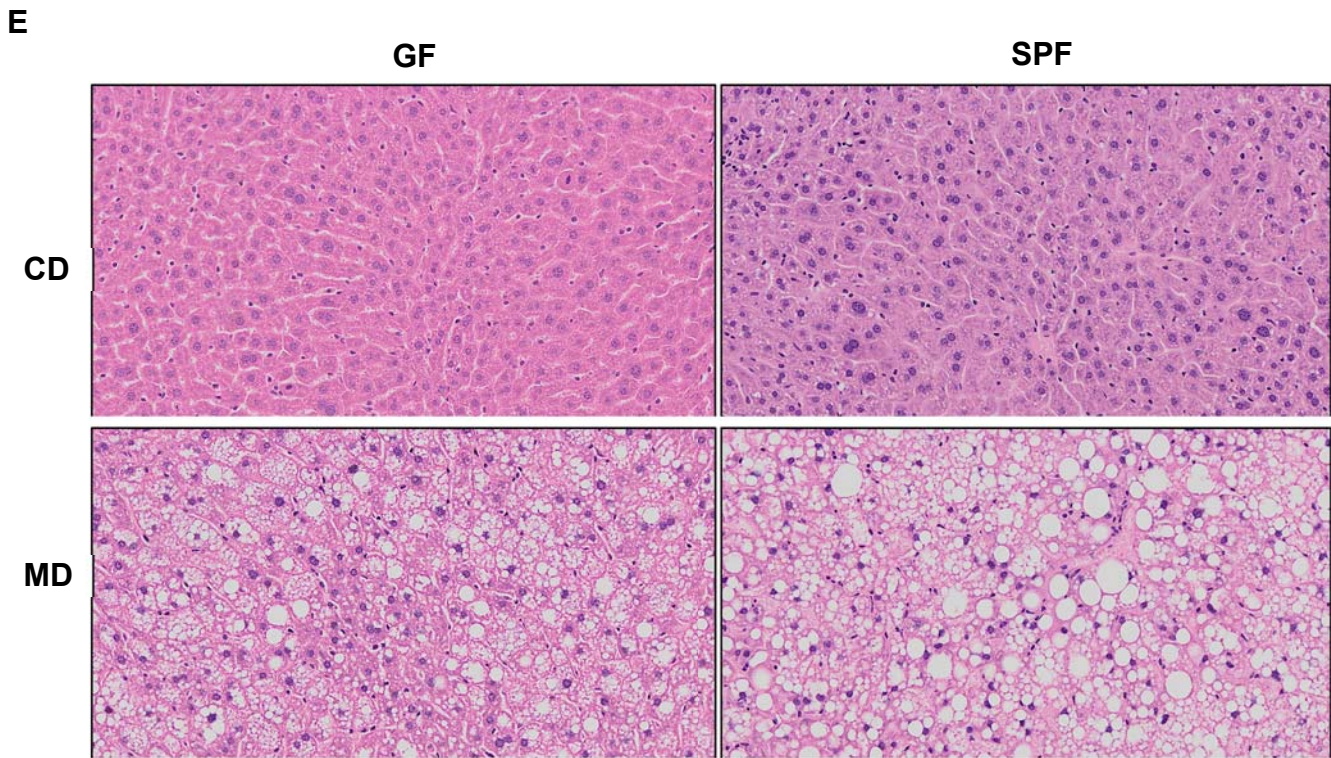


**C** Liver weight

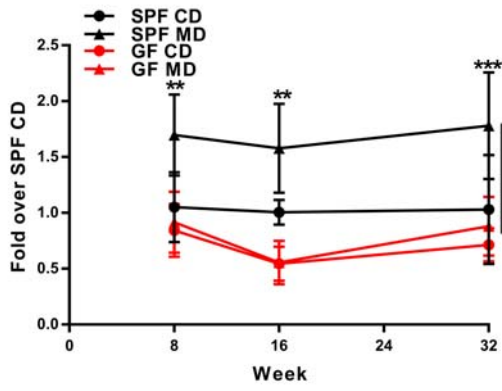
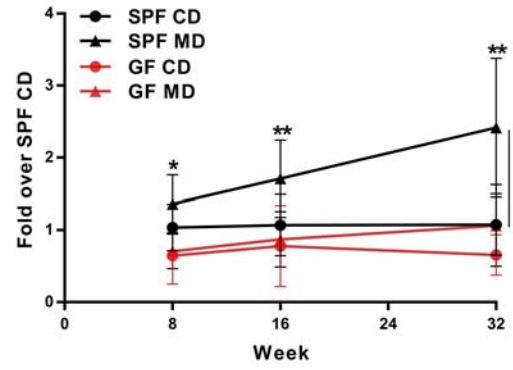
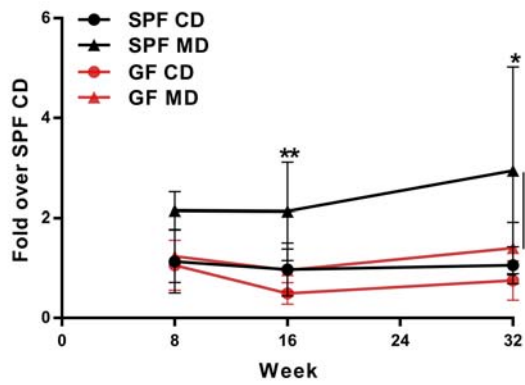
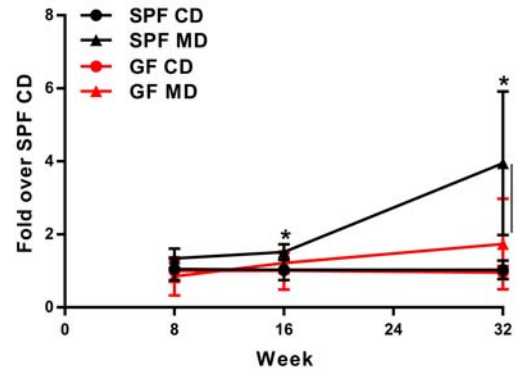


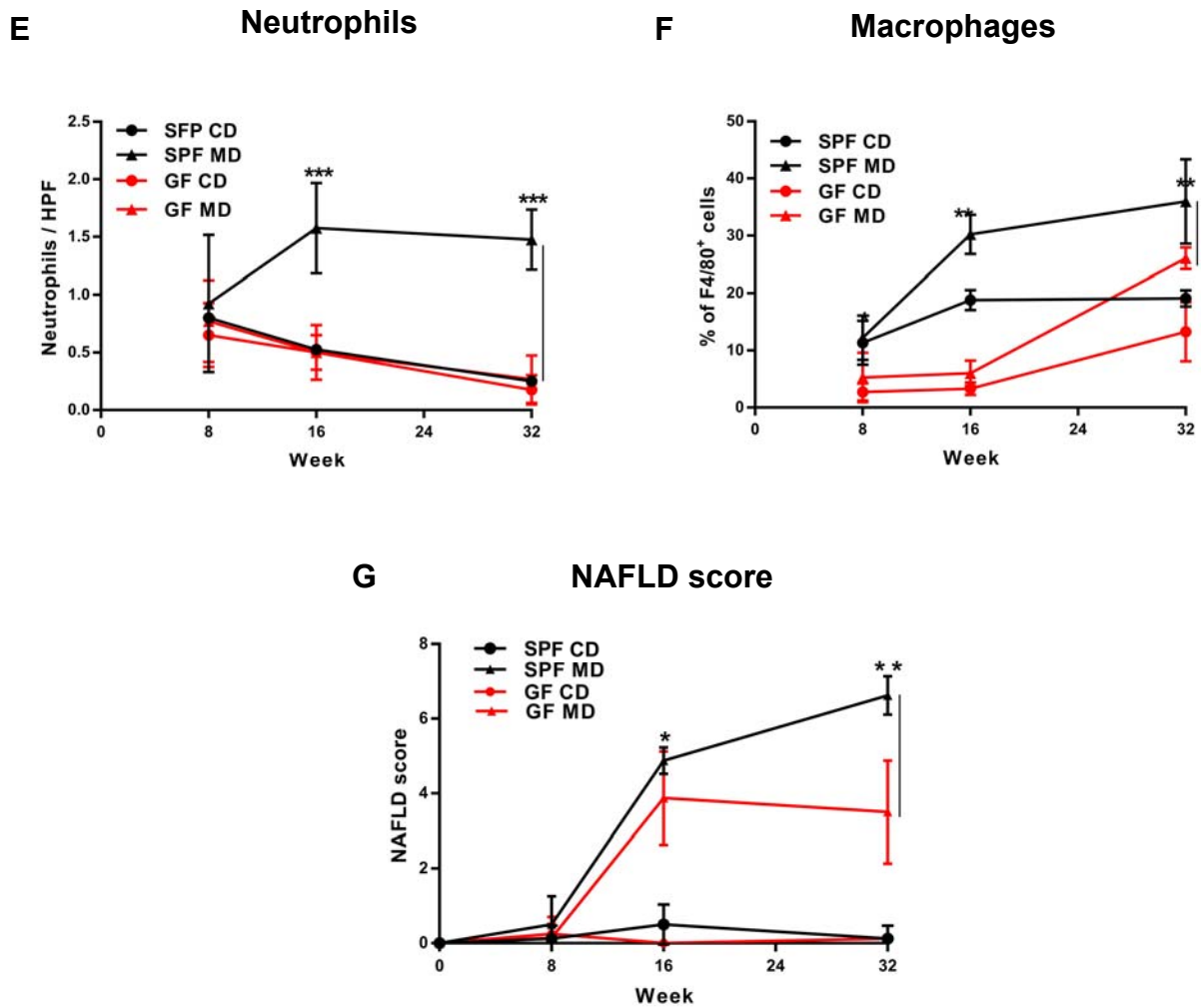
**D** Liver / body





**Figure 5.1. Germ free mice fed high fat diet developed less hepatic steatosis compared to the specific pathogen free mice.** Feeding with high fat diet resulted in less (A) body weight, (B) body weight change, (C) livers weight and (D) liver-to-body weight ratio in germ free mice compared to the specific pathogen free mice. Less steatosis was observed in the livers of germ free mice fed high fat diet compared to the specific pathogen free mice fed high fat diet as shown by the (E) representative images of H&E stained liver sections (at 16 weeks) and (F) steatosis score. GF, SPF, CD and MD denote germ free mice, specific pathogen free mice, control diet and milk-based high fat diet, respectively. \* $P < 0.05$ , \*\* $P < 0.01$ , \*\*\* $P < 0.001$  (Man-Whitney test); data are expressed as mean  $\pm$  SEM;  $n = 6-8$ .

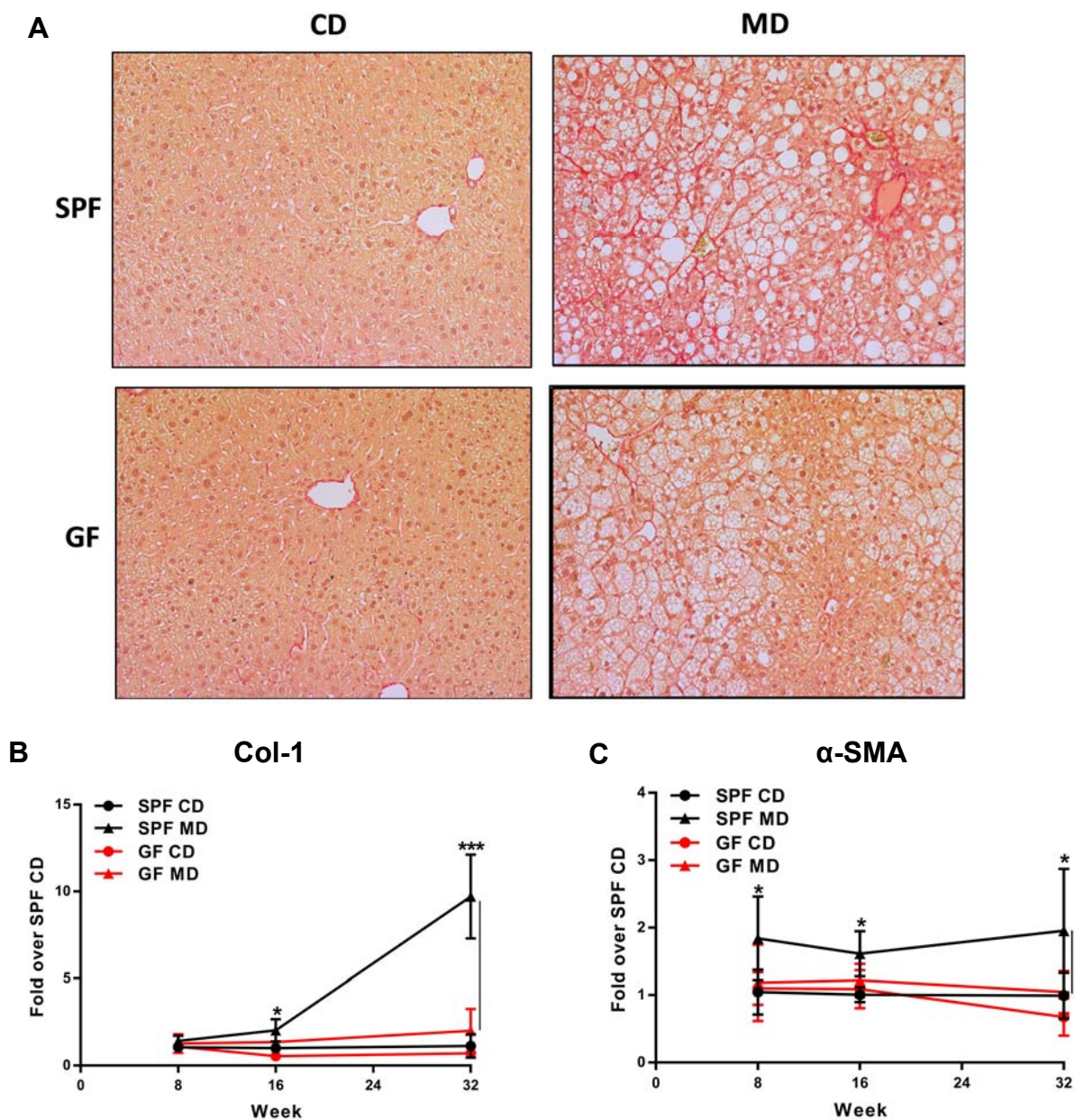
**A****TNF- $\alpha$** **B****IL-1 $\beta$** **C****CCL-2****D****TGF- $\beta$** 



**Figure 5.2. Germ free mice fed high fat diet showed lower levels of NASH-indicative markers in their livers compared to the specific pathogen free mice fed high fat diet.** Germ mice fed high fat diet showed lower levels of (A-D) expression of TNF- $\alpha$ , IL-1 $\beta$ , CCL-2 and TGF- $\beta$ , (E-F) infiltration of neutrophils and macrophages, and (G) NAFLD score in their livers compared to the specific pathogen free mice fed high fat diet. GF, SPF, CD and MD denote germ free mice, specific pathogen free mice, control diet and milk-based high fat diet, respectively. \*P<0.05, \*\*P<0.01, \*\*\*P<0.001 (Man-Whitney test); data are expressed as mean $\pm$ SEM; n=6-8.

**GF mice fed MD had decreased level of collagen accumulation in their livers compared to the SPF mice fed MD**

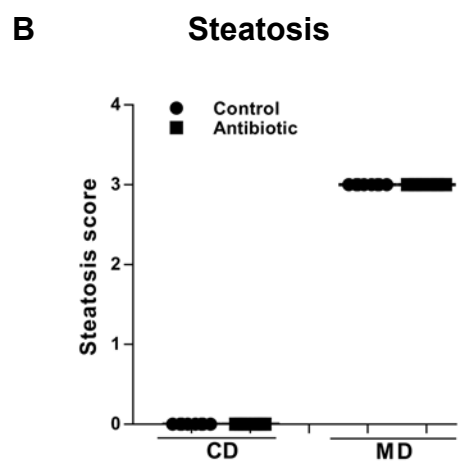
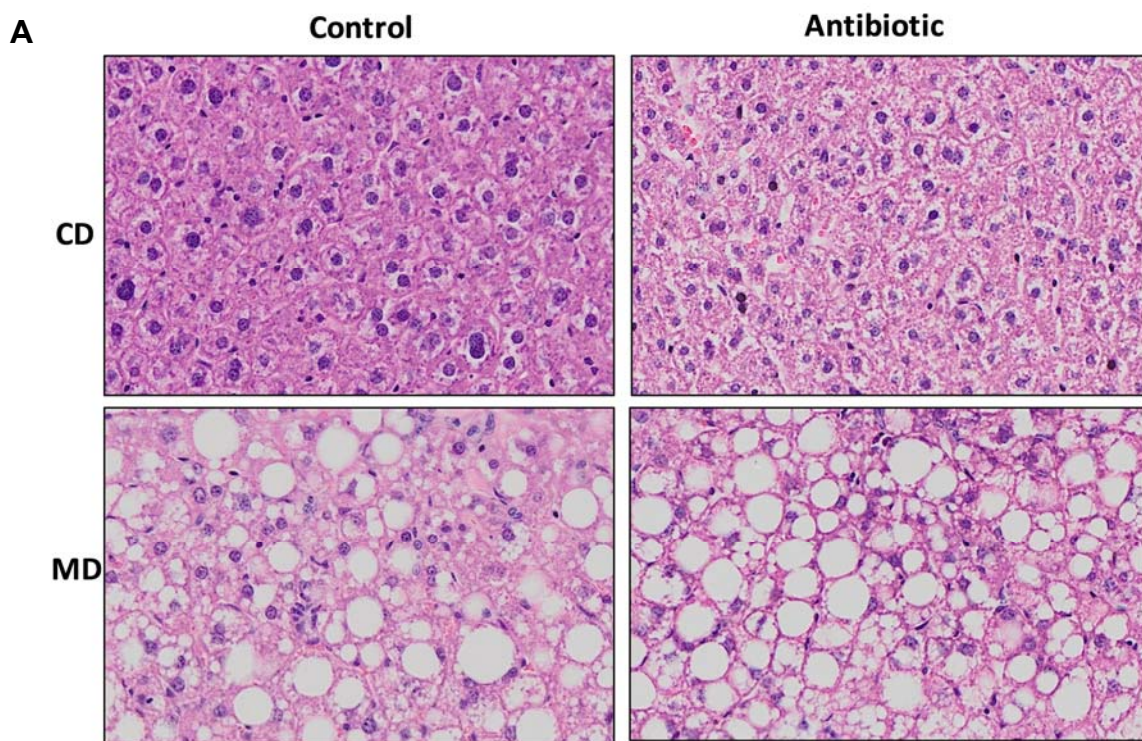
Collagen accumulation, a sign of hepatic fibrosis, is very common in chronic inflammation in fatty liver [140]. Therefore, the level of collagen accumulation was determined as a strong indicator of NASH. Reduced level of collagen accumulation was observed in picosirius red-stained liver sections of GF mice fed MD compared to the SPF mice fed MD at week 16 and 32 (data shown at 16 week, Fig. 5.3A). Reduced level of collagen accumulation was reflected in the decreased expression of Col-1 and  $\alpha$ -SMA, two important pro-fibrotic proteins [214, 215], in the livers of GF mice fed MD compared to the SPF mice fed MD (Fig. 5.3B-C).



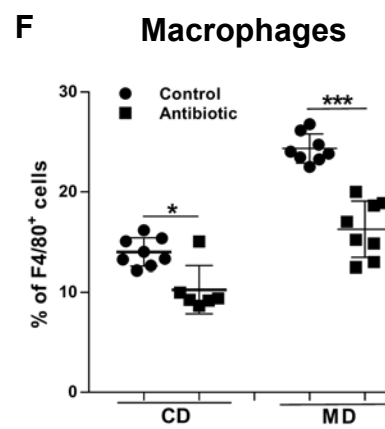
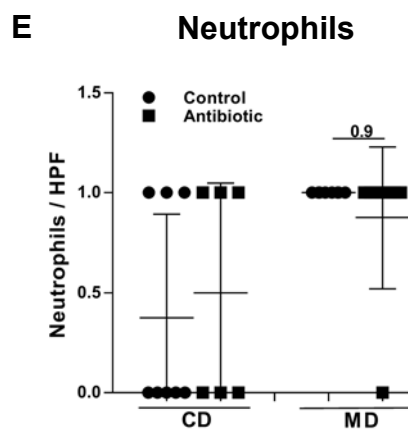
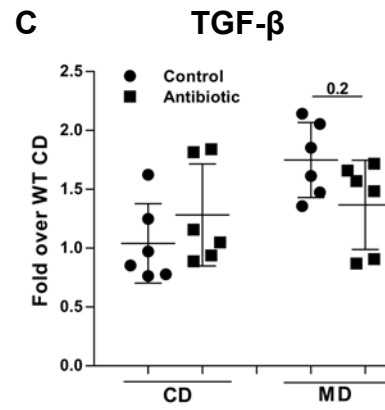
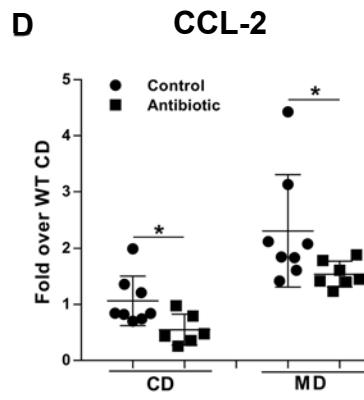
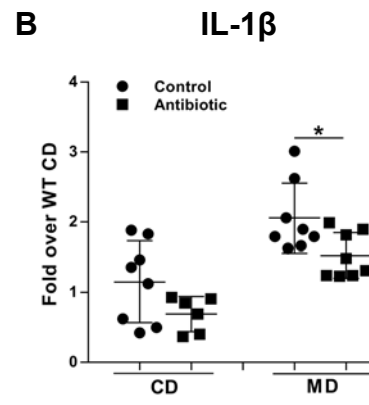
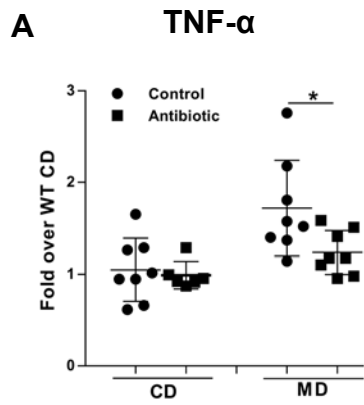
**Figure 5.3. Germ free mice fed high fat diet showed decreased level of collagen accumulation in their livers compared to the specific pathogen free mice.** Feeding high fat diet resulted in decreased level of collagen accumulation in the livers of germ free mice compared to the specific pathogen free mice as shown by the (A) representative images of picrosirius red stained liver sections (at 16 weeks) and expression of (B) Col-1a and (C)  $\alpha$ -SMA. GF, SPF, CD and MD denote germ free mice, specific pathogen free mice, control diet and milk-based high fat diet, respectively. \* $P < 0.05$ , \*\* $P < 0.01$ , \*\*\* $P < 0.001$  (Man-Whitney test); data are expressed as mean  $\pm$  SEM; n=6-8.

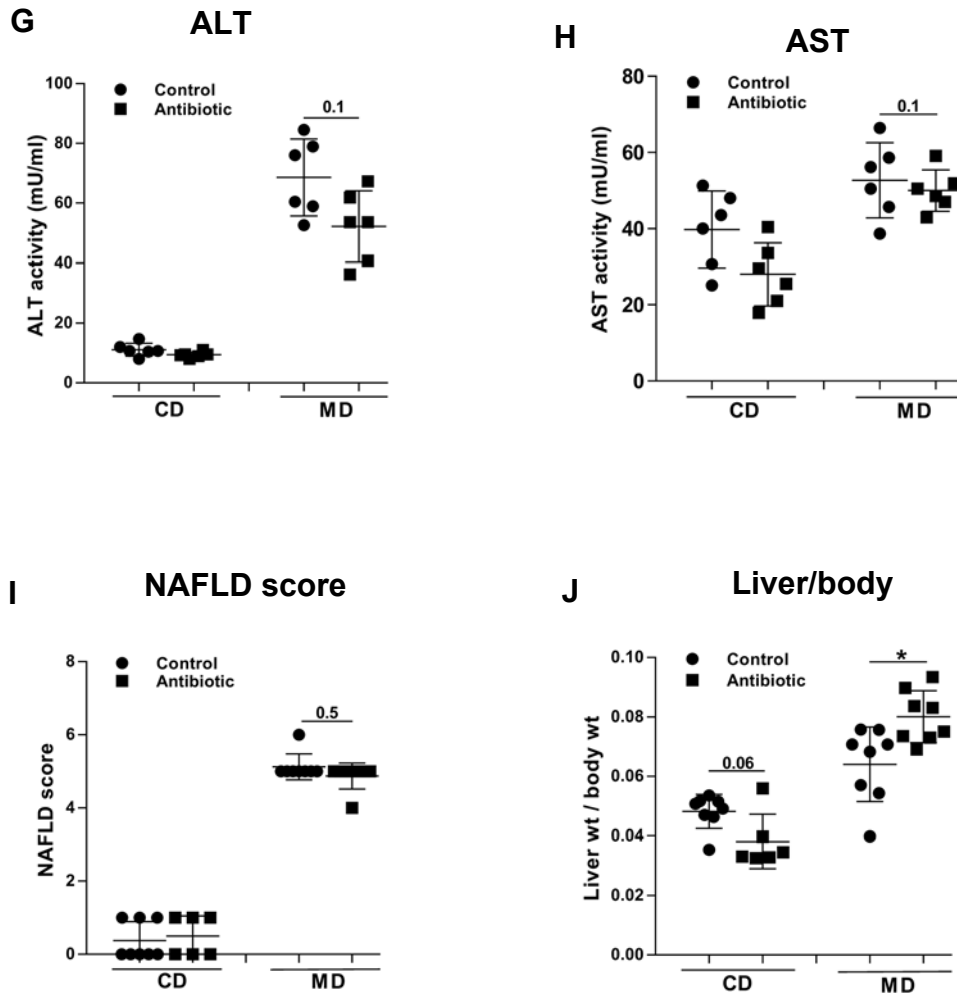
**Broad spectrum antibiotics-treated mice fed MD showed similar levels of steatosis, but had a decreased level of NASH compared to the control mice fed MD**

The treatment of mice fed MD with broad spectrum antibiotics failed to make any difference in the level of steatosis in their livers compared to the control mice fed MD (Fig. 5.4A). Similar clinical scores of steatosis were observed in the livers of broad spectrum antibiotic-treated mice and control mice (Fig. 5.4B). Although the treatment of mice fed MD with broad spectrum antibiotic did not result in any difference in the level of hepatic steatosis, it resulted in decreased levels of NASH-indicative markers in the livers of antibiotic-treated mice fed MD compared to the control mice fed MD (Fig. 5.5). Broad spectrum antibiotic-treated mice fed MD showed decreased expression of TNF- $\alpha$ , IL-1 $\beta$ , CCL-2 and TGF- $\beta$ , reduced infiltration of neutrophils and macrophages, and lower trends of serum activities of ALT and AST and NAFLD scores when compared to the control mice fed MD (Fig. 5.5A-I). Decreased level of NASH in the livers of broad spectrum antibiotic-treated mice fed MD resulted in improved liver health as demonstrated by significantly higher liver-to-body weight ratio compared to the control mice fed MD (Fig. 5.5J). Picrosirius red stained liver sections demonstrated that broad spectrum antibiotic-treated mice fed MD had decreased accumulation of collagen in their livers when compared to the control mice fed MD (Fig. 5.6A). Broad spectrum antibiotic-treated mice fed MD showed a lower trend of expression of pro-fibrotic Col-1 and  $\alpha$ -SMA in their livers, (Fig. 5.6A) which corroborates the reduced accumulation of collagen. Collectively, decreased levels of NASH-indicative and pro-fibrotic markers in the livers of broad spectrum antibiotic-treated mice fed MD, when compared to the control mice fed MD, suggesting the role of gut microbiota in mediating chronic inflammation in steatotic liver.

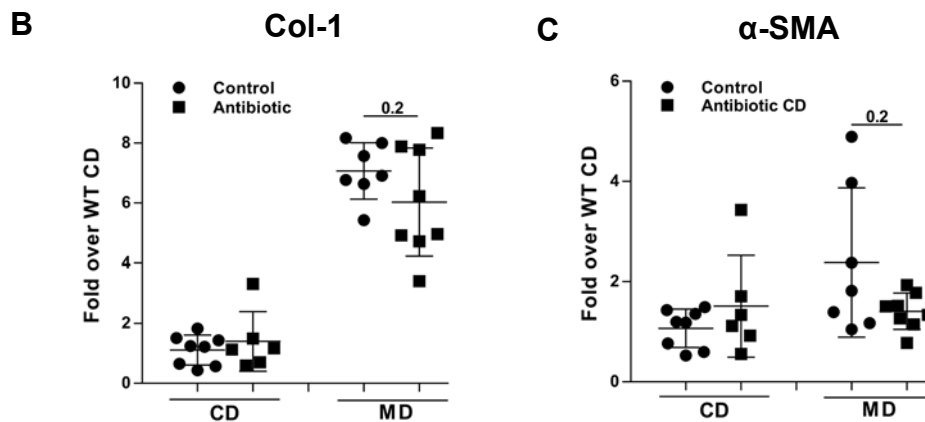
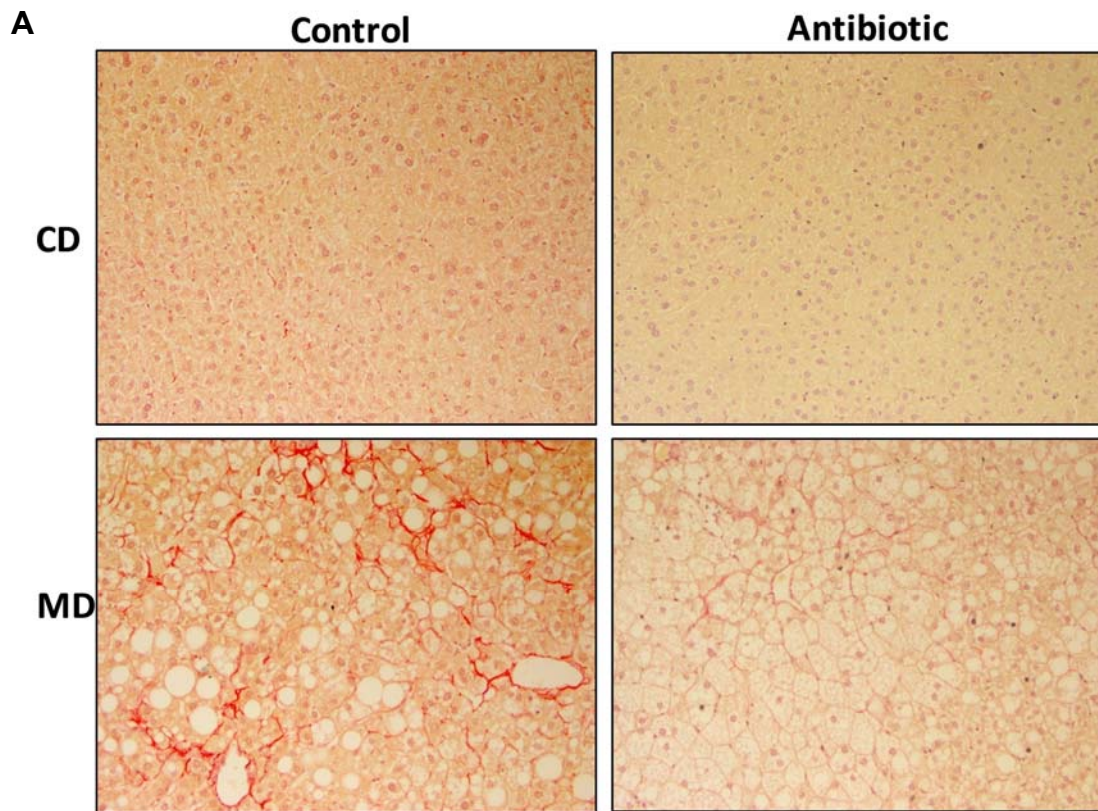


**Figure 5.4. Broad spectrum antibiotic-treated mice fed high fat diet developed similar level of hepatic steatosis compared to the control mice.** Feeding with high fat diet resulted in similar steatosis in the livers of broad spectrum antibiotic-treated mice compared to the control mice as shown by the (A) representative images of H&E stained liver sections and (B) steatosis score. CD and MD denote control diet and milk-based high fat diet, respectively. Data are expressed as mean±SEM; n=6-8.





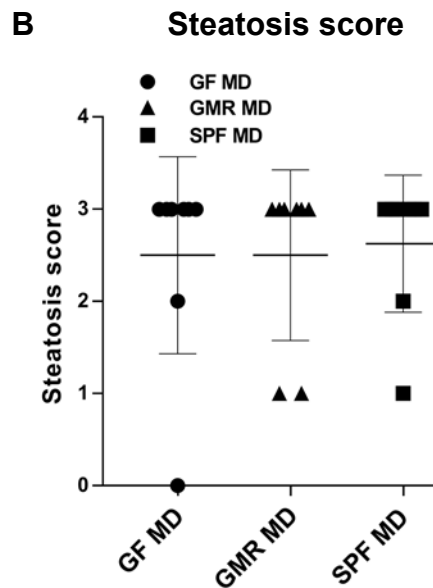
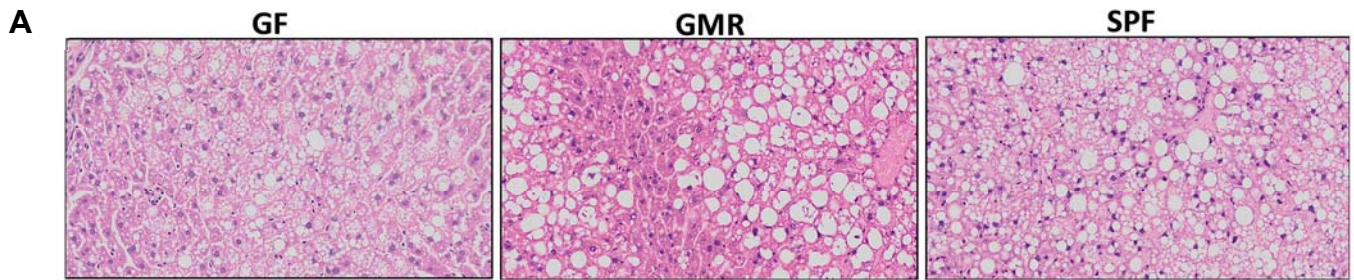
**Figure 5.5. Broad spectrum antibiotic-treated mice fed high fat diet showed decreased levels of NASH-indicative markers compared to the control mice fed high fat diet.** Broad spectrum antibiotic-treated mice fed high fat diet showed lower levels of (A-D) expression of TNF- $\alpha$ , IL-1 $\beta$ , CCL-2 and TGF- $\beta$ , (E-F) infiltration of neutrophils and macrophages, (G-H) serum activities of ALT and AST, and (I) NAFLD scores in their livers compared to the control mice fed high fat diet. (J) Decreased level of NASH resulted in better liver health as demonstrated by higher liver-to-body weight ratio in broad spectrum antibiotic-treated mice fed MD compared to the control mice fed MD. CD and MD denote control diet and milk-based high fat diet, respectively. \*P<0.05, \*\*P<0.01, \*\*\*P<0.001 (Man-Whitney test); data are expressed as mean $\pm$ SEM; n=6-8.



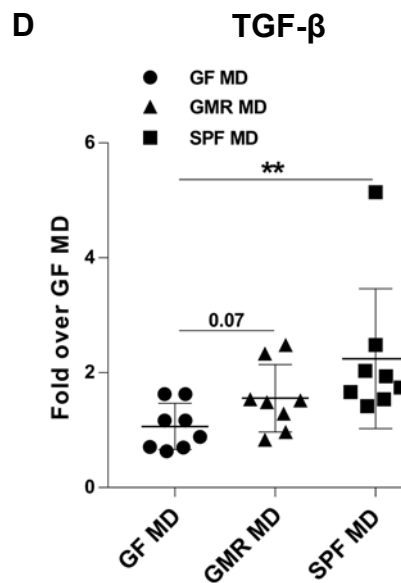
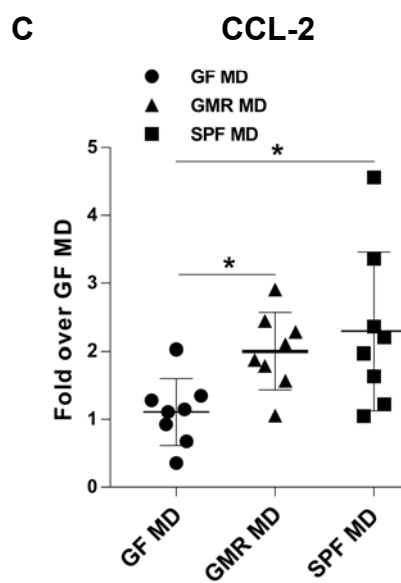
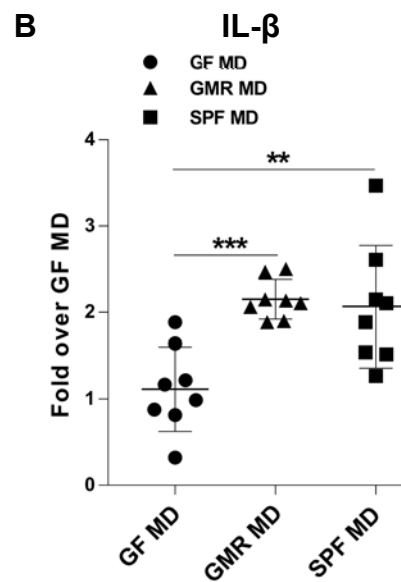
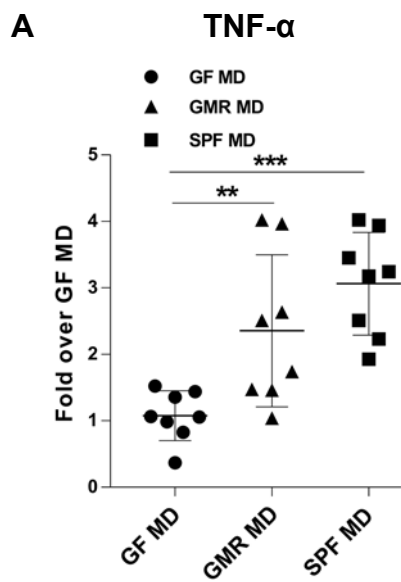
**Figure 5.6. Broad spectrum antibiotic-treated mice fed high fat diet showed decreased level of collagen accumulation in their livers compared to the control mice fed high fat diet.** Broad spectrum antibiotic-treated mice fed high fat diet displayed a lower trend of collagen accumulation in their livers compared to the control mice fed high fat diet as shown by the **(A)** representative images of picrosirius red stained liver sections and expression of **(B-C)** Col-1a and  $\alpha$ -SMA. CD and MD denote control diet and milk-based high fat diet, respectively. (Man-Whitney test); data are expressed as mean $\pm$ SEM; n=6-8.

## **Conventionalization of GF mice fed MD resulted in increased level of NASH**

To gain further evidence for the role of gut microbiota in mediating NASH, GF mice fed MD were conventionalized through the re-constitution of gut microbiota by fecal transplantation from SPF mice fed MD. Re-constitution of gut microbiota in GF mice fed MD did not result in any difference in the level of steatosis in their livers as compared to the GF mice fed MD. H&E staining of liver sections and their clinical scores for steatosis displayed a level of steatosis in the livers of gut microbiota re-constituted mice fed MD, that was similar to the steatosis observed in the livers of GF and control SPF mice fed MD (Fig. 5.7A-B). Although the level of steatosis remained unchanged, the levels of different NASH-indicative markers significantly increased in the livers of gut microbiota re-constituted mice when compared to the GF mice (Fig. 5.8A-G). Expression of TNF- $\alpha$ , IL-1 $\beta$ , CCL-2 and TGF- $\beta$  (Fig. 5.8A-D) and infiltration of neutrophils and macrophages (Fig. 5.8E-F) were increased in the livers of gut microbiota reconstituted mice fed MD as compared to the GF mice fed MD. Increased levels of these inflammatory markers resulted in a higher trend of NAFLD score in gut microbiota re-constituted mice as compared to the GF mice (Fig. 5.8G). Re-constitution of gut microbiota in GF free mice fed MD also resulted in an increased accumulation of collagen as demonstrated by picrosirius red staining of liver sections (Fig. 5.9A). This increase in collagen accumulation was also reflected in increased expression of Col-1 and  $\alpha$ -SMA in the livers of gut microbiota re-constituted mice fed MD compared to the GF mice fed MD (Fig. 5.9B-C). These data clearly demonstrated the role of gut microbiota in causing NASH.



**Figure 5.7. Reconstitution of gut microbiota in germ free mice fed high fat diet did not make any difference in the hepatic steatosis.** Feeding with high fat diet resulted in similar steatosis in the livers of conventionalized (gut microbiota re-constituted) mice compared to the germ free mice as shown by the **(A)** representative images of H&E stained liver sections and **(B)** steatosis score. GF, GMR, SPF and MD denote germ free mice, gut microbiota re-constituted mice, specific pathogen free mice and milk-based high fat diet, respectively. Data are expressed as mean $\pm$ SEM; n=6-8.



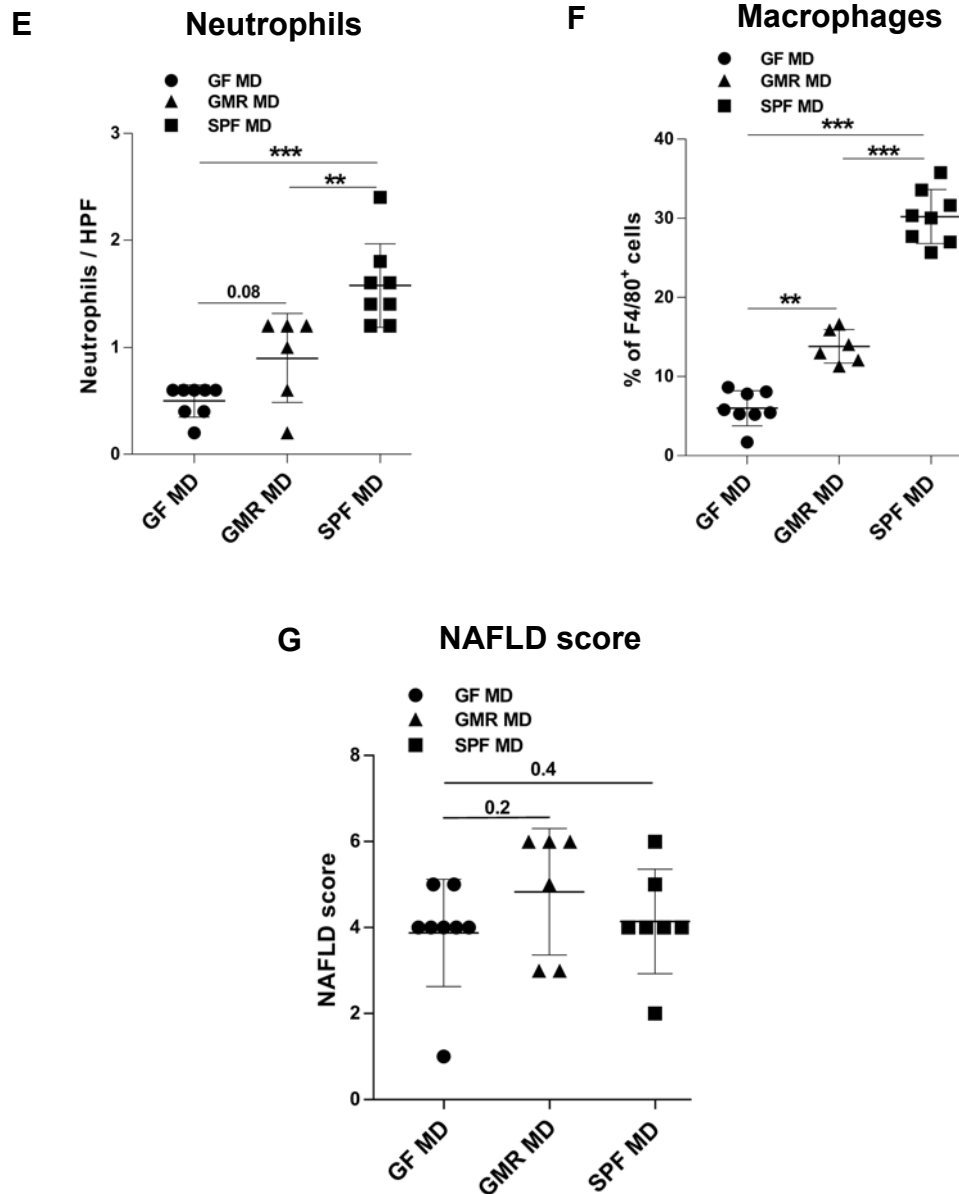


**Figure 5.8. Reconstitution of gut microbiota in germ free mice fed high fat diet showed elevated levels of NASH-indicative markers in their steatotic livers.** Reconstitution of gut microbiota in germ free mice fed high fat diet resulted in increased levels of (A-D) expression of TNF- $\alpha$ , IL-1 $\beta$ , CCL-2 and TGF- $\beta$ , (E-F) infiltration of neutrophils and macrophages, and (G) NAFLD scores in their livers compared to the germ free mice. GF, GMR, SPF and MD denote germ free mice, gut microbiota re-constituted mice, specific pathogen free mice and milk-based high fat diet, respectively. \* $P < 0.05$ , \*\* $P < 0.01$ , \*\*\* $P < 0.001$  (Man-Whitney test); data are expressed as mean  $\pm$  SEM; n=6-8.

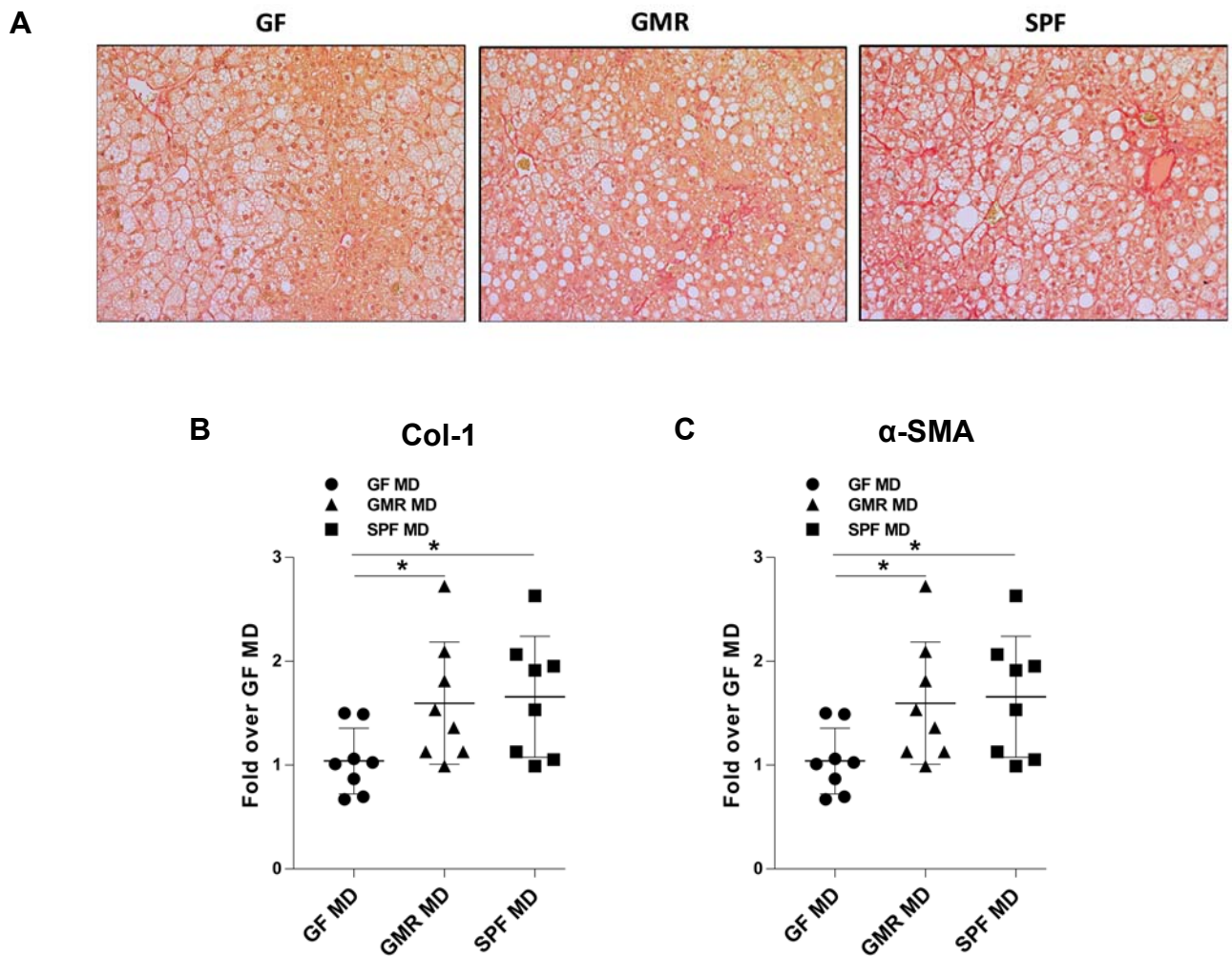


**Figure 5.9. Reconstitution of gut microbiota in germ free mice fed high fat diet resulted in increased collagen accumulation in their steatotic livers.** Reconstitution of gut microbiota in germ free mice fed high fat diet displayed an increase in collagen accumulation in their livers compared to the germ free mice fed high fat diet as shown by the **(A)** representative images of picrosirius red stained liver sections and expression of **(B-C)** Col-1a and  $\alpha$ -SMA. GF, GMR, SPF and MD denote germ free mice, gut microbiota re-constituted mice, specific pathogen free mice and milk-based high fat diet, respectively. \* $P < 0.05$  (Man-Whitney test); data are expressed as mean  $\pm$  SEM;  $n = 6-8$ .

### **Composition of gut microbial community was altered in mice fed MD**

To determine whether a high fat diet could bring about a change in the structure of gut microbial community, which might better explain the observed role of gut microbiota in mediating NASH in the livers of mice fed MD, the composition of cecal microbiota was determined at phylum level using 16s rRNA analysis. Indeed, the composition of gut microbial community was changed in mice fed MD. Stacked bar diagram of gut microbial community revealed a shift in phylum level in mice fed MD as compared to the mice fed CD (Fig. 5.10A). Structure of gut microbial community in mice fed MD became similar to mice fed CD when the diet was switched from MD to CD. Relative abundances of Bacteroidetes, Actinobacteria, and Tenericutes were significantly decreased in mice fed MD as compared to the mice fed CD. On the other hand, relative abundances of Proteobacteria, Verrucobacteria, and Firmicutes were significantly increased in mice fed MD as compared to the mice fed CD (Fig. 5.10B-G). When the diet was switched from MD to CD, relative abundances of these six gut microbial phyla became similar to the mice fed CD. Within the phylum Firmicutes, relative abundance of genus *Clostridium* trended to be higher in mice fed MD which became similar to the mice fed CD upon the change of diet from MD to CD (Fig. 5.10H). Principal component analysis was performed based on the composition of gut microbiota in order to assess whether the mice fed MD were clustered differently than the mice fed CD. Likewise, as we anticipated mice fed MD clustered differently versus the mice fed CD (Fig. 5.11A-B). However, mice fed MD clustered similarly to the mice fed CD when the diet was changed from MD to CD, demonstrating that the composition of gut microbial community differs in mice fed MD versus mice fed CD.

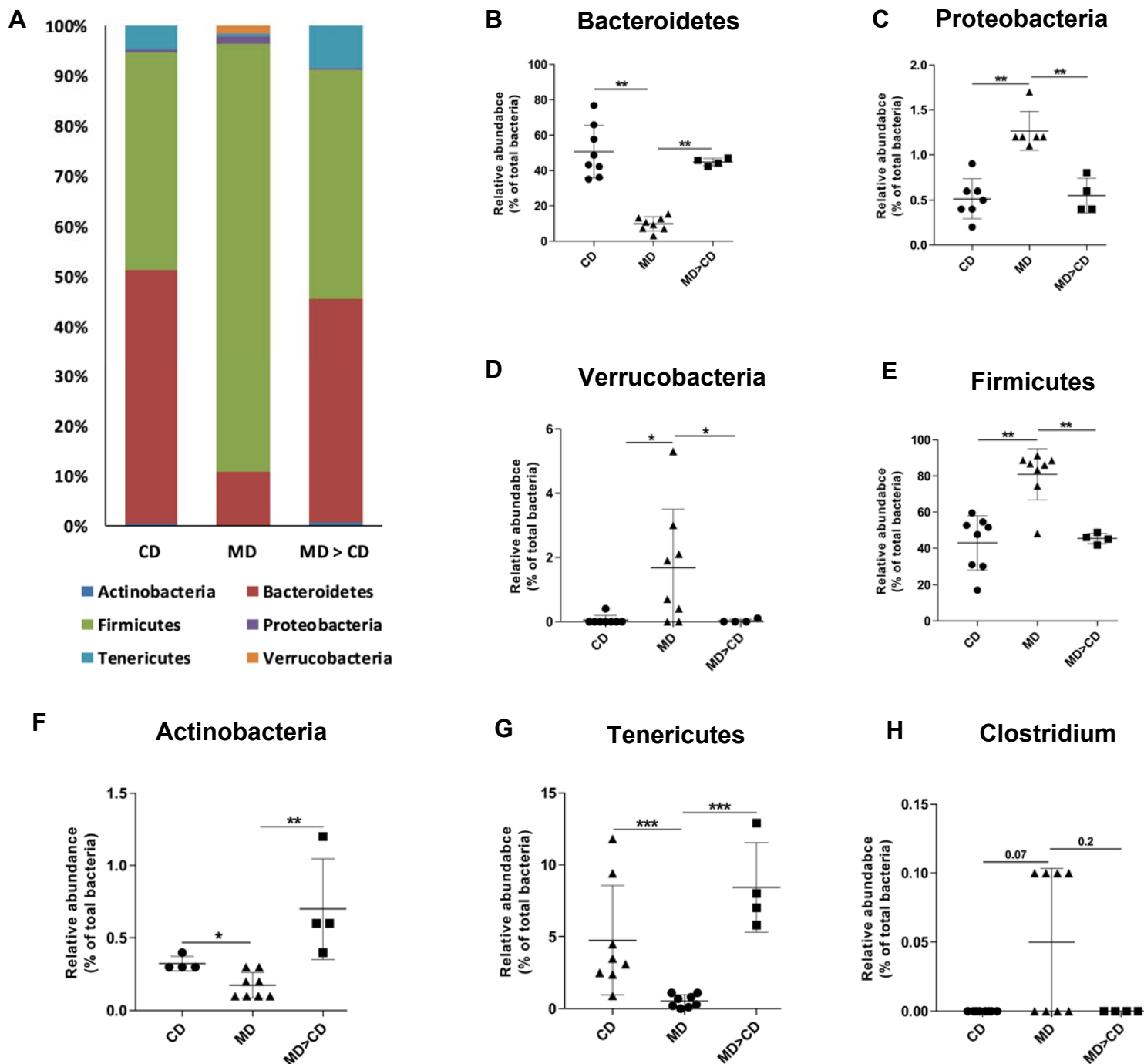


**Figure 5.10. Composition of gut microbiota changed in mice fed high fat diet.** Feeding of mice with high fat diet for 16 weeks resulted in alteration of composition of gut microbial community which became similar to that of mice fed control diet upon the switch of diet from control diet to high fat diet as represented by (A) stacked bar diagram at phylum level and changes in relative abundances of (B) Bacteroidetes, (C) Proteobacteria, (D) Verrucobacteria, (E) Firmicutes, (F) Actinobacteria, (G) Tenericutes, and (H) Clostridium. CD, MD and MD>CD denote control diet, milk-based high fat diet and switched diet, respectively. \* $P < 0.05$  (Man-Whitney test); data are expressed as mean  $\pm$  SEM;  $n = 4-8$ .

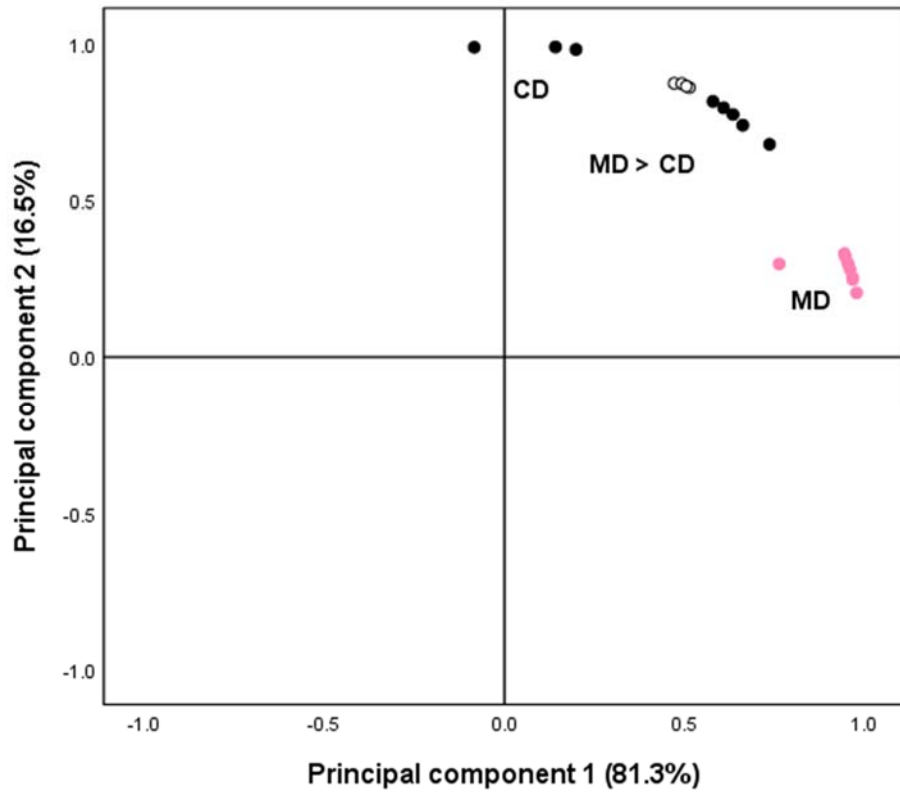


**Figure 5.11. Principal component analysis resulted in different clustering of mice fed high fat diet.** Principal component analysis based on the relative abundances of gut microbes at phylum level resulted in different clustering of mice fed high fat diet than mice fed control diet. When the diet was switched from high fat diet to control diet, mice fed high fat diet clustered similar to the mice fed control diet. CD, MD and MD>CD denote control diet, milk-based high fat diet and switched diet, respectively. Dark-filled dots, pink-filled dots and open dots indicate the mice fed CD, MD and MD>CD respectively.

## **Discussion**

In order to demonstrate the association of gut microbiota in transferring a steatotic liver to one with NASH, three specific experiments were conducted in this study. First experiment was performed using GF mice which showed that GF mice fed MD are protected from NASH. Second experiment was performed by the treatment of SPF mice fed MD with broad spectrum antibiotics. Diminishing of gut microbiota through the treatment with broad spectrum antibiotics resulted in decreased levels of NASH-indicative markers in SPF mice fed MD. Data from the experiment with broad spectrum antibiotics treatment was in line with the findings of GF mice experiment. Finally, in conventionalization experiment, gut microbiota was reconstituted in GF mice fed MD through fecal transfer from SPF mice fed MD, which resulted in increased levels of NASH-indicative markers.

Although the level of chronic inflammation in steatotic liver was decreased in both GF and broad spectrum antibiotics-treated mice as compared to the control mice, GF mice demonstrated better protection than broad spectrum antibiotics-treated mice. Whereas the GF mice fed MD were completely protected from elevated expression of pro-inflammatory cytokines and increased infiltration of innate immune cells, broad spectrum antibiotics-treated mice fed MD showed only a partial decrease in these NASH-indicative markers, perhaps because gut microbes are not completely eliminated through broad spectrum antibiotic treatment [216], while GF mice are free from all microbes. Therefore, it is possible that pro-inflammatory components coming from the remaining gut microbes of broad spectrum antibiotics-treated mice still have some causative effect on

the mediation of NASH. At the same time, plausible direct therapeutic effect of antibiotics on the pathogenesis of NASH cannot be ruled out.

Although the re-constitution of gut microbiota in GF mice fed MD resulted in an increase in the level of immune infiltration in their livers, it did not reach the level of immune infiltration in the livers of control SPF mice fed MD. Perhaps, that occurred due to the fact that gut microbiota-derived metabolites (e.g. short chain fatty acids) play an important role in the differentiation of embryonic immune progenitor cells, particularly the macrophage progenitor cells [217]. A defective prenatal differentiation of these immune progenitor cells may occur in the liver of GF mice due to the deficiency of gut microbiota-derived metabolites. Immune cells derived from this progenitor cells are called sessile cells. It is possible that a portion of the sessile immune cells is deficient in the liver of GF mice due to the lack of gut microbiota-derived factors. Postnatal re-constitution of gut microbiota in GF mice through fecal transplantation could only facilitate the differentiation of bone marrow-derived innate cells in the liver, but not compensate the missing sessile cells [218]. Therefore, the level of immune cell count in the liver of conventionalized GF mice never reached the level in SPF mice.

Data from 16s rRNA analysis, as displayed by stacked bar diagram and principal component analysis, demonstrated a change in the composition of gut microbiota in mice fed MD as compared to the mice fed CD. Although the relative abundance of Bacteroidetes, the major Gram negative phylum in the gut microbiota of mice, decreased, the relative abundance of two different Gram negative phyla, Proteobacteria and Verrucobacteria, significantly increased in the mice fed MD [219]. The important change in the relative abundance of Gram negative bacteria is mainly due to their contribution in

producing endotoxin. It is still unclear how much of a role Proteobacteria or Verrucobacteria plays in maintaining the level of circulating endotoxin. Apart from the alteration of gut microbial composition in the phylum level, we also observed a change in genus *Clostridium* in mice fed MD. *Clostridium* produces ethanol which, importantly, contributes to oxidative stress in the liver leading to NASH [220]. It requires further investigation to identify specific microbes potentially associated with the production of pro-inflammatory molecules or metabolites associated with NASH. In that case, application of microbe-specific antibiotics other than broad spectrum antibiotics may create a new therapeutic option for NASH.

# Chapter 6

Role of Gut Microbiota in Causing NASH is Dependent on LPS-TLR-4-Kupffer Cell Axis

## **Summary**

Increased level of LPS has been reported both in obese patients and experimental models of obesity. It has also been reported that chronic administration of LPS in mice results in increased adipose tissue and body weight in a TLR-4 pathway-dependent manner. In the previous chapter, we demonstrated the obvious role of gut microbiota in causing NASH. LPS is known as a major gut-derived pro-inflammatory component in the liver. Therefore, it demands a comprehensive study to investigate the potential role of LPS-TLR-4 pathway in the modulation of NASH by gut microbiota. Treatment of mice fed MD with broad spectrum antibiotics resulted in decreased concentration of serum LPS and indicators of NASH. Chronic injection of low dose LPS restored the higher level of serum LPS in mice fed MD. The level of NASH was also increased upon injection of LPS corroborating the role of LPS in causing NASH. Simultaneous injection of TAK-242, a TLR-4 inhibitor, protected the mice fed MD from NASH demonstrating the role of LPS-TLR-4 pathway in causing the disease. It was also observed that TLR-4 KO mice fed MD had decreased level of NASH. Chronic injection of LPS in TLR-4 KO mice fed MD failed to increase the level of NASH. This observation further confirmed the involvement of LPS-TLR-4 pathway in causing NASH. Because kupffer cells are the principal member of TLR-4-expressing community in the liver, we also attempted to investigate the role of kupffer cells in mediating NASH. It was found that reconstitution of TLR-4 KO kupffer cells in the livers of wild-type mice fed MD by bone marrow transplantation resulted in a decreased level of NASH. Conversely, reconstitution of wild-type kupffer cells in the livers of TLR-4 KO mice fed MD resulted in an increased level of NASH. This experiment clearly indicated the role of kupffer cells in mediating NASH in a TLR-4 dependent manner.

## **Introduction**

Once the involvement of gut microbiota in causing NASH is demonstrated, the next question to resolve is the mechanism how gut microbiota contributes to NASH modulation. One potential mechanism might be the engagement of TLRs and their gut microbiota-derived ligands known as microbe-associated molecular patterns. LPS is a major microbe-associated molecular pattern drained into the portal circulation from intestine. The concentration of LPS has been shown to be increased in obese patients as well as animal models of obesity [122, 123, 221, 222]. Role of LPS-TLR-4 pathway in metabolic syndrome was first studied by Cani et al. They showed that chronic endotoxemia created through the infusion of LPS using a subcutaneously implanted osmotic mini-pump had resulted in an increased body weight and adipose tissue in mice [122]. In the same report, they also showed that interruption of TLR-4 pathway through the knockout of CD14 prevents the LPS-infused mice from gaining increased body weight and adipose tissue. These data demonstrated the role of LPS-TLR-4 pathway in obesity. In a follow-up report, Cani et al. showed that treatment of mice fed high fat diet with broad spectrum antibiotics had resulted in a reduced concentration of serum LPS and decreased body weight and adipose tissue, when compared to the control mice fed a high fat diet. This result demonstrated that gut microbiota plays a role in controlling obesity through metabolic endotoxemia. Due to the close association of obesity and NAFLD, a similar role for the LPS-TLR-4 pathway is postulated in the pathogenesis of NASH. Therefore, the current study was designed to investigate the role of a gut-derived low grade chronic endotoxemia in causing NASH in mice fed high fat diet in a TLR-4 pathway-dependent manner.

## **Results**

### **Diminishing of gut microbiota resulted in reduced concentration of serum endotoxin which was restored upon LPS injection**

Diminishing of gut microbiota through the treatment of mice fed CD or MD with broad spectrum antibiotics resulted in reduced concentration of endotoxin in portal serum and feces (Fig. 6.1A-B). This indicates that the concentration of serum endotoxin is dependent on the normal abundance of gut microbiota. Injection i.p. of low dose LPS for four weeks led to the increase of concentration of endotoxin in portal serum (Fig. 6.1A).

### **LPS injection resulted in increased level of NASH in broad spectrum antibiotics-treated mice that were fed MD**

As discussed in the last chapter, treatment of mice fed MD with broad spectrum antibiotics resulted in decreased level of NASH. This improvement of disease might be due to the reduced concentration of gut-derived endotoxin in the circulation of broad spectrum antibiotics-treated mice. This assumption led us to test if the restoration of an increased level of serum endotoxin through the injection i.p. of a subclinical dose of exogenous LPS in broad spectrum antibiotics-treated mice could increase the severity of NASH. LPS injection in broad spectrum antibiotics-treated mice fed MD, however, did not make any difference in fat accumulation and steatosis score (Fig. 6.2A and Fig. 6.2B), but that LPS injection did result in increased levels of expression of TNF- $\alpha$ , IL-1 $\beta$ , CCL-1 and TGF- $\beta$ , infiltration of neutrophils and macrophages, serum activities of ALT and AST and clinical scores of NAFLD as compared to the non-LPS injected/antibiotics-treated mice fed MD (Fig. 6.3A-I). Elevated levels of the aforementioned indicators of NASH

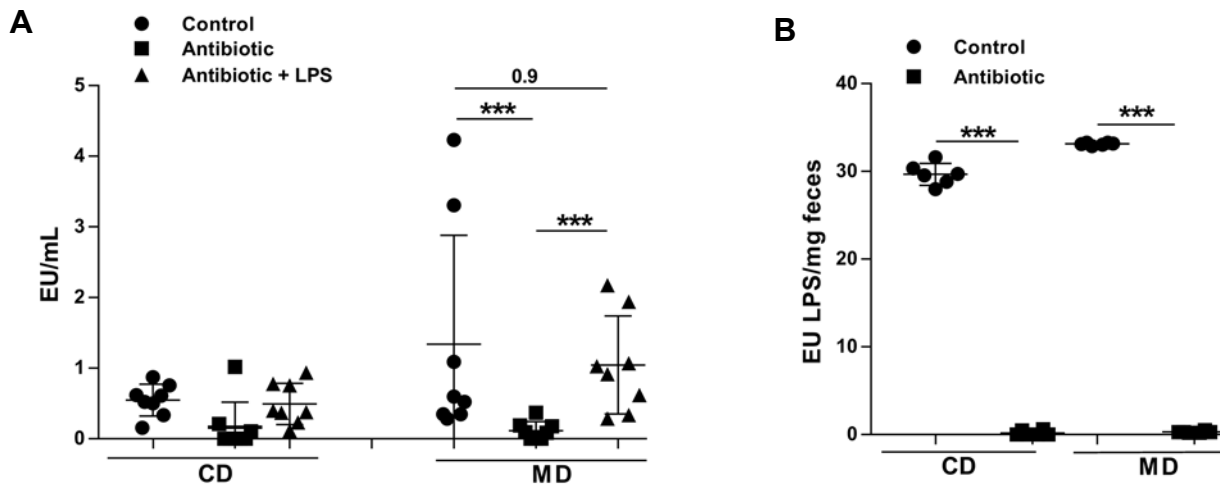


**Figure 6.1. Diminishing of gut microbiota resulted in reduced concentration of endotoxin in portal serum and feces.** Treatment of mice fed CD or MD with broad spectrum antibiotics resulted in reduced concentration of endotoxin in **(A)** portal serum and **(B)** feces. **(A)** Intraperitoneal injection of low dose LPS restored the serum endotoxin level in mice fed MD. CD and MD denote control diet and milk-based high fat diet, respectively. \*\*\* $P < 0.001$  (Man-Whitney test); data are expressed as mean  $\pm$  SEM;  $n = 6-8$ .

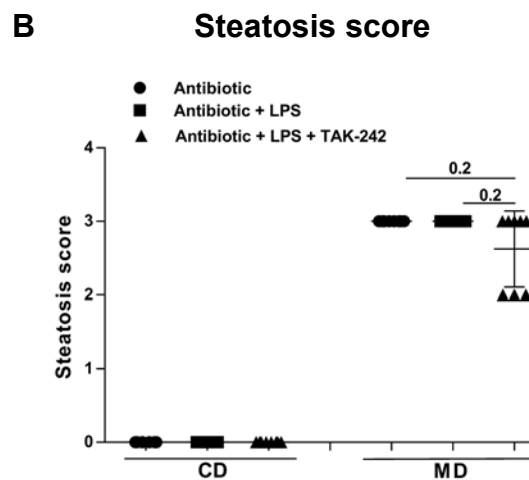
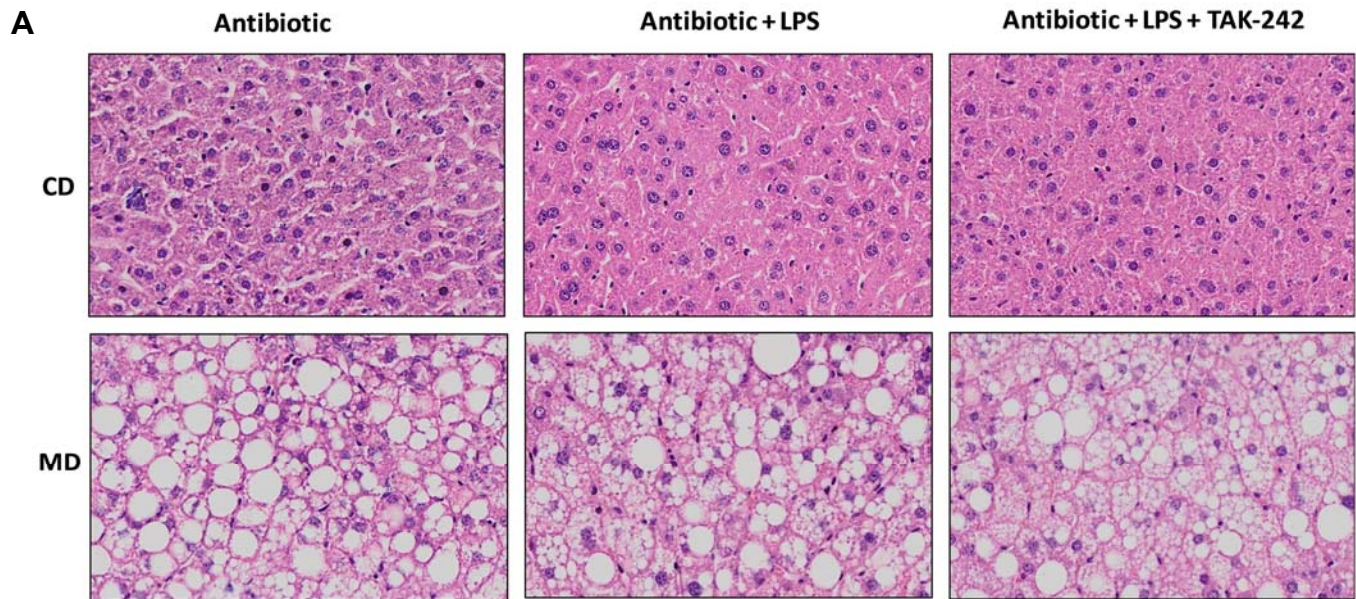
were reflected in exacerbated liver health as shown by the reduced liver-to-body weight ratios of LPS-injected/antibiotics-treated mice fed MD, when compared to the only antibiotics-treated mice fed MD (Fig. 6.3J).

LPS injection also resulted in increased collagen accumulation in the fatty livers of broad spectrum antibiotics-treated mice fed MD compared to the only antibiotics-treated mice fed MD, as demonstrated by elevated levels of picosirius red staining of collagen and expression of col-1 and  $\alpha$ -SMA (Fig. 6.4A-C). These data demonstrated the role of the low concentration of gut-derived endotoxin in mediating NASH in the fatty liver.

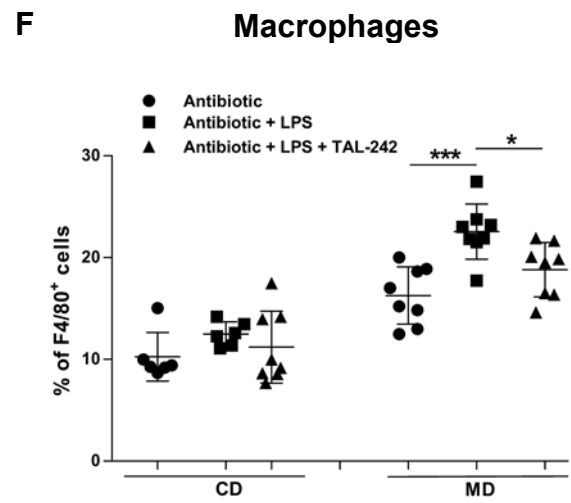
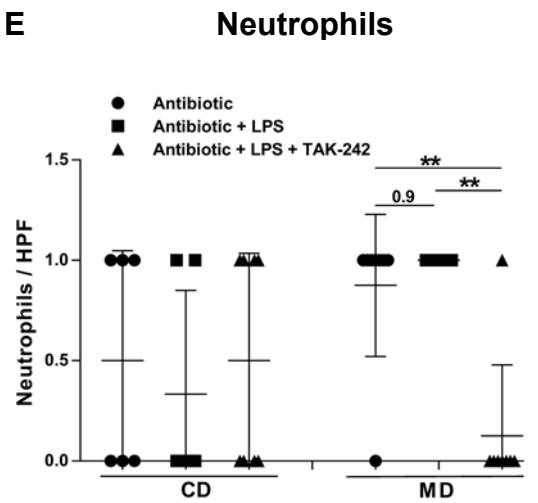
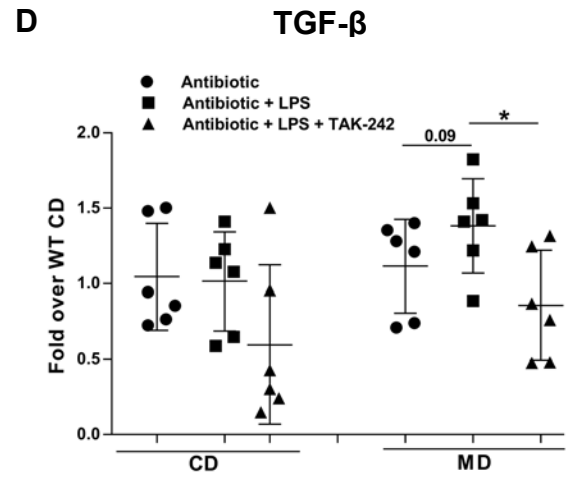
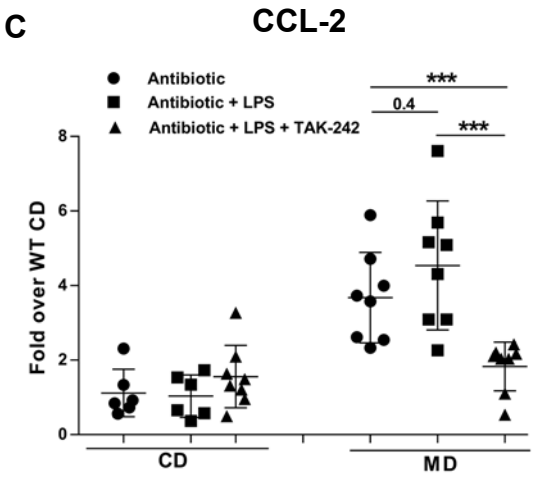
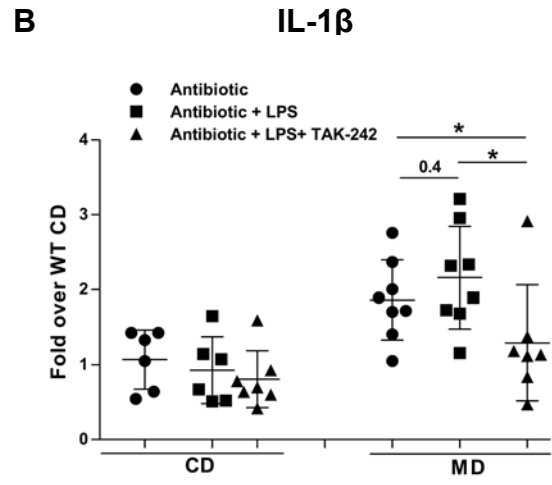
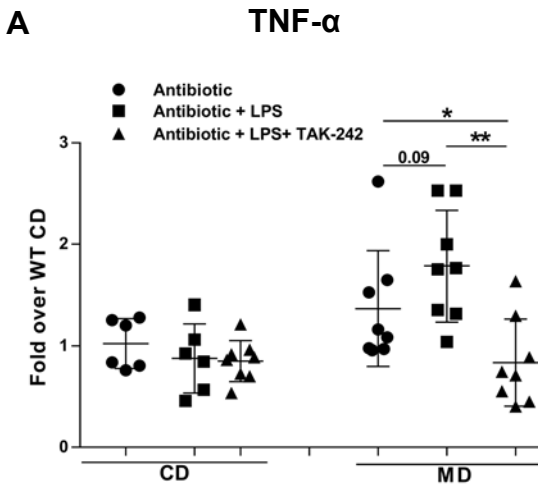
#### **Administration of TLR-4 inhibitor (TAK-242) blunted the effect of injection of low dose LPS resulting in decreased level of NASH**

Administration of TAK-242 in antibiotics-treated/LPS-injected mice fed MD did not make any significant decrease in fat accumulation or steatosis score (Fig. 6.2A and Fig. 6.2B), but resulted in reduced levels of expression of TNF- $\alpha$ , IL-1 $\beta$ , CCL-1 and TGF- $\beta$ , infiltration of neutrophils and macrophages, serum activities of ALT and AST and clinical scores of NAFLD compared to the only antibiotics-treated/LPS-injected mice fed MD (Fig. 6.3A-I). Reduced level of NASH was consistent with the improved liver health as shown by the increased liver-to-body weight ratios in antibiotics-treated/LPS-injected/TAK-242-administered mice fed MD, as compared to the only antibiotics-treated/LPS-injected mice fed MD (Fig. 6.3J).

Administration of TAK-242 also resulted in reduced collagen accumulation in the fatty livers of broad spectrum antibiotics-treated/LPS-injected mice fed MD compared to



**Figure 6.2. Injection of LPS or TLR-4 inhibitor in broad spectrum antibiotics-treated mice fed high fat diet did not make alter hepatic steatosis.** Intraperitoneal injection of low dose LPS or TLR-4 inhibitor (TAK-242) in mice fed CD or MD did not alter hepatic steatosis as shown by **(A)** representative images of H&E stained liver sections and **(B)** steatosis score. CD and MD denote control diet and milk-based high fat diet, respectively. Data are expressed as mean±SEM; n=6-8.



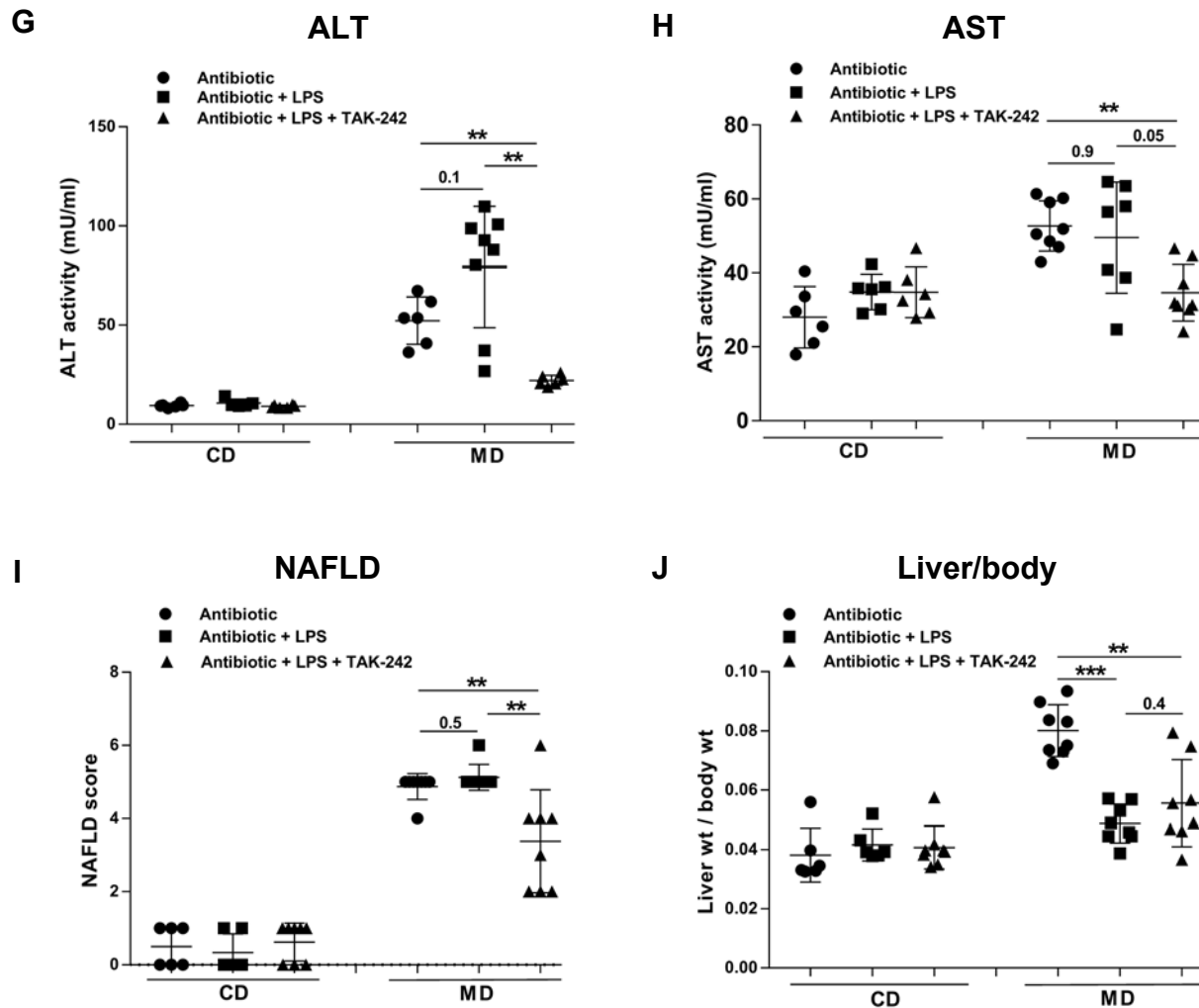


**Figure 6.3. Injection of low dose LPS in broad spectrum antibiotics-treated mice fed high fat diet resulted in increased level of NASH which was reversed upon administration of TLR-4 inhibitor.** Injection of low dose LPS in broad spectrum antibiotics-treated mice fed MD resulted in increased levels of (A-D) expression of TNF- $\alpha$ , IL-1 $\beta$ , CCL-2 and TGF- $\beta$ , (E-F) infiltration of neutrophils and macrophages, (G-H) serum activities of ALT and AST, and (I) NAFLD scores in their livers which was reversed upon administration of TLR-4 inhibitor (TAK-242). (J) Increased level of NASH in LPS-injected/antibiotics-treated mice fed MD resulted in exacerbated liver health as demonstrated by reduced liver-to-body weight ratio which was reversed upon administration of TAK-242. CD and MD denote control diet and milk-based high fat diet, respectively. \* $P < 0.05$ , \*\* $P < 0.01$ , \*\*\* $P < 0.001$  (Man-Whitney test); data are expressed as mean  $\pm$  SEM; n=6-8.

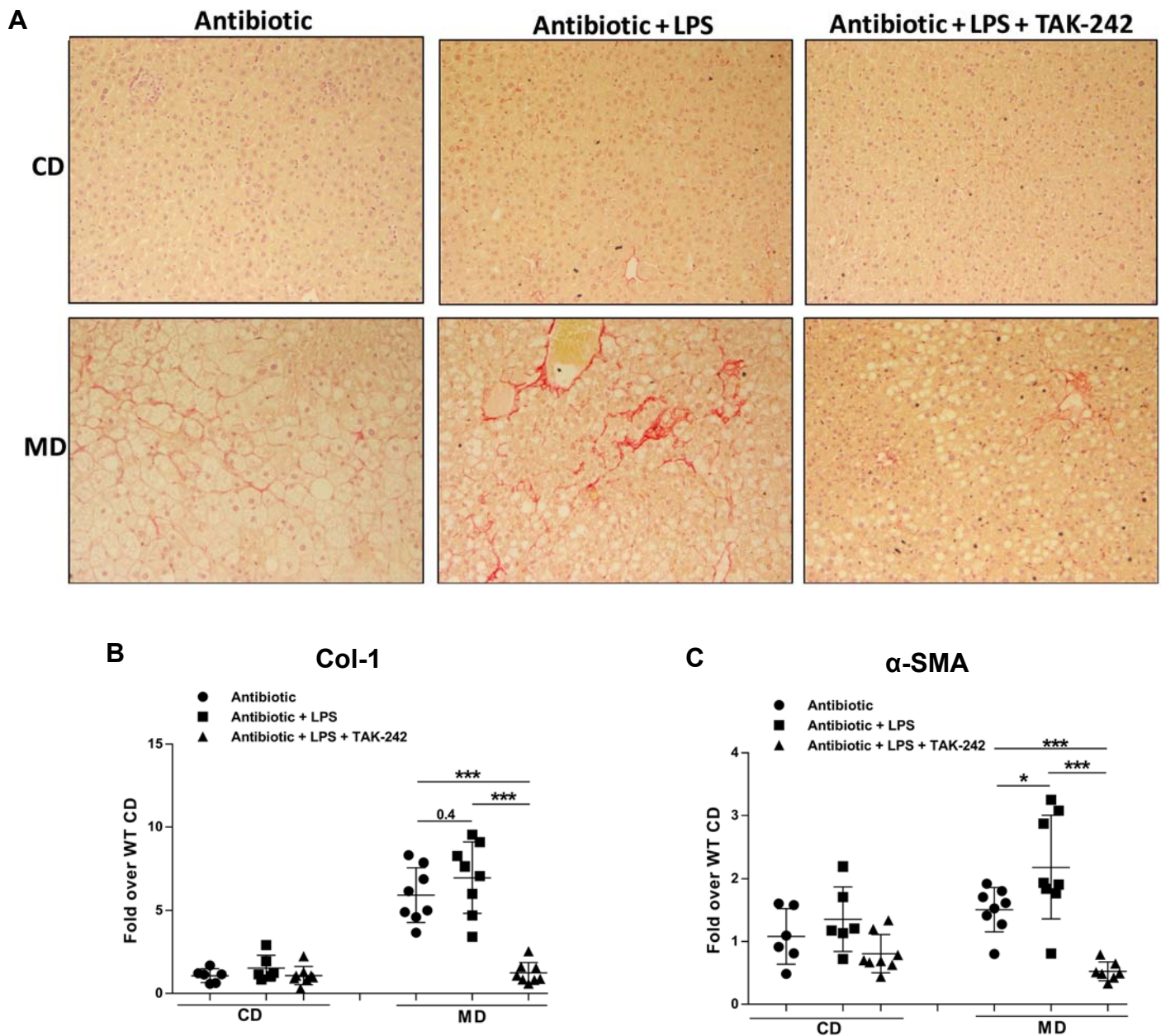


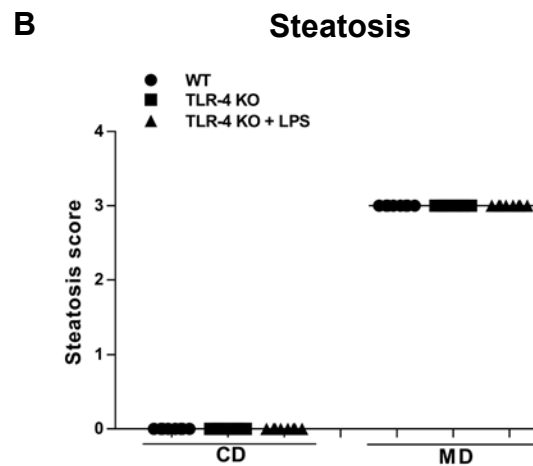
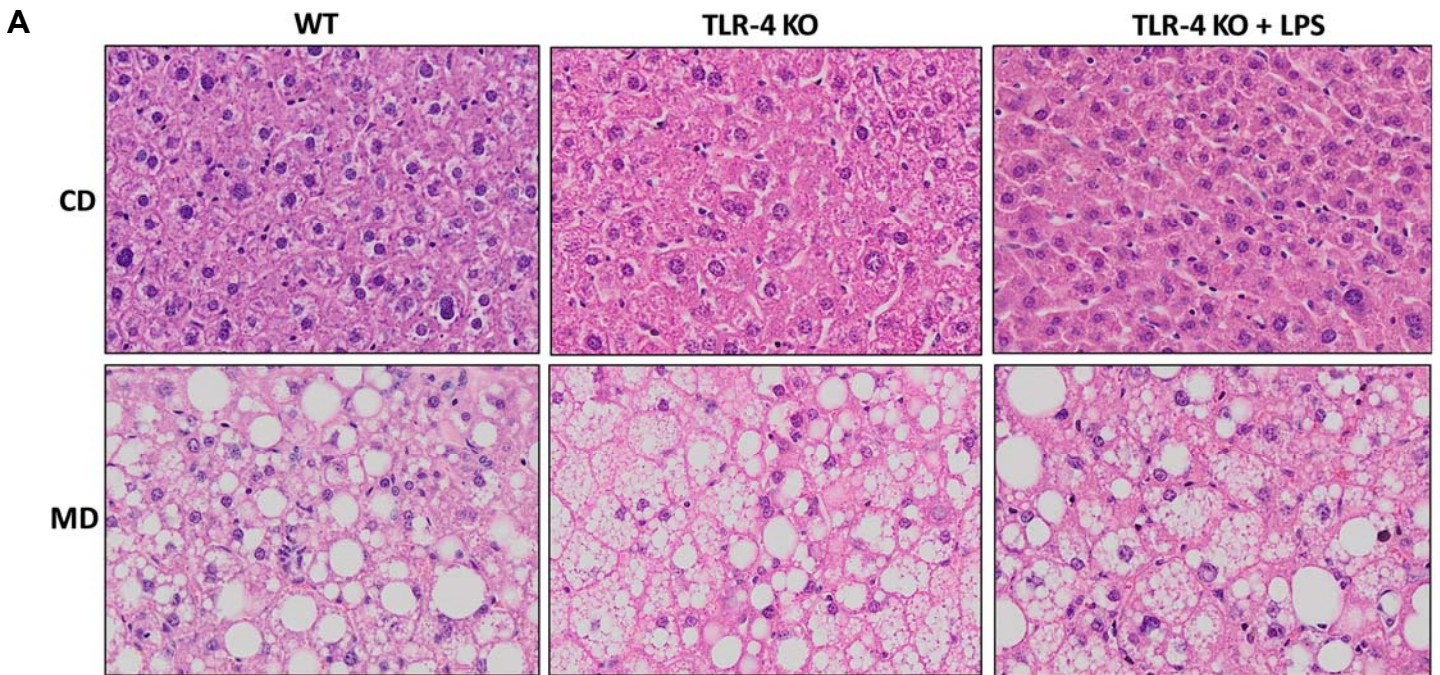
**Figure 6.4. Injection of low dose LPS in broad spectrum antibiotics-treated mice fed high fat diet resulted in increased accumulation of collagen which was reversed upon administration of TLR-4 inhibitor.** Injection of low dose LPS in broad spectrum antibiotics-treated mice fed MD displayed an increased level of collagen accumulation in their livers which was reversed upon administration of TLR-4 inhibitor (TAK-242) as shown by the (A) representative images of picosirius red stained liver sections and expression of (B-C) Col-1a and α-SMA. CD and MD denote control diet and milk-based high fat diet, respectively. \*P<0.05, \*\*\*P<0.001 (Man-Whitney test); data are expressed as mean±SEM; n=6-8.

the antibiotics-treated/LPS-injected mice fed MD, as demonstrated by reduced levels of picosirius red staining of collagen and expression of col-1 and  $\alpha$ -SMA (Fig. 6.4A-C). These results demonstrate that circulating LPS induces inflammation in the fatty liver through the interaction with TLR-4 indicating an important role of LPS-TLR-4 axis in causing NASH.

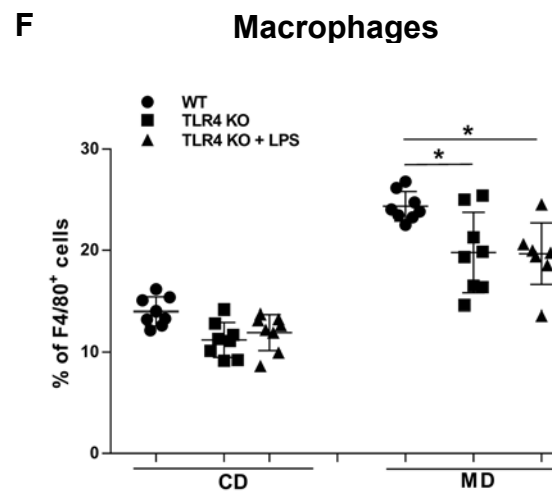
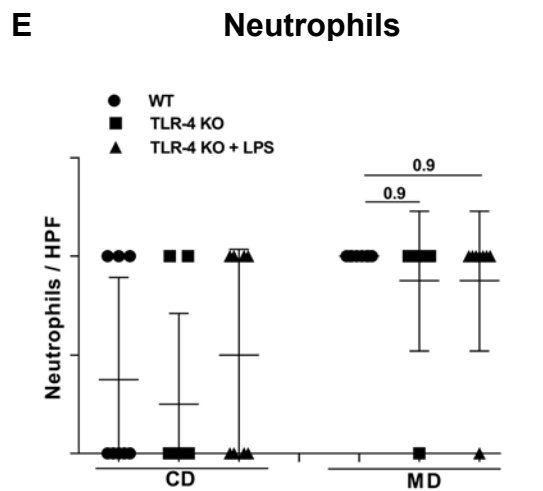
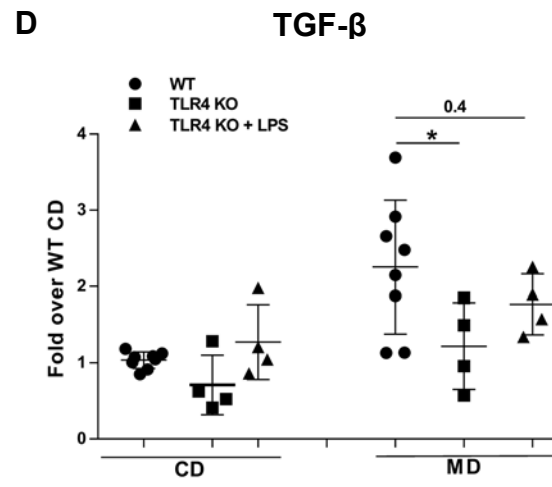
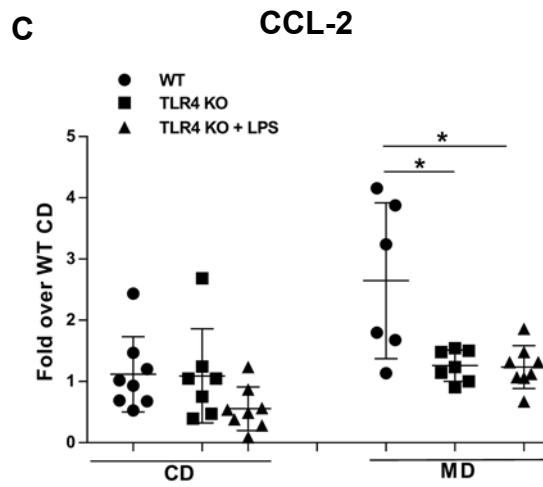
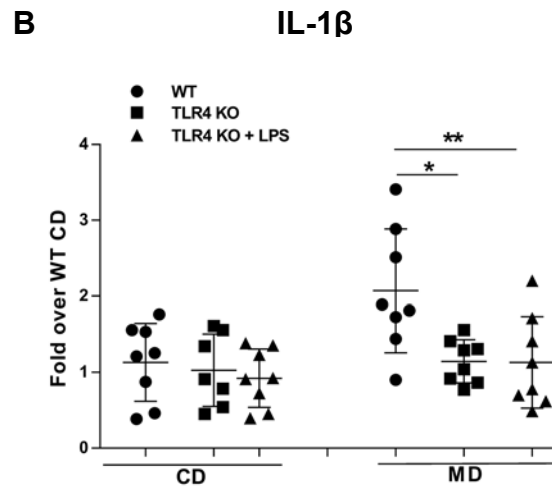
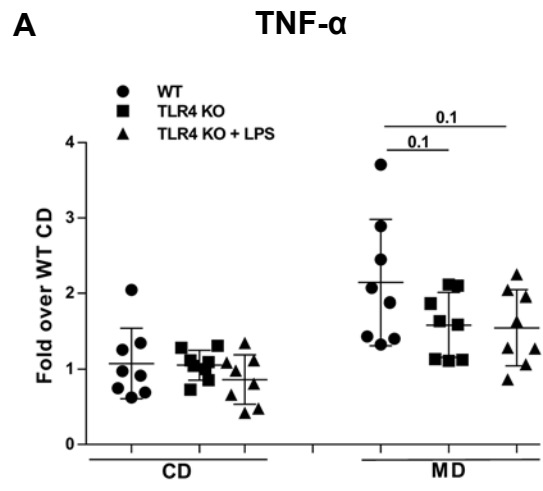
### **TLR-4 has an obvious role in the modulation of NASH in mice fed MD**

Livers from TLR-4 KO mice fed MD did not show any difference in fat accumulation or steatosis score as compared to the wild-type mice fed MD (Fig. 6.7A-B). Likewise, injection of low dose LPS in TLR-4 KO mice fed MD did not cause any difference in fat accumulation or steatosis score as compared to the wild-type or TLR-4 KO mice fed MD (Fig. 6.7A-B). These data indicate that TLR-4 does not have a clear role in fat deposition in the liver.

Although TLR-4 did not show any role in fat accumulation in the livers of mice fed MD, yet it showed important role in the transitioning of fatty livers to chronic inflammatory stage. TLR-4 KO mice fed MD exhibited reduced levels of expression of TNF- $\alpha$ , IL-1 $\beta$ , CCL-1 and TGF- $\beta$ , infiltration of neutrophils and macrophages, serum activities of ALT and AST and clinical scores of NAFLD, as compared to the wild-type mice fed MD (Fig. 6.8A-I). Injection of low dose LPS in TLR-4 KO mice did not result in any increase in the levels of NASH-indicative markers as compared to the Only TLR-4 KO mice fed MD. The reduced level of NASH was consistent with the improved liver health, as shown by the increased liver-to-body weight ratios in TLR-4 KO mice fed MD, when compared to the wild-type mice fed MD (Fig. 6.8J). Injection of low dose LPS in TLR-4 KO mice fed MD



**Figure 6.7. TLR-4 KO mice fed high fat diet displayed similar level of hepatic steatosis as compared to the wild-type mice fed high fat diet.** TLR-4 KO and wild-type mice fed MD did not display any difference in hepatic steatosis as shown by the (A) representative images of H&E stained liver sections and (B) steatosis score. Intraperitoneal injection of low dose LPS in TLR-4 KO mice fed MD did not make any difference in hepatic steatosis as compared to the wild-type or TLR-4 KO mice fed MD. CD and MD denote control diet and milk-based high fat diet, respectively. Data are expressed as mean $\pm$ SEM; n=6-8.



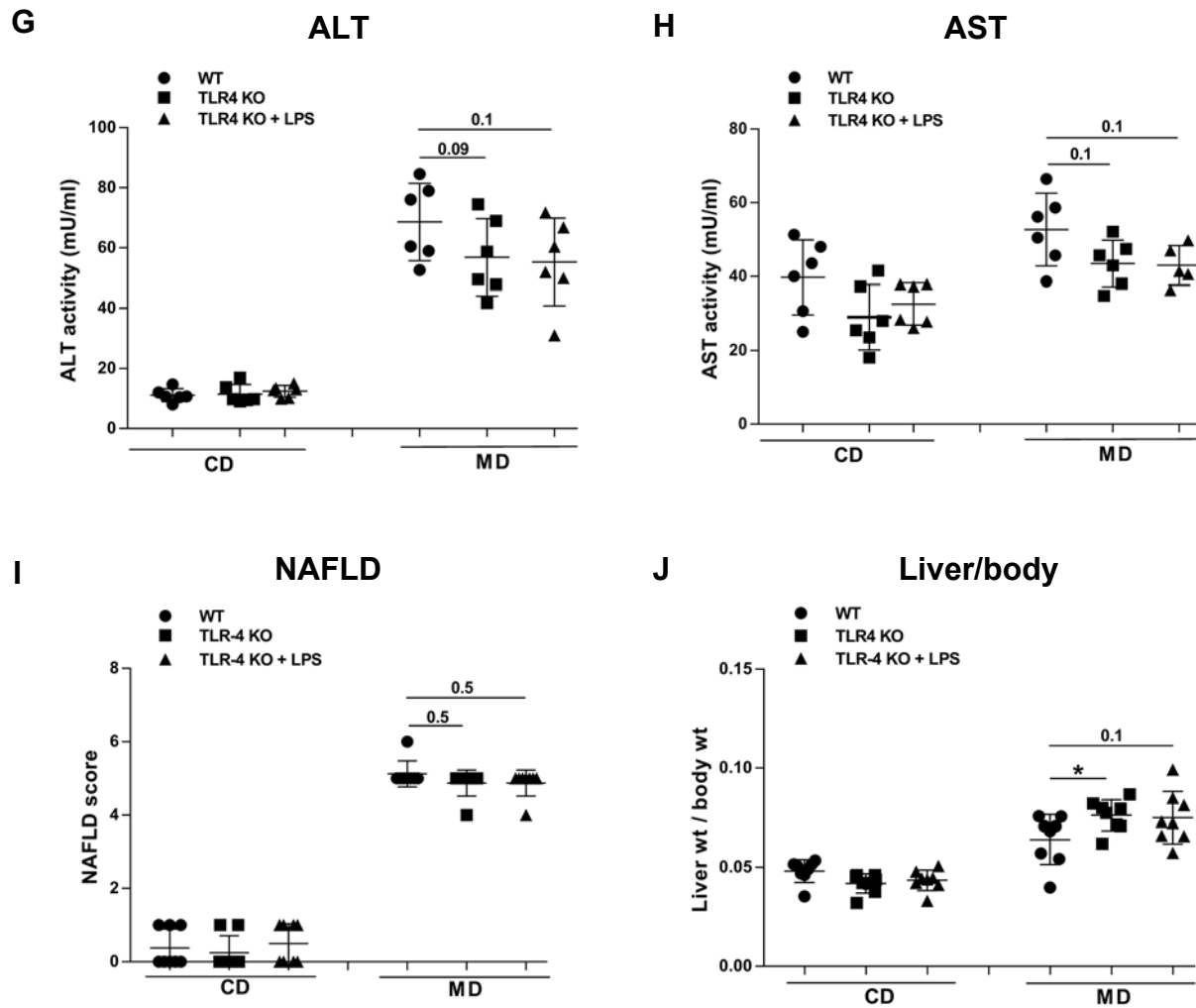


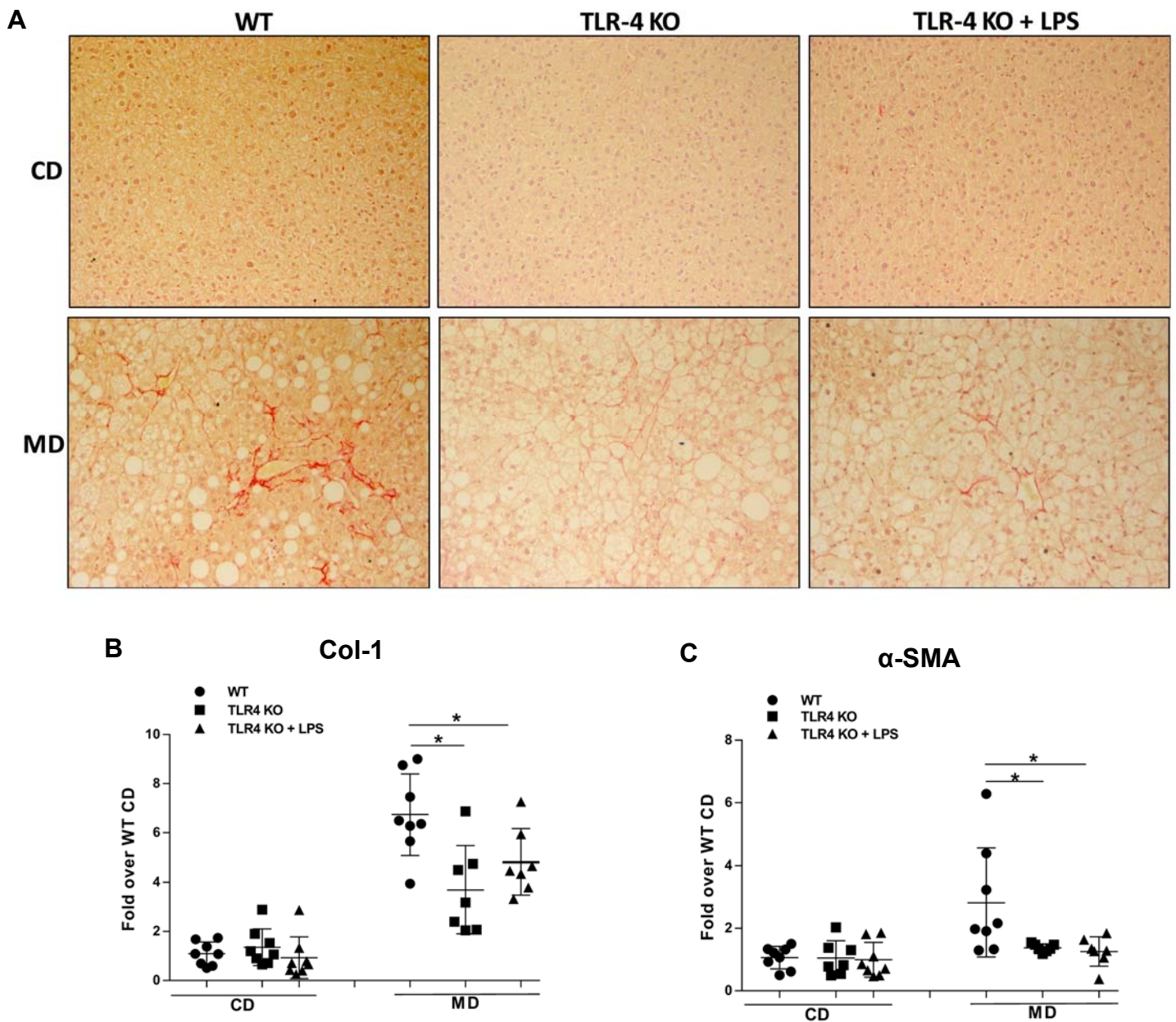
**Figure 6.8. TLR-4 KO mice fed high fat diet exhibited decreased level of NASH which remained unchanged upon injection of low dose LPS.** TLR-4 KO mice fed MD showed decreased levels of (A-D) expression of TNF- $\alpha$ , IL-1 $\beta$ , CCL-2 and TGF- $\beta$ , (E-F) infiltration of neutrophils and macrophages, (G-H) serum activities of ALT and AST, and (I) NAFLD scores in their livers as compared to the wild-type mice fed MD which remained unchanged upon low dose LPS injection. (J) Decreased level of NASH in TLR-4 KO mice fed MD resulted in improved liver health as demonstrated by increased liver-to-body weight ratio which remained unchanged upon low dose LPS injection. CD and MD denote control diet and milk-based high fat diet, respectively. \* $P < 0.05$ , \*\* $P < 0.01$ , \*\*\* $P < 0.001$  (Man-Whitney test); data are expressed as mean  $\pm$  SEM; n=6-8.

did not result in any significant difference in the levels of NASH-indicative markers as compared to the TLR-4 KO mice fed MD with no LPS injection.

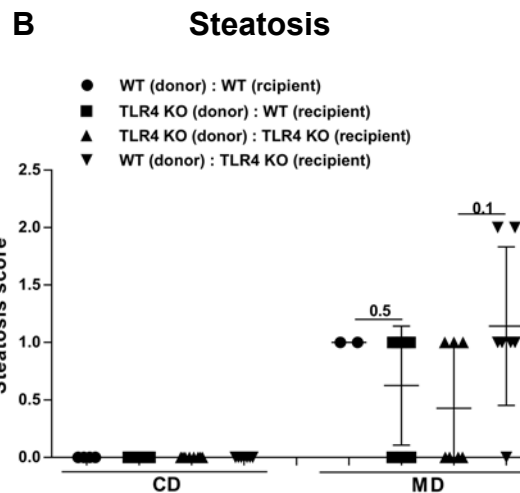
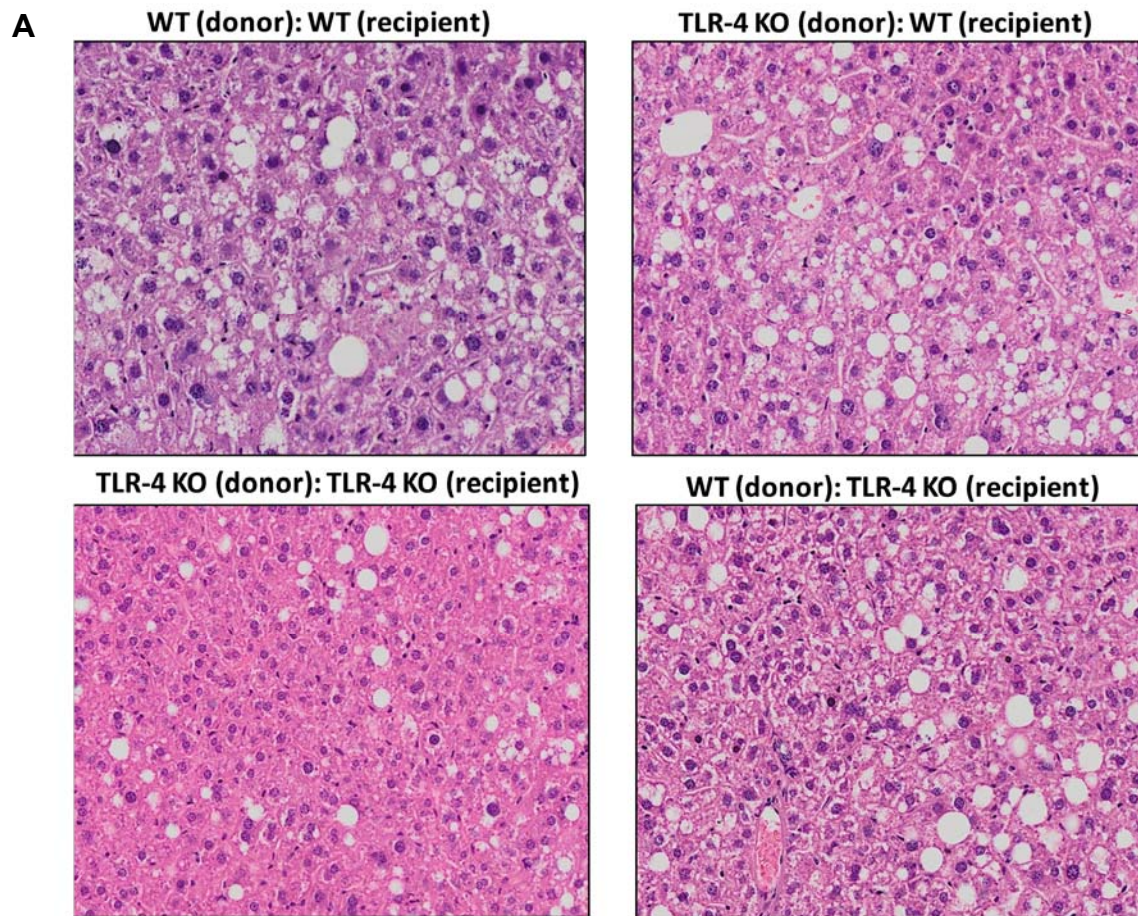
TLR-4 KO mice fed MD exhibited reduced collagen accumulation in their fatty livers as compared to the wild-type mice fed MD as demonstrated by reduced levels of picrosirius red staining of collagen and expression of col-1 and  $\alpha$ -SMA (Fig. 6.9A-C). Injection of low dose LPS in TLR-4 KO mice fed MD did not make any increase in collagen accumulation in their livers as compared to the TLR-4 KO mice fed MD with no LPS injection. These data demonstrate the role of TLR-4 in mediating NASH in mice fed MD.

### **TLR-4-expressing kupffer cells play a crucial role in mediating NASH in mice fed MD**

Once the role of LPS-TLR-4 axis in causing NASH is demonstrated, the next question naturally rises is the role of kupffer cells, as they are the major TLR-4-expressing cells in the liver. To address this question, wild-type mice fed CD or MD were reconstituted with TLR-4 KO kupffer cells, and TLR-4 KO mice fed CD or MD were reconstituted with wild-type kupffer cells through bone marrow transplantation. It was observed that the reconstitution of TLR-4 KO kupffer cells in the livers of wild-type mice fed MD by bone marrow transplantation resulted in a decreasing trend of fat accumulation and steatosis score, as compared to the TLR-4<sup>+</sup> kupffer cells-containing wild-type mice fed MD. On the other hand, reconstitution of wild-type kupffer cells in the livers of TLR-4 KO mice fed MD resulted in an increasing trend of fat accumulation and steatosis score, as compared to the TLR-4 KO kupffer cells-containing TLR-4 KO mice fed MD (Fig. 6.10A-B). These data indicate that TLR-4-expressing kupffer cells are involved in the process of fat accumulation in the livers of mice fed MD.



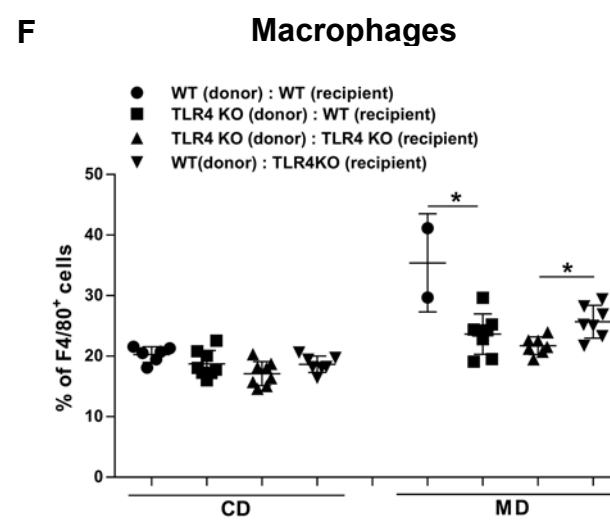
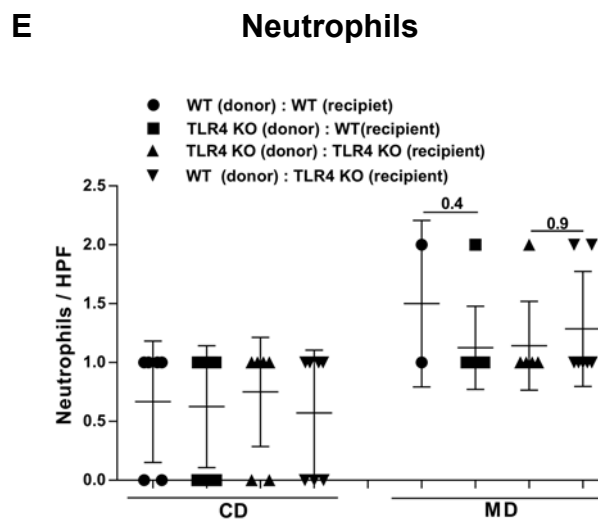
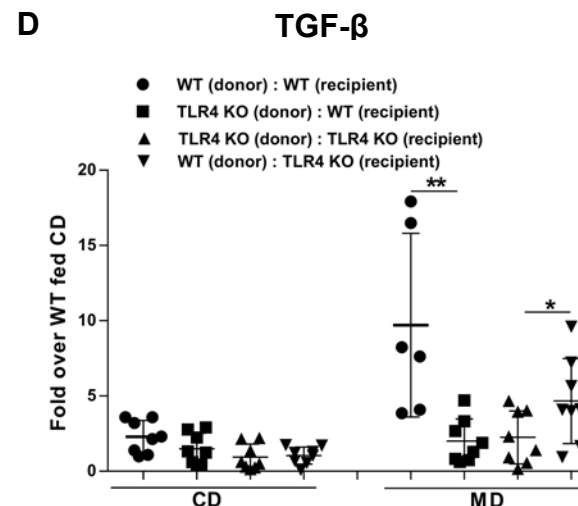
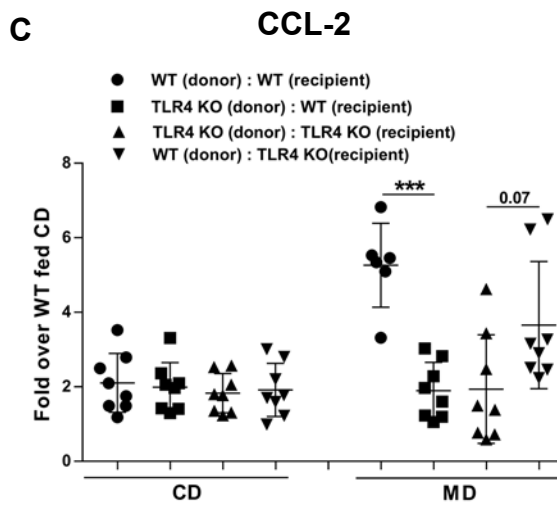
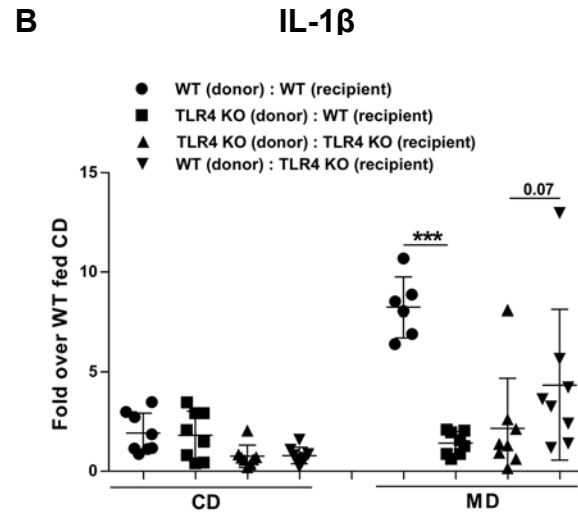
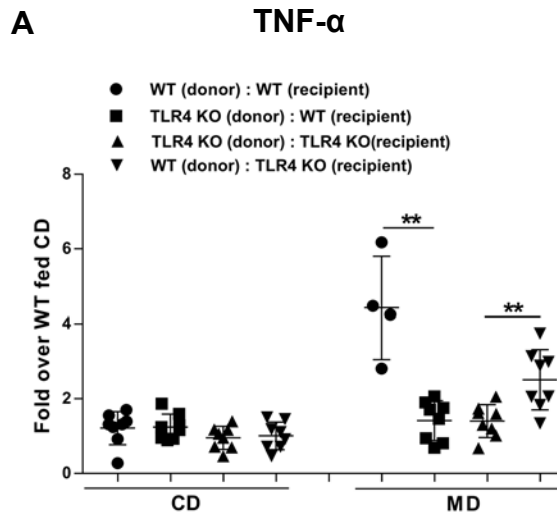
**Figure 6.9. TLR-4 KO mice fed high fat diet displayed decreased level of collagen accumulation in their livers which remained unchanged upon injection of low dose LPS.** TLR-4 KO mice fed MD showed decreased level of collagen accumulation in their livers as compared to the wild-type mice fed MD which remained unchanged upon injection of low dose LPS as shown by the (A) representative images of picosirius red stained liver sections and expression of (B-C) Col-1a and  $\alpha$ -SMA. CD and MD denote control diet and milk-based high fat diet, respectively. \* $P < 0.05$ , \*\*\* $P < 0.001$  (Man-Whitney test); data are expressed as mean  $\pm$  SEM;  $n = 6-8$ .



**Figure 6.10. TLR-4-expressing kupffer cells are involved in the accumulation of fat in mice fed high fat diet.** Reconstitution of TLR-4 KO kupffer cells in the livers of wild-type mice fed MD resulted in a decreasing trend of hepatic steatosis as compared to the TLR-4<sup>+</sup> kupffer cells-containing wild-type mice fed MD; also, reconstitution of wild-type kupffer cells in the livers of TLR-4 KO mice fed MD resulted in an increasing trend of hepatic steatosis as compared to the TLR-4 KO kupffer cells-containing TLR-4 KO mice fed MD as shown by the **(A)** representative images of H&E stained liver sections and **(B)** steatosis score. CD and MD denote control diet and milk-based high fat diet, respectively. Data are expressed as mean±SEM; n=6-8.

Regarding the inflammation in the fatty liver, reconstitution of TLR-4 KO kupffer cells in the livers of wild-type mice fed MD by bone marrow transplantation resulted in reduced levels of expression of TNF- $\alpha$ , IL-1 $\beta$ , CCL-1 and TGF- $\beta$ , infiltration of neutrophils and macrophages, serum activities of ALT and AST and clinical scores of NAFLD, when compared to the TLR-4<sup>+</sup> kupffer cells-containing wild-type mice fed MD. In the same time, reconstitution of wild-type kupffer cells in the livers of TLR-4 KO mice fed MD resulted in increased levels of expression of TNF- $\alpha$ , IL-1 $\beta$ , CCL-1 and TGF- $\beta$ , infiltration of neutrophils and macrophages, serum activities of ALT and AST and clinical scores of NAFLD, when compared to the TLR-4 KO kupffer cells-containing TLR-4 KO mice fed MD. (Fig. 6.11A-I). Decreased level of NASH in the livers of wild-type mice fed MD reconstituted with TLR4-KO kupffer cells was reflected in improved liver health, as demonstrated by the increased liver-to-body weight ratios. Increased level of NASH in the livers of TLR-4 KO mice fed MD reconstituted with wild-type kupffer cells was reflected in exacerbated liver health, as shown by the decreased liver-to-body weight ratios (Fig. 6.11J).

Wild-type mice fed MD reconstituted with TLR4-KO kupffer cells exhibited reduced collagen accumulation in their livers, when compared to the wild-type mice fed MD containing TLR-4<sup>+</sup> kupffer cells, as demonstrated by reduced levels of picosirius red staining of collagen and expression of col-1 and  $\alpha$ -SMA (Fig. 6.12A-C). On the other hand, reconstitution of wild-type kupffer cells in the livers of TLR-4 KO mice fed MD resulted in increased collagen accumulation in their livers, when compared to the TLR-4 KO mice fed MD containing TLR-4 KO kupffer cells, as shown by increased levels of picosirius red staining of collagen and expression of col-1 and  $\alpha$ -SMA (Fig. 6.12A-C).



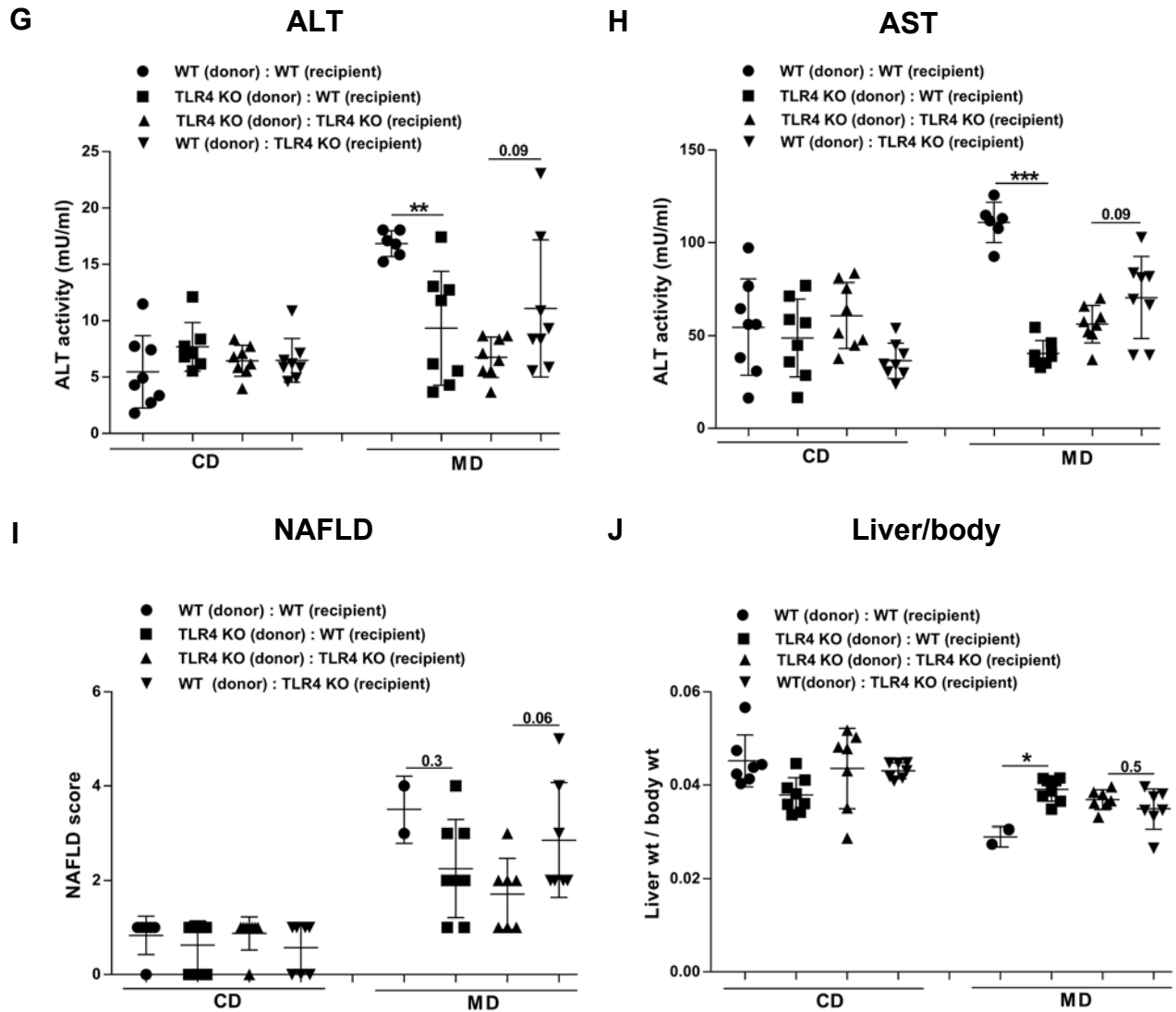


**Figure 6.11. TLR-4-expressing kupffer cells play crucial role in mediating NASH in mice fed high fat diet.** Reconstitution of TLR-4 KO kupffer cells in the livers of wild-type mice fed MD resulted in decreased levels of (A-D) expression of TNF- $\alpha$ , IL-1 $\beta$ , CCL-2 and TGF- $\beta$ , (E-F) infiltration of neutrophils and macrophages, (G-H) serum activities of ALT and AST, and (I) NAFLD scores as compared to the TLR-4<sup>+</sup> kupffer cells-containing wild-type mice fed MD. (J) Decreased level of NASH in wild-type mice fed MD reconstituted with TLR-4 KO kupffer cells resulted in improved liver health as demonstrated by increased liver-to-body weight ratios. On the other hand, Reconstitution of wild-type kupffer cells in the livers of TLR-4 KO mice fed MD resulted in increased levels of (A-D) expression of TNF- $\alpha$ , IL-1 $\beta$ , CCL-2 and TGF- $\beta$ , (E-F) infiltration of neutrophils and macrophages, (G-H) serum activities of ALT and AST, and (I) NAFLD scores as compared to the TLR-4 KO kupffer cells-containing TLR-4 KO mice fed MD. (J) Increased level of NASH in TLR-4 KO mice fed MD reconstituted with wild-type kupffer cells resulted in exacerbated liver health as demonstrated by decreased liver-to-body weight ratios. CD and MD denote control diet and milk-based high fat diet, respectively. \*P<0.05, \*\*P<0.01, \*\*\*P<0.001 (Man-Whitney test); data are expressed as mean $\pm$ SEM; n=6-8.

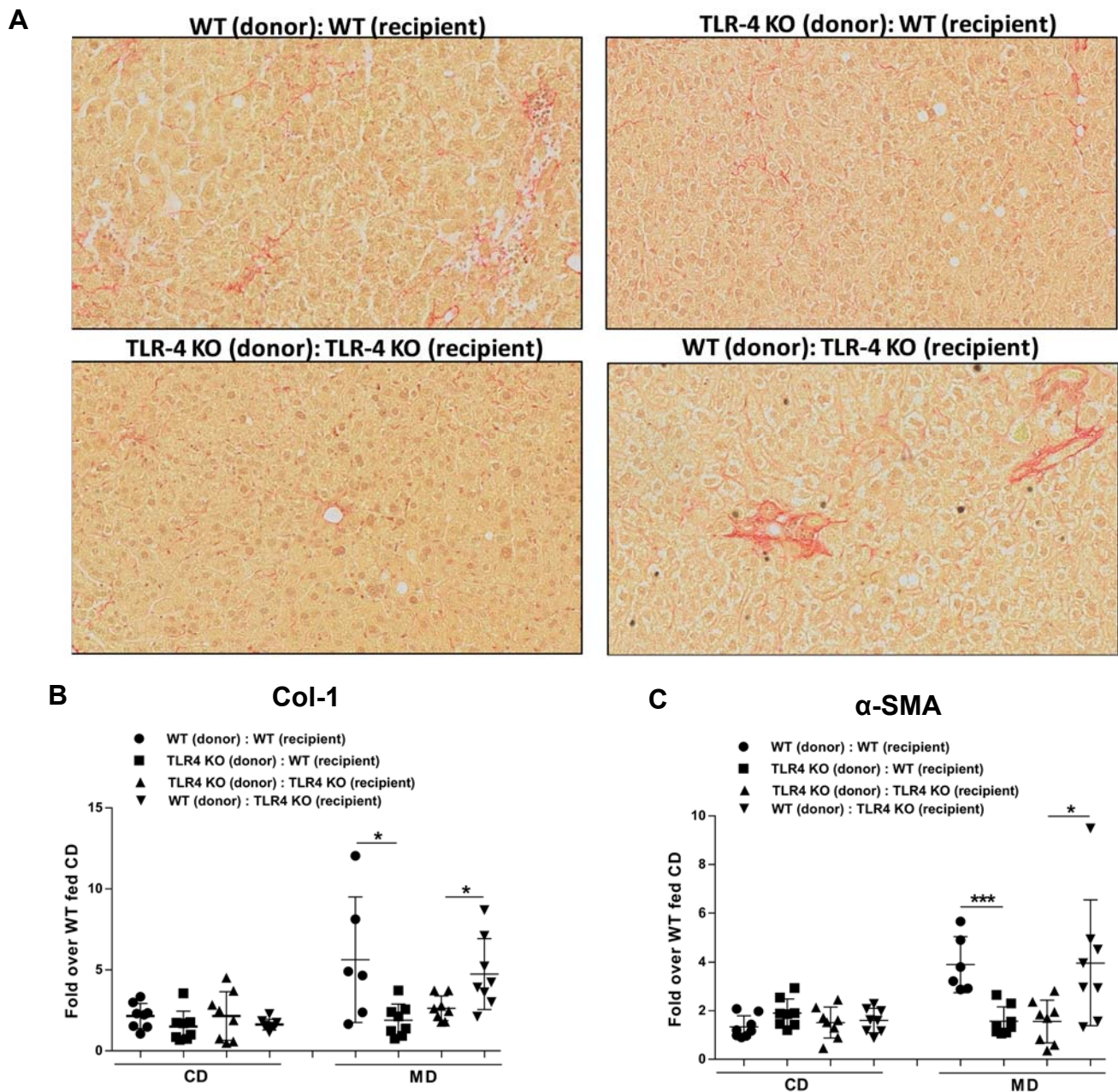
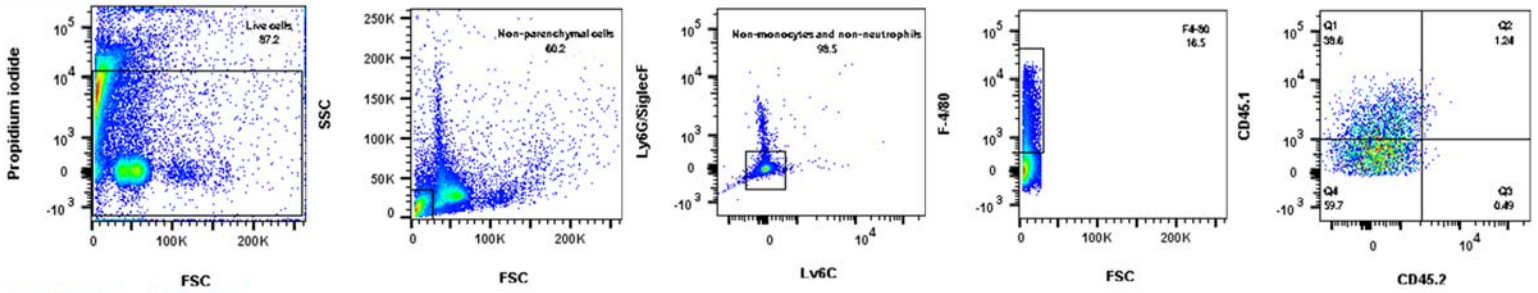


**Figure 6.12. TLR-4-expressing kupffer cells play an important role in collagen accumulation in the livers of mice fed high fat diet.** Reconstitution of TLR-4 KO kupffer cells in the livers of wild-type mice fed MD resulted in decreased level of collagen accumulation in their livers as compared to TLR-4<sup>+</sup> kupffer cells-containing wild-type mice fed MD as shown by the (A) representative images of picrosirius red stained liver sections and expression of (B-C) Col-1a and α-SMA. On the other hand, reconstitution of wild-type kupffer cells in the livers of TLR-4 KO mice fed MD resulted in increased level of collagen accumulation in their livers as compared to TLR-4 KO kupffer cells-containing TLR-4 KO mice fed MD as shown by the (A) representative images of picrosirius red stained liver sections and expression of (B-C) Col-1a and α-SMA. CD and MD denote control diet and milk-based high fat diet, respectively. \*P<0.05, \*\*\*P<0.001 (Man-Whitney test); data are expressed as mean±SEM; n=6-8.

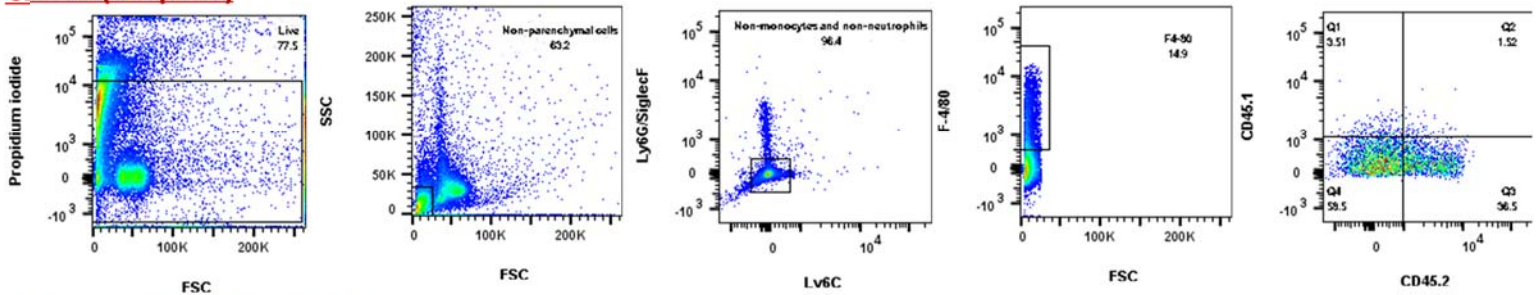
## Reconstituted kupffer cells were derived from the transplanted bone marrow

It is an important question whether the kupffer cells can actually be reconstituted from the transplanted bone marrow. To address this question, bone marrow cells isolated from CD45.1 mice were transplanted into lethally-irradiated and clodronate-treated (to deplete existing kupffer cells) congenic CD45.2 mice. Flow cytometric analyses of non-parenchymal cells isolated from the livers of chimeric mice displayed that 45.9% of the Ly6G/SiglecF<sup>low</sup>Ly6C<sup>low</sup>F-4/80<sup>+</sup> cells were CD45.1<sup>+</sup>. That finding was in line with the results for non-parenchymal cells isolated from the livers of donor mice where 38.6% of the Ly6G/SiglecF<sup>low</sup>Ly6C<sup>low</sup>F-4/80<sup>+</sup> cells were CD45.1<sup>+</sup>. In contrast, 36.5% of the Ly6G/SiglecF<sup>low</sup>Ly6C<sup>low</sup>F-4/80<sup>+</sup> non-parenchymal cells isolated from the livers of recipient mice were CD45.2<sup>+</sup>. These data demonstrate that bone marrow transplantation in lethally-irradiated and clodronate-treated recipient mice results in the reconstitution of kupffer cells in their livers from the transplanted cells (Fig. 6.13).

**A CD45.1 (donor)**



**B CD45.2 (recipient)**



**C CD45.1 → CD45.2 (chimeric)**

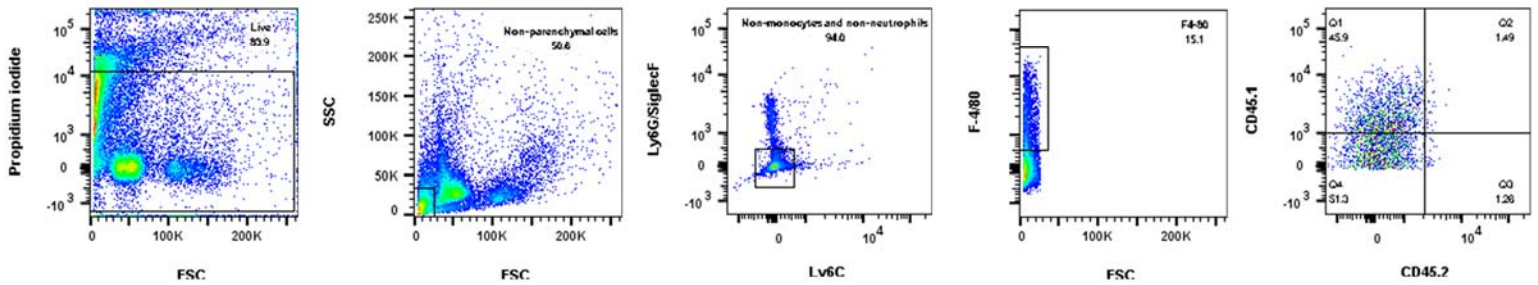


**Figure 6.13. Reconstituted kupffer cells in the livers of bone marrow recipient mice are derived from the transplanted cells.** Representative plots of flow cytometric analyses are showing that most of the live, non-parenchymal and Ly6G/SiglecF<sup>low</sup>Lv6C<sup>low</sup>F-4/80<sup>+</sup> cells in the livers of (A) donor, (B) recipient and (C) chimeric mice were CD45.1<sup>+</sup>, CD45.2<sup>+</sup> and CD45.1<sup>+</sup> respectively.

## **Discussion**

In chapter 5, the generalized involvement of gut microbiota in mediating NASH has been demonstrated. Therefore, the next question to address is about the mechanism of how gut microbiota contributes to the modulation of chronic inflammation on the grounds of a fatty liver. One important mechanism to associate gut microbiota with the pathogenesis of diseases is the production of microbe-associated molecular patterns to induce pro-inflammatory pathways through the interaction with pattern recognition receptors mostly expressed by the innate cells [223].

Gut microbiota produces numerous types of microbe-associated molecular patterns in the intestine that can enter the systemic circulation and induce inflammatory responses through the interaction with their corresponding pattern recognition receptors [224, 225]. Therefore, it is not possible to distinguish the pro-inflammatory capability of individual microbe-associated molecular patterns when they are present together in the system. In this study, we treated mice with broad spectrum antibiotics to diminish their gut microbiota and then injected them with LPS, which allowed us to study the effect solely mediated by this pro-inflammatory molecule without being affected by the responses mediated by others.

TAK-242 is a small compound that selectively inhibits TLR-4 signaling through the interference with interactions between TLR-4 and its adaptor molecules [226]. Therapeutic effect of TAK-242 was shown in mouse models of sepsis and endotoxin-shock [227, 228]. It was also trialed for the treatment of severe sepsis in human [229]. To demonstrate the role of TLR-4 in the modulation of low grade LPS-mediated chronic inflammation in the fatty liver, broad spectrum antibiotics/LPS-treated mice fed MD were

injected with TAK-242 which blunted the inflammation induced by LPS. The outcome from this experiment in mice promises TAK-242 as a potential therapeutic option for NASH in human. Therefore, it could be used for clinical trial as a NASH drug in future.

Noticeably, administration of TAK-242 in mice fed MD not only blunted the increase in levels of pro-inflammatory indicators of NASH in LPS-injected mice fed MD, but also reduced their levels lower than non LPS-injected control mice fed MD (Fig. 6.3-6.4). It indicates a possibility that TAK-242 may interfere not only the LPS-TLR-4 pathway, but also other pro-inflammatory pathways in NASH. Therefore, it could be a new topic of study to investigate the role of TAK-242 in the inhibition of different pro-inflammatory signaling in NASH.

Besides kupffer cells, other types of cells in the liver e.g. hepatocytes, sinusoidal endothelial cells, stellate cells, and hepatic dendritic cells, are also known to express TLR-4 [230, 231]. Therefore, the sole contribution of TLR-4-expressing kupffer cells in mediating NASH had remained unclear. To address this question, kupffer cells in wild-type mice were reconstituted by TLR-4 KO kupffer cells and kupffer cells in TLR-4 KO mice were reconstituted by wild-type kupffer cells through bone marrow transplantation. After induction of NASH, wild-type mice containing TLR-4 KO kupffer cells showed a reduced level of NASH as compared to the wild-type mice containing wild-type kupffer cells. On the other hand, TLR-4 KO mice containing wild-type kupffer cells displayed an elevated level of NASH as compared to the TLR-4 KO mice containing TLR-4 KO kupffer cells. Thus, our experiment clarified the essential role of TLR-4-expressing kupffer cells in mediating NASH.

# Chapter 7

Peroxisomal Structure and Anti-oxidative Function is Compromised in  
NASH in a TLR-4 Dependent Manner

## **Summary**

Peroxisomes are one of the major sites for the generation and decomposition of reactive oxygen species (ROS), in particular hydrogen peroxide (H<sub>2</sub>O<sub>2</sub>). Catalase is the H<sub>2</sub>O<sub>2</sub>-decomposing enzyme exclusively localized in peroxisomes. Catalase detoxifies H<sub>2</sub>O<sub>2</sub> produced not only in peroxisomes but also in mitochondria through peroxisome-mitochondria communication. Therefore, a compromised peroxisomal structure and function can lead to the accumulation of H<sub>2</sub>O<sub>2</sub> that can exacerbate oxidative stress and inflammation. Sublethal dose of endotoxin in rat was reported to induce structural and functional alterations in liver peroxisomes which led us to investigate the role of TLR-4 pathway in mediating any alteration in peroxisomal structure and anti-oxidative function in the steatotic livers of mice. Fluorescent Immunohistochemistry of peroxisomal membrane protein 70 (PMP70) and catalase in the liver sections of mice fed MD displayed a reduced level of immunofluorescence intensity, when compared to the mice fed control diet, indicating an altered peroxisomal structure and anti-oxidative function respectively. Fluorescence intensity of immuno-stained PMP70 and catalase significantly increased in the livers of TLR-4 KO mice fed MD, when compared to the wild-type mice fed MD, indicating that alteration of peroxisomal structure and anti-oxidative function in NASH is dependent on TLR-4 pathway. Catalase activity assay using tissue homogenates from mice fed MD demonstrated a reduced level of catalase activity, as compared to the mice fed CD, which increased in TLR-4 KO mice fed MD. These data indicated that TLR-4 pathway mediates an alteration in peroxisomal structure and anti-oxidative function in NASH. Thus, our study provides a new insight into the pathophysiological mechanism of how TLR-4 pathway contributes to the pathogenesis of NASH.

## **Introduction**

Peroxisomes are essential subcellular organelles which are ubiquitous in eukaryotic cells [232]. They have indispensable role in the synthesis of bile acids, myelin lipid plasmalogens, and docosahexaenoic acids and catabolism of long-chain fatty acids, very-long-chain fatty acids, and branched-chain fatty acids through a set of  $\alpha$  and  $\beta$ -oxidation reactions [232-234]. Apart from lipid catabolism, peroxisomes are also involved in degradation of polyamines, glyoxylate, certain amino acids, arachidonic acids, and several xenobiotics [234]. In addition, peroxisomes are also involved in generation and scavenging of reactive oxygen species (ROS) produced inside and outside this organelle [235]. Thus, peroxisomes play an important role in cell metabolism and metabolic homeostasis through communication with other organelles especially mitochondria [236]. Critical metabolic role of peroxisome is closely associated with the exertion of control over inflammatory responses. Peroxisomes exert control over inflammation in three different ways. First, degradation of pro-inflammatory arachidonic acids; second, synthesis of anti-inflammatory docosahexaenoic acids; and third, scavenging of ROS.

One important catabolic function of peroxisome is the degradation of arachidonic acid derivatives known as eicosanoids. Commonly known eicosanoids are prostaglandins, thromboxanes, leukotrienes, and prostacyclins which have tremendous role in the elicitation of broad ranging inflammatory responses. Most important pro-inflammatory activities mediated by these molecules are vasodilation/vasoconstriction, leukocyte migration and platelet aggregation [237, 238].

Peroxisomes contain enzymes which contribute to the synthesis of docosahexaenoic acids. Docosahexaenoic acids are peroxisomally produced omega-3

fatty acids used as precursors for resolvins, maresins and protectins. These molecules possess potent anti-inflammatory and immunoregulatory functions [239-241].

Peroxisomes play a dual role in generation and detoxification of ROS particularly hydrogen peroxide ( $H_2O_2$ ). Peroxisomes contain different oxidases that generate  $H_2O_2$  as a byproduct of their oxidation reactions. These oxidases are co-localized with catalase which is exclusively found in peroxisomes. Catalase decomposes  $H_2O_2$  into  $H_2O$  and molecular oxygen [242]. Catalase scavenges  $H_2O_2$  generated not only in peroxisomes but also in extra-peroxisomal sites like mitochondria. Peroxisomes and mitochondria can exchange their metabolites including  $H_2O_2$  through intra-organellar diffusion, vesicular traffic or direct physical contact [236]. Therefore, depending on the abundance of peroxisomes within the cells and their catalase content, they can efficiently detoxify cellular  $H_2O_2$  generated within the cells during the metabolic reactions [232, 233, 243]. Impaired detoxification of  $H_2O_2$  by peroxisomes due to their structural and functional alterations in an inflamed milieu can result in an increased level of oxidative stress and thereby exacerbate the inflammation [235].

Liver is the key metabolic organ which governs the energy balance of the body [244]. Peroxisomes are most abundant in hepatocytes where they constitute round 1-2% of the total cell volume [245]. Thus, peroxisomes play the major role in the neutralization of bulk amount of  $H_2O_2$  continuously produced in this metabolically active organ. Hepatic steatosis results in enhanced production of  $H_2O_2$  making the organ more dependent on peroxisomes for safe disposal of  $H_2O_2$  [246]. Therefore, there is a concern about any impairment in peroxisomal function that can potentially exacerbate the oxidative stress in the steatotic liver and facilitate the progression of the disease to NASH.

Knowledge about an impaired peroxisomal function in NASH first came from the observation that homozygous mutation of the peroxisome proliferator-activated receptor- $\alpha$  gene (PPAR- $\alpha$ ), the key regulator of genes involved in peroxisomal proliferation, accumulate fat in the liver of mice under a starved condition [247]. Subsequent study showed that acyl-coenzyme A oxidase null mice, the rate limiting enzyme for peroxisomal  $\beta$ -oxidation, leads to the development of NASH, further indicating the role of impaired peroxisomal function in mediating NASH [248]. Therefore, we anticipated that there occurs an impairment in peroxisomal structure and antioxidative function in dietary fat mediated NASH. It was reported that intraperitoneal injection of sublethal dose of LPS in rat alters the structure, number, and function of peroxisomes [249, 250]. Elevated expression of TLR-4 in the steatotic liver has been associated with the increased sensitivity to gut-derived LPS resulting in chronic inflammation [251, 252]. Therefore, in this current study, we examined the effect of TLR-4 pathway on peroxisomal structure and antioxidative function in the modulation of NASH in mice fed MD.

## **Results**

### **Peroxisomal structure is altered in the livers of mice fed MD in a TLR-4 dependent manner**

Fluorescence immunohistochemistry of PMP70, a major component of peroxisomal membrane [253], in the liver sections of mice fed MD demonstrated a decreased fluorescence intensity as compared to the mice fed CD. In the same time, immunofluorescence-stained liver sections of TLR-4 KO mice fed MD displayed an increased level of fluorescence intensity than WT mice fed MD (Fig. 7.1). This data indicated that peroxisomal structure is altered in mice fed MD in a TLR-4-dependent manner.

### **Catalase level and activity are decreased in the livers of mice fed MD in a TLR-4 dependent manner**

An alteration in peroxisomal structure led us to investigate the plausible change in peroxisomal antioxidative function. Fluorescence immunohistochemistry of catalase, a major antioxidative enzyme exclusively found in peroxisomes, in the liver sections of mice fed MD demonstrated a decreased fluorescence intensity as compared to the mice fed CD. In the same time, immunofluorescence-stained liver sections of TLR-4 KO mice fed MD displayed an increased level of fluorescence intensity than WT mice fed MD (Fig. 7.2). This data indicated that catalase level is altered in mice fed MD in a TLR-4-dependent manner.

Western blot analysis demonstrated a decreased level of catalase in the livers of wild-type mice fed MD as compared to the wild-type mice fed CD. In the same time,

Catalase level was increased in TLR-4 KO mice fed MD (Fig. 7.3A-B). This data indicated that the level of catalase in mice fed MD is decreased in a TLR-4 dependent manner which was consistent with the observation in fluorescence immunohistochemistry of catalase. Of note, catalase level was also increased in TLR-4 KO mice fed CD compared to the WT mice fed CD. This indicated the catalase level is very sensitive to the basal activity of TLR-4 pathway.

Catalase activity assay was performed using liver tissue homogenates. Catalase activity was decreased in wild-type mice fed MD as compared to the wild-type mice fed CD. Catalase activity significantly increased in TLR-4 KO mice fed MD as compared to the wild-type mice fed MD indicating the role of TLR-4 pathway-mediated chronic inflammation on catalase activity in NASH (Fig. 7.3C). Catalase activity data was consistent with the level of catalase displayed by fluorescence immunohistochemistry and Western blot analysis.

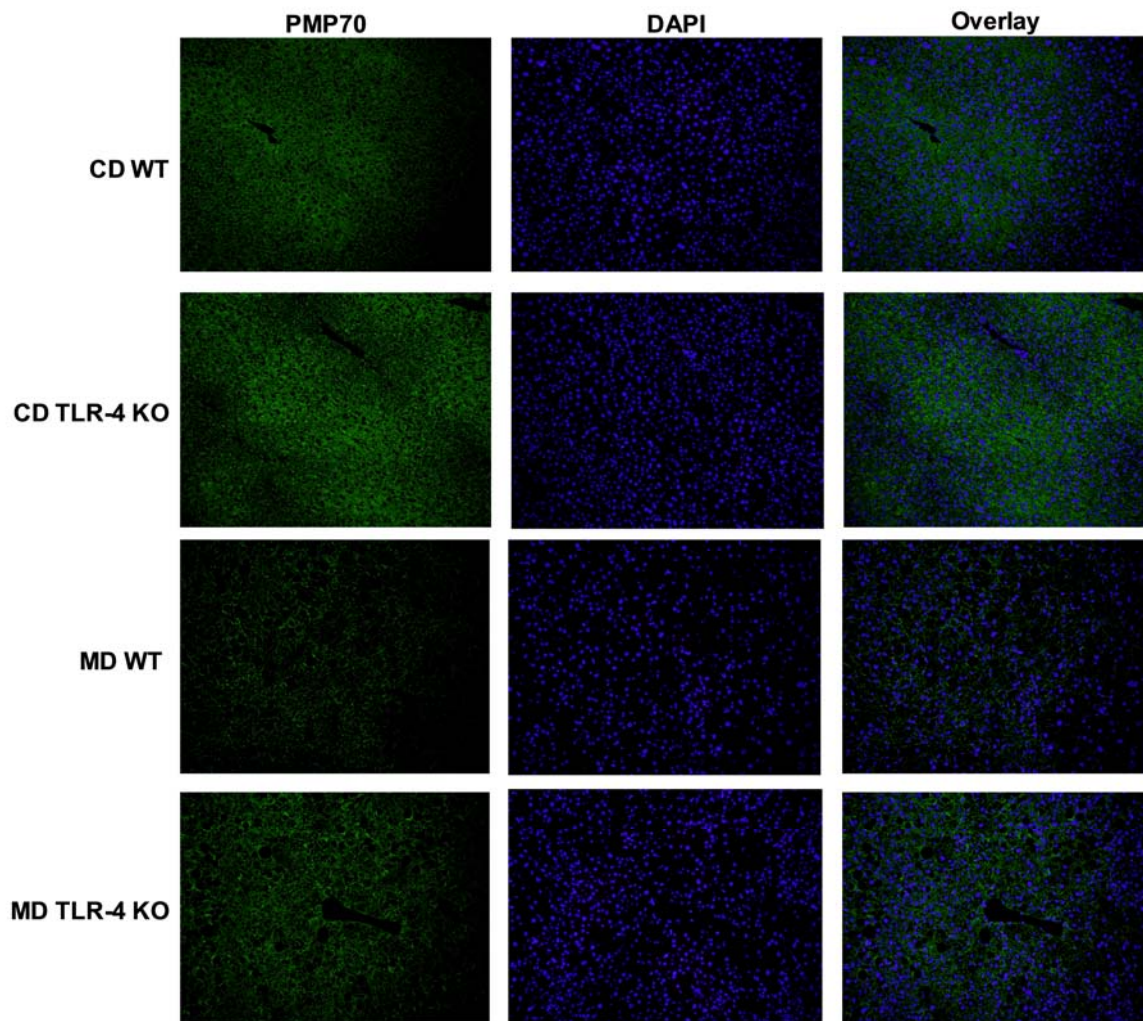


**Figure 7.1. Fluorescence immunohistochemistry of peroxisomal membrane protein 70 in liver sections displayed a reduced level of fluorescence intensity in mice fed milk-based high fat diet in a TLR-4 dependent manner.** Immunofluorescence staining of peroxisomal membrane protein 70 in liver sections displayed a reduced level of fluorescence intensity in WT mice fed MD as compared to the WT mice fed CD. Fluorescence intensity increased in TLR-4 KO mice fed MD as compared to the WT mice fed MD. CD and MD denote control diet and milk-based high fat diet, respectively.

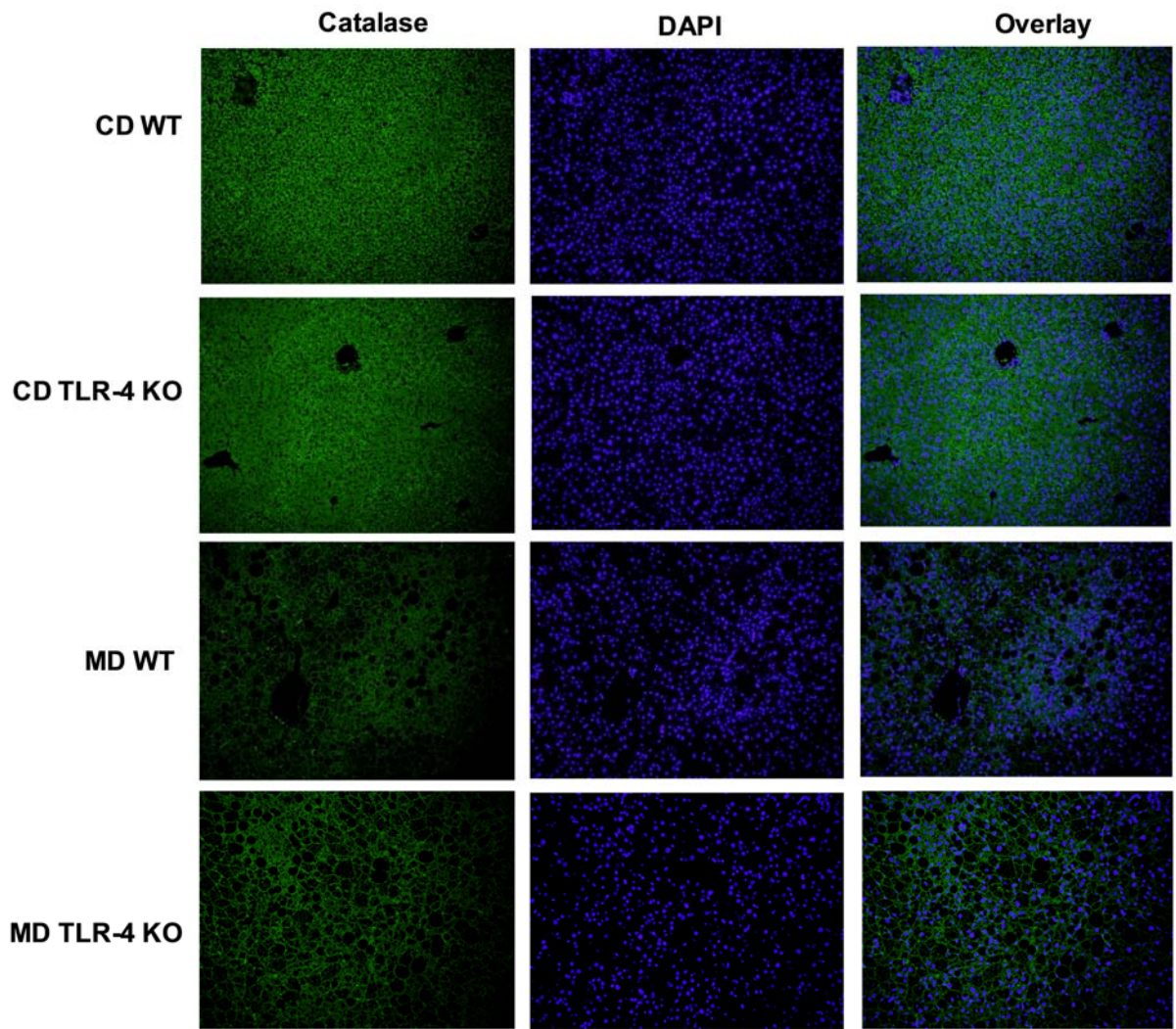


**Figure 7.2. Fluorescence immunohistochemistry of catalase in liver sections displayed a reduced level of fluorescence intensity in mice fed milk-based high fat diet in a TLR-4 dependent manner.** Immunofluorescence staining of catalase in liver sections displayed a reduced level of fluorescence intensity in WT mice fed MD as compared to the WT mice fed CD. Fluorescence intensity increased in TLR-4 KO mice fed MD as compared to the WT mice fed MD. CD and MD denote control diet and milk-based high fat diet, respectively.

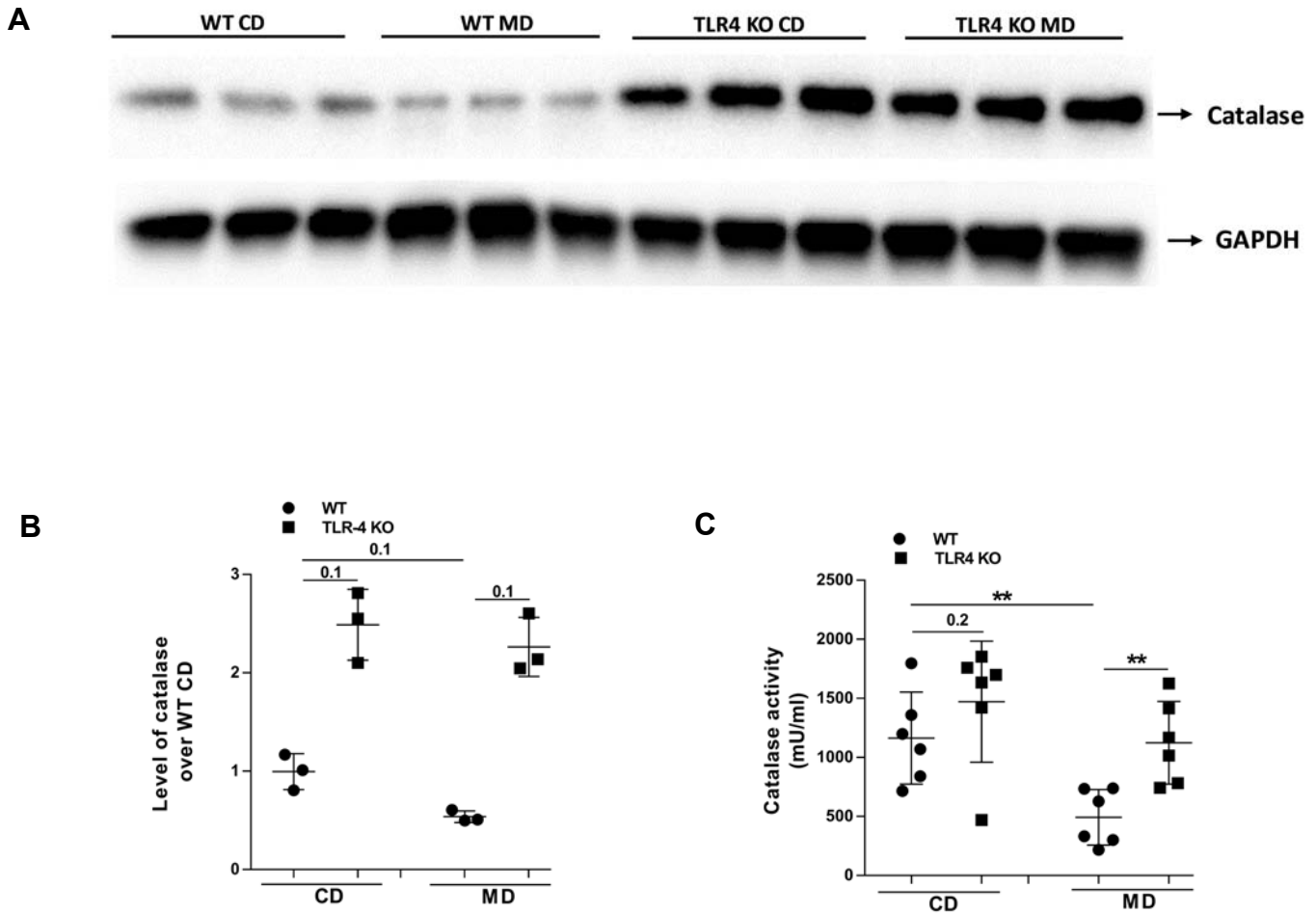


**Figure 7.3. Catalase level and activity are decreased in the livers of mice fed milk-based high fat diet which is dependent on TLR-4.** Catalase level and activity were decreased in the livers of mice fed MD as compared to the mice fed CD in TLR-4 dependent manner as shown by (A) Western blot analysis (B) Image J analysis of the Western blot image and (C) catalase activity assay. CD and MD denote control diet and milk-based high fat diet, respectively. \* $P < 0.05$ , \*\* $P < 0.01$  (Man-Whitney test); data are expressed as mean  $\pm$  SEM;  $n = 3-6$ .

## **Discussion**

Reactive oxygen species (ROS) are endogenously produced as byproducts of cellular metabolic processes in mitochondria and peroxisomes [254, 255]. Cellular homeostasis mediated by anti-oxidant defense system prevents the accumulation of ROS within the cells. When the level of ROS overwhelms the anti-oxidant defense system, whether through an excessive production of ROS or a reduction of anti-oxidant defense capacity, oxidative stress occurs [256]. A sustained oxidative stress can lead to chronic inflammation which can potentially serve as a cause of different advanced stage diseases [257, 258].

Peroxisomes are single membrane-bounded ubiquitous organelles in eukaryotic cells [255]. Several metabolic processes, including catalase-mediated detoxification of  $\text{H}_2\text{O}_2$ , exclusively occur in peroxisomes [259]. The number, morphology, and activity of peroxisomes can remarkably vary depending on the tissue, organ, and nutritional and metabolic status [236]. Peroxisomes produce different ROS from different metabolic pathways that are neutralized by enzymatic and non-enzymatic anti-oxidant defense systems. Catalase is a unique member of peroxisomal anti-oxidant defense system which neutralizes  $\text{H}_2\text{O}_2$  in a catalytic ( $2 \text{H}_2\text{O}_2 \rightarrow 2 \text{H}_2\text{O} + \text{O}_2$ ) or peroxidatic ( $\text{H}_2\text{O}_2 + \text{AH}_2 \rightarrow \text{A} + 2 \text{H}_2\text{O}$ ) manner [259]. Although catalase is localized exclusively within peroxisomes, they can decompose  $\text{H}_2\text{O}_2$  produced not only in peroxisomes but also in extra-peroxisomal sites such as mitochondria through inter-organellar exchange of metabolites [236]. Thus, catalase-mediated detoxification of  $\text{H}_2\text{O}_2$  in peroxisomes plays an indispensable role in preventing the cell from reaching the stage of oxidative stress. Besides catalase, peroxisomes are also required for the biosynthesis of plasmalogens.

Plasmalogens are ether-phospholipids known to have anti-oxidative function, but it is still unclear how much role they play in providing anti-oxidative defense [260].

Oxidative stress is the key mediator of NASH, which is caused by the increased availability of free fatty acids in the steatotic livers [261, 262]. Therefore, NASH-affected livers are in increased demand of anti-oxidative mediators. Impaired detoxification of H<sub>2</sub>O<sub>2</sub> in NASH-affected livers due to any alteration in peroxisomal structure and function may exacerbate the severity of the disease. In this study, we have shown that the catalase level and activity decrease in the livers of mice model of NASH which are reversed in TLR-4 KO mice indicating the role of TLR-4 pathway in the modulation of anti-oxidative function of catalase. It may be due to the adverse effect of TLR-4 pathway-mediated low grade chronic inflammation on the structure and/or function of peroxisomes in the fatty liver. Not only in TLR-4 KO mice fed MD, we have also observed an increase in catalase level and activity in the livers of TLR-4 KO mice fed CD as compared to the wild-type mice fed CD. It might be due to the sensitivity of peroxisomal structure and function to the basal activation of TLR-4.

The findings presented in this study are in line with previous reports demonstrating the role of endotoxin-induced inflammation in alteration of peroxisomal structure-function in the liver [249, 250]. Endotoxin-induced inflammation causes change in lipid composition of peroxisomes in the liver [250]. Because the concentration of circulating endotoxin is increased in NASH, it is important to know how the lipid composition of peroxisomes are affected in NASH. Besides endotoxin-induced inflammation, increased concentration of free fatty acids is also an important contributor to organelle malfunction. Increased concentration of free fatty acids alters the lipid composition in mitochondria and

endoplasmic reticulum, resulting in their impaired function [263, 264]. Because fat accumulation in the liver results in an increased concentration of free fatty acids, it demands a comprehensive study to determine the changes in structural composition of peroxisomes to have a clearer picture on their impaired anti-oxidative function in NASH. TLR-4 pathway-mediated alteration of peroxisomal structure/function in NASH may not only reduce their anti-oxidative activity but also impact the peroxisome-mediated synthesis of anti-inflammatory and degradation of pro-inflammatory molecules. Therefore, it requires a further investigation to study the effect of TLR-4 pathway on the peroxisomal metabolism of different pro and anti-inflammatory molecules potentially associated with NASH.

# Chapter 8

## Conclusions and Overall Discussion

Because chronic inflammation is the principal reason for the progression of a benign fatty liver into an end stage disease, the ultimate goal of all NASH research is to stop the inflammation. To stop the inflammation in the fatty liver, it is urgent to reduce the availability of causative agents of inflammation, or therapeutically interfere with their signaling pathways. In this project, gut microbiota has been studied as a potential source of pro-inflammatory agents of NASH. We have comprehensively investigated the role of the gut microbiota-derived LPS-TLR-4 pathway as a potential mediator of NASH with therapeutic relevance, using an appropriate experimental model.

### **Study of NASH in mice fed high fat diet represents a clinically relevant model**

When compared to other genetic and diet-based models of NASH, high fat diets are clinically more relevant for some genuine reasons. First, high fat diets do not contain any ingredient that is unusual in the regular human diet. In fact, high fat diets are prepared from sources that are commonly consumed by humans, e.g., vegetable oil, coconut oil, milk fat, beef tallow, lard and other sources [265]. Second, high fat diets mimic western diets in having high fat content [266]. Third, high fat diets induce the development of NASH spontaneously without requiring any additional dietary intervention [150]. When compared to other dietary models, high fat diets require a longer period of feeding to induce NASH. For instance, a methionine and choline deficient diet induces NASH at day 10 of feeding, whereas a high fat diet requires 8-12 weeks [133, 142, 150, 267]. This requirement of long-term feeding is consistent with NASH patients requiring a long period of pathogenesis [150]. Finally, high fat diets result in the development of obesity and NASH simultaneously, which is a common scenario in the case of NASH patients [150].

Therefore, high fat diets offer an opportunity to study NASH within the context of metabolic syndrome, which is known to manifest as NAFLD in the liver.

Both unsaturated and saturated fats are present in regular human diets [157]. The role of saturated fats in inducing steatosis and chronic inflammation in the liver has been demonstrated in numerous reports [160-163]. In line with those findings, we designed a comparisomal study between a milk-based saturated high fat diet and a lard-based saturated diet, thus demonstrating the higher efficiency of a milk-based saturated high fat diet over a lard-based unsaturated high fat diet in inducing NASH. We also performed an experiment where mice were fed at three different time points (8, 16 or 32 weeks) resulting in a significantly higher level of NASH at weeks 16 and 32, as compared to week 8. Based on these results, we fed mice with a milk-based saturated high fat diet for 16 weeks to ensure a maximum level of steatosis and inflammation in the remaining experiments of the study.

To keep our animal study consistent with human patients, it was important to evaluate the level of disease with methods similarly used for diagnostic purposes in humans. We used both noninvasive and invasive methods to detect and measure the level of NASH in mice. In the case of human patients, noninvasive methods are of first preference. Imaging techniques, e.g., ultrasonography, computerized tomography, and magnetic resonance imaging are widely used noninvasive methods to identify fat deposition in the liver. One major limitation of those imaging methods is that they cannot distinguish steatosis from NASH [268-271]. Therefore, imaging methods were of no use in our NASH study on animal models. Assays employed for determining ALT and AST activities in serum are also commonly used noninvasive methods of NASH diagnosis.

Elevated levels of ALT and AST activity in serum indicates hepatocyte damage subsequent to hepatic inflammation. Those levels can rise up to five fold in NASH patients compared to their upper limits in healthy individuals. Although ALT and AST activity in serum cannot give an accurate indication about the degree or severity of liver disease, those markers were used as an important indicator of NASH in our study [268, 272, 273]. Apart from those noninvasive methods, liver biopsy is the most reliable invasive technique to diagnose NASH. Biopsy samples are used for histology that can diagnose as well as evaluate the level of disease. Biopsy sections are evaluated based on steatosis, inflammation, hepatocyte ballooning, necrosis, and fibrosis. Yet liver histology is a controversial tool to diagnose NASH in humans due to the risks of biopsy and the validity of a tiny biopsy for representing NASH in the entire liver [272, 274]. Due to the availability of tissue post euthanization, liver histology is an unquestionably useful method for disease evaluation in animal models of NASH. Thus, because of the application of different, clinically used noninvasive and invasive indicators of NASH, our study outcome has strong clinical relevance.

### **Gut microbiota spans gut-liver axis in causing NASH**

In this project, we also studied the role of gut microbiota in mediating NASH. We found a reduced level of dietary fat-mediated chronic inflammation in the livers of mice that were germ free or treated with broad spectrum antibiotics, as compared to control mice. Mechanisms explaining the communication between the gut microbiota and NASH are still widely investigated. A large body of evidence from both population and animal studies clearly indicates that changes in the composition of gut microbiota are closely associated with NASH. One widely studied mechanism of gut microbiota in inducing

NASH is altered production of metabolites. For instance, changes in gut microbiota of NASH patients result in higher abundance of *Escherichia* and increase the level of endogenous alcohol in the circulation, leading to the increased production of ROS in the liver [275, 276]. Another important metabolic role of gut microbiota is the production of short chain fatty acids, which provide nutrients and energy essential for maintaining gut health and integrity. An altered production of short chain fatty acids results in defective gut permeability, leading to an increase of pro-inflammatory microbial elements in the portal circulation [277]. Gut microbiota also has an important role in the regulation of intestinal lipid absorption mediated by the deconjugation of bile acids in intestine. Deconjugation of bile acids is mediated by the removal of polar groups of glycine and taurine catalyzed by gut microbial enzymes. Impaired deconjugation of bile acids can lead to increased emulsification and absorption of dietary fat, resulting in hepatic steatosis [277, 278]. It is still not clear whether the abundance of microbes expressing the enzymes associated with bile acid deconjugation is altered in NASH.

Apart from their metabolic functions, the supply of pro-inflammatory microbes-associated molecular patterns into the liver is also a potential mechanism of gut microbiota in mediating NASH. Prominent microbes-associated molecular patterns involved in NASH include endotoxin, peptidoglycan, flagellin, and microbial nucleic acids [279]. In this comprehensive study, we demonstrated the role of gut-derived LPS in mediating NASH through the TLR-4 receptor.

### **Gut microbial community gets changed in NASH**

The role of specific microbes has been reported to induce different inflammatory diseases in mice fed a high fat diet. A milk-based saturated fat diet can induce colitis in

IL10<sup>-/-</sup> mice through the expansion of *Bilophila wadsworthia* [159]. The *Enterobacter cloacae* B29 strain isolated from the gut of an obese human has been shown to induce obesity and insulin resistance in germ free C57BL/6J mice fed a high fat diet, whereas germ free control mice on a high-fat diet were protected from disease phenotypes [280]. Our current project revealed an overall change in the structure of gut microbial community in mice fed MD, but we could not identify a specific microbe associated with NASH. Therefore, it is important to undertake a future investigation to identify microbes whose presence could be directly related to the pathogenesis of NASH.

Feeding mice with a high fat diet has been reported to result in increased concentration of circulating endotoxin [122, 123]. Consistent with those reports, we have shown a trend of higher concentration of endotoxin in the portal serum of mice fed MD, as compared to the mice fed CD. Those data led us to investigate whether the composition of gut microbiota is changes, resulting in an increased abundance of Gram negative bacteria in mice fed MD. However, our 16s rRNA analysis displayed a decrease in the relative abundance of *Bacteroidetes*, the major Gram negative phylum in gut microbiota in mice [281]. Yet the relative abundance of *Proteobacteria*, another important Gram negative phylum in the gut microbiota of mice, was significantly increased [282]. Further investigation is required to determine if the entire phylum of *Proteobacteria* or any specific microbe within the phylum, plays a key role in mediating chronic endotoxemia in mice fed MD.

### **Altered gut permeability facilitates the elevation of circulating endotoxin level**

The elevated concentration of gut microbiota-derived pro-inflammatory components in the circulation of NASH patients, especially endotoxin, is mediated by

increased gut permeability [283, 284]. However, a comprehensive assessment in an animal model is yet to be performed in order to explain the relationship between gut permeability and NASH. In the case of obesity, an increased level of TNF- $\alpha$  in the serum has been associated with inflammation in the intestine leading to gut leakage [285]. In our study, a higher level of expression of TNF- $\alpha$  was observed in the livers of NASH-affected mice. Therefore, it is possible that an increased production of TNF- $\alpha$  in the altered cytokine milieu of NASH eventually leads to the inflammation in intestine. Additionally, changes in gut microbiota in NASH may also alter intestinal permeability through the pathways driven by bacterial metabolites. Zhu and colleagues reported that expression of alcohol-metabolizing enzymes are up-regulated in NASH livers [276]. In a follow-up study, they reported that the abundance of alcohol-producing *Escherichia* is increased in the gut of NASH patients as compared to non-obese and obese non-NASH controls, leading to an elevated concentration of alcohol in the blood serum of NASH patients [275]. Gut microbiota-produced alcohol is known to have a potential role in increasing gut permeability [286] and the generation of reactive oxygen species in the liver [287]. Thus, gut permeability and NASH participate in a positive feedback loop in causing the disease. In our animal study, *Clostridium* was the only alcohol-producing genus whose abundance was increased in the gut microbiota of NASH. Further investigation is required to determine the extent to which *Clostridium* contributes to the mediation of gut permeability.

### **LPS-TLR-4 pathway plays an essential role in mediating NASH**

Using a unique approach, we studied the role of LPS in causing NASH through the injection of LPS in mice treated with broad spectrum antibiotics. The purpose of LPS

injection in broad spectrum antibiotics-treated mice was to ensure the presence of LPS in the system as the sole pro-inflammatory agent derived from microbes. Therefore, the TLR-4-mediated inflammation in the fatty liver was attributed only to LPS, not to any other microbial agents. Apart from microbes-derived LPS, there are many endogenous host-derived ligands of TLR-4 with varying activation potential, e.g., low-molecular weight hyaluronic acid, heparin sulfate, saturated fatty acid, fibrinogen, fibronectin, heat shock proteins 60 and 70, high mobility group box-1, and degraded matrix [288]. It is still not clear what level of TLR-4 activation is contributed by these endogenous ligands.

The level of TLR-4 pathway activation can vary depending on the types of LPS. Acylation of lipid A, the actual site of LPS recognized by TLR-4, can vary in terms of number, length, and saturation level of fatty acyl chains [289]. While human TLR-4 can sense only hexaacyl lipid A, murine TLR-4 can sense pentaacyl or tetraacyl lipid A [290]. Furthermore, lipid A attached with saturated fatty acyl chains with lengths of 12 or 14 (or occasionally 16) are better agonists of TLR-4 [291]. In the complex ecology of gut microbiota, LPS molecules with different types of lipid A are produced. Therefore, it is important to investigate whether the altered gut microbiota in the mice fed a high fat diet produce higher levels of those types of LPS, which are stronger agonists of TLR-4.

### **TLR-4 pathway is a promising target for therapeutic intervention against NASH and ischemia/reperfusion injury in liver transplantation**

High fat diet-mediated hepatic steatosis in TLR-4 KO mice displayed a reduced level of inflammation as compared to the wild-type mice; even the chronic administration of low dose LPS could not increase the level of inflammation in the fatty liver of TLR-4 KO mice. Those data demonstrated the prospect of TLR-4 pathway as a therapeutic target

for the treatment of NASH. In our study, we administered TAK-242, an inhibitor of TLR-4, in LPS-injected mice fed a high fat diet, resulting in a significant decrease in the levels of NASH-indicative markers. TAK-242, a novel synthetic molecule with the chemical name resatorvid, suppresses TLR-4 signaling by selectively binding to the TIR domain via Cys747 [292-294]. Although several studies have reported the protective role of TAK-242 against acute inflammation in different disease conditions, it is still not clear how efficient TAK-242 may be in inhibiting chronic inflammation. TAK-242 has demonstrated protective effects against *Escherichia coli*-induced sepsis and acute endotoxemic shock in mice [227, 228]. Most importantly, TAK-242 has been tested on a trial to treat severe sepsis in human patients [229]. The findings from studies on TLR-4-mediated acute inflammation indicate a plausible role for TAK-242 in inhibiting TLR-4-induced chronic inflammation. Thus, in our study, data on the protective role of TAK-242 against NASH in mice offer therapeutic promise for the treatment of NASH in human patients.

The TLR-4 pathway has been correlated not only with chronic inflammation in NASH, but also with warm ischemia/reperfusion injury in liver transplantation [295]. Circulating endotoxin is a critical factor in causing injury in the liver following ischemia/reperfusion. Steatotic livers are more sensitive to endotoxin in developing ischemia/reperfusion injury compared to their lean counterparts [296]. Our lab has reported that the neutralization of endotoxins through treatment with anti-endotoxin monoclonal antibody dramatically improved survival rate and liver function after ischemia/reperfusion injury in mice with hepatic steatosis [297]. We also reported that deficiency of TLR4 is protective against ischemia/reperfusion injury in the mouse steatotic liver [296]. Therefore, we anticipate that inhibition of the TLR-4 pathway through the

treatment with TAK-242 would be protective against ischemia/reperfusion injury in steatotic liver.

**Therapeutic interference of LPS-TLR-4 pathway may improve hepatic regeneration following partial hepatectomy in steatotic liver**

We have studied the impact of dietary fat mediated NASH in the impairment of hepatic regeneration following partial hepatectomy. No study has yet investigated the role of gut microbiota or the role of the LPS-TLR-4 pathway in modulating the impairment of hepatic regeneration following partial hepatectomy in the steatotic liver. Such a study could result in a novel drug with therapeutic potential for the treatment of impaired hepatic regeneration in NASH. In this project, we have shown that the TLR-4 inhibitor, TAK-242, can suppress chronic inflammation in the fatty liver. Therefore, treatment of mice with TAK-242 before surgical resection is anticipated to inhibit the pro-inflammatory insult on the regenerating lobes of the liver and thereby improve impaired regeneration. It has also been demonstrated in this project that diminishing of gut microbiota through treatment with broad spectrum antibiotics results in a reduced concentration of serum endotoxin and a decreased level of NASH. Therefore, treatment of mice with broad spectrum antibiotics before partial hepatectomy surgery is anticipated to result in an improved regeneration outcome.

A published study from our lab demonstrated that pre-treatment of obese mice (ob/ob) with anti-endotoxin monoclonal antibodies could protect them from subsequent hepatic ischemia/reperfusion injury, indicating the role of circulating endotoxin in mediating the inflammatory cascade in the steatotic liver [298]. Therefore, pretreatment of mice with anti-endotoxin monoclonal antibodies prior to partial hepatectomy could

potentially reduce the level of inflammation by sequestering the endotoxins from binding to Kupffer cells, thereby ameliorating hepatic regeneration.

### **Why peroxisomes are important in controlling oxidative stress**

In mammals, peroxisomes play an indispensable role in numerous metabolic pathways including fatty acid  $\alpha$ - and  $\beta$ -oxidation. During those metabolic processes, peroxisomes produce a bulk amount of ROS as byproducts of different biochemical reactions that are efficiently neutralized, using a set of enzymatic and non-enzymatic defense mechanisms [236]. Except for catalase, most of those anti-oxidant defense mechanisms are common in other metabolically active organelles, especially mitochondria [242]. Catalase is the  $H_2O_2$ -detoxifying enzyme in the cell [299]. Catalase is exclusively localized in peroxisomes, but  $H_2O_2$  is generated in both peroxisomes and mitochondria. In fact, only 35% of  $H_2O_2$  within the cell is generated by peroxisomes in the rat liver [242].  $H_2O_2$  generated in mitochondria is also decomposed by peroxisomal catalase, which is mediated by peroxisome-mitochondrial communication [236]. Therefore, peroxisomes play a major role in controlling oxidative stress by preventing the accumulation of ROS.

### **Peroxisomal anti-oxidative function is impaired in NASH**

Regular peroxisomal function in the healthy liver serves two important beneficial roles simultaneously. One is the degradation of very long chain and branched-chain fatty acids, thus preventing them from being accumulated in the liver to induce hepatic steatosis; the other is the neutralization of ROS, preventing them from causing oxidative stress [246, 300]. Up-regulation of peroxisomal biogenesis leads to a resistance to

dietary fat-mediated hepatic steatosis in mice [301]. On the other hand, peroxisome-deficient mice develop an increased level of hepatic steatosis [302]. Recently, Park and colleagues have reported that expression of peroxisomal proliferator-activated receptor- $\alpha$  (PPAR- $\alpha$ ), the master regulator of peroxisomal fatty acid oxidation and proliferation, is reduced in methionine- and choline-deficient diet-induced NASH in mice [303]. They have also shown that statin-mediated inhibition of hepatic steatosis and NASH recovers the expression level of PPAR- $\alpha$ . Those data indicate an impaired peroxisomal function in NASH that is consistent with the reduced catalase level and activity demonstrated in the livers of mice fed MD in our study. It is still not clear if the decreased level and activity of catalase in NASH is due to the reduced biogenesis or structural alteration of peroxisomes.

#### **Intervention of TLR-4 pathway can improve peroxisomal anti-oxidative function**

In this project, we have demonstrated that the catalase level and function increase in TLR-4 KO mice fed MD as compared to the wild-type mice fed MD, indicating an important role for the TLR-4 pathway in regulating peroxisomal function in NASH. The impact of the TLR-4 pathway on peroxisomal function might be mediated in two different ways: a) alteration of peroxisomal structure as a direct influence of pro-inflammatory milieu, and b) cross-talk between the TLR-4 pathway and the biogenesis of peroxisomes, leading to their reduced proliferation. The impact of the TLR-4 pathway in the alteration of peroxisomal structure has been indicated in studies by Khan and colleagues [249, 250]. They have shown that administration of a sub-lethal dose of endotoxin induces changes in peroxisomal structure and function in the rat liver.

Possible crosstalk between the TLR-4 pathway and peroxisomal biogenesis has been indicated in a study by Necela and colleagues [304]. They have shown that activation of the TLR-4 pathway leads to the downregulation of peroxisomal proliferator-activated receptor- $\gamma$  (PPAR- $\gamma$ ) through an NF- $\kappa$ B-dependent mechanism in macrophages. They have also shown that knockout of PPAR- $\gamma$  results in an increased expression of pro-inflammatory genes, indicating a regulatory feedback loop between TLR-4 pathway and expression of PPAR- $\gamma$ . Because PPAR- $\alpha$  and PPAR- $\gamma$  share similarity in their ligands and mechanism of inducing gene expression [305], the existence of similar type of regulatory feedback loop between TLR-4 and PPAR- $\alpha$  cannot be ruled out. Because PPAR- $\alpha$  is the key transcription factor in the PPAR family that regulates the expression of genes involved in peroxisomal  $\beta$ -oxidation and proliferation, it is important to investigate a potential crosstalk between TLR-4 and PPAR- $\alpha$ .

## References

1. Benedict, M. and X. Zhang, *Non-alcoholic fatty liver disease: An expanded review*. World J Hepatol, 2017. **9**(16): p. 715-732.
2. Gordon, H., *Detection of alcoholic liver disease*. World J Gastroenterol, 2001. **7**(3): p. 297-302.
3. Savolainen, V.T., et al., *Alcohol consumption and alcoholic liver disease: evidence of a threshold level of effects of ethanol*. Alcohol Clin Exp Res, 1993. **17**(5): p. 1112-7.
4. Calzadilla Bertot, L. and L.A. Adams, *The Natural Course of Non-Alcoholic Fatty Liver Disease*. Int J Mol Sci, 2016. **17**(5).
5. Angulo, P., et al., *The NAFLD fibrosis score: a noninvasive system that identifies liver fibrosis in patients with NAFLD*. Hepatology, 2007. **45**(4): p. 846-54.
6. Ekstedt, M., et al., *Long-term follow-up of patients with NAFLD and elevated liver enzymes*. Hepatology, 2006. **44**(4): p. 865-73.
7. Satapathy, S.K. and A.J. Sanyal, *Epidemiology and Natural History of Nonalcoholic Fatty Liver Disease*. Semin Liver Dis, 2015. **35**(3): p. 221-35.
8. Sayiner, M., et al., *Epidemiology of Nonalcoholic Fatty Liver Disease and Nonalcoholic Steatohepatitis in the United States and the Rest of the World*. Clin Liver Dis, 2016. **20**(2): p. 205-14.
9. Dixon, J.B., P.S. Bhathal, and P.E. O'Brien, *Nonalcoholic fatty liver disease: predictors of nonalcoholic steatohepatitis and liver fibrosis in the severely obese*. Gastroenterology, 2001. **121**(1): p. 91-100.

10. Fingas, C.D., et al., *Epidemiology of nonalcoholic steatohepatitis and hepatocellular carcinoma*. *Clinical Liver Disease*, 2016. **8**(5): p. 119-122.
11. Williams, C.D., et al., *Prevalence of nonalcoholic fatty liver disease and nonalcoholic steatohepatitis among a largely middle-aged population utilizing ultrasound and liver biopsy: a prospective study*. *Gastroenterology*, 2011. **140**(1): p. 124-31.
12. Vernon, G., A. Baranova, and Z.M. Younossi, *Systematic review: the epidemiology and natural history of non-alcoholic fatty liver disease and non-alcoholic steatohepatitis in adults*. *Aliment Pharmacol Ther*, 2011. **34**(3): p. 274-85.
13. Lazo, M., et al., *Prevalence of nonalcoholic fatty liver disease in the United States: the Third National Health and Nutrition Examination Survey, 1988-1994*. *Am J Epidemiol*, 2013. **178**(1): p. 38-45.
14. Ray, K., *NAFLD-the next global epidemic*. *Nat Rev Gastroenterol Hepatol*, 2013. **10**(11): p. 621.
15. Powell, E.E., et al., *The natural history of nonalcoholic steatohepatitis: a follow-up study of forty-two patients for up to 21 years*. *Hepatology*, 1990. **11**(1): p. 74-80.
16. Caldwell, S.H., et al., *Cryptogenic cirrhosis: clinical characterization and risk factors for underlying disease*. *Hepatology*, 1999. **29**(3): p. 664-9.
17. Poonawala, A., S.P. Nair, and P.J. Thuluvath, *Prevalence of obesity and diabetes in patients with cryptogenic cirrhosis: a case-control study*. *Hepatology*, 2000. **32**(4 Pt 1): p. 689-92.
18. Teli, M.R., et al., *The natural history of nonalcoholic fatty liver: a follow-up study*. *Hepatology*, 1995. **22**(6): p. 1714-9.

19. Wong, V.W., et al., *Disease progression of non-alcoholic fatty liver disease: a prospective study with paired liver biopsies at 3 years*. Gut, 2010. **59**(7): p. 969-74.
20. Pais, R., et al., *A systematic review of follow-up biopsies reveals disease progression in patients with non-alcoholic fatty liver*. J Hepatol, 2013. **59**(3): p. 550-6.
21. McPherson, S., et al., *Evidence of NAFLD progression from steatosis to fibrosing-steatohepatitis using paired biopsies: implications for prognosis and clinical management*. J Hepatol, 2015. **62**(5): p. 1148-55.
22. Anthony, P.P., et al., *The morphology of cirrhosis: definition, nomenclature, and classification*. Bull World Health Organ, 1977. **55**(4): p. 521-40.
23. Ascha, M.S., et al., *The incidence and risk factors of hepatocellular carcinoma in patients with nonalcoholic steatohepatitis*. Hepatology, 2010. **51**(6): p. 1972-8.
24. White, D.L., F. Kanwal, and H.B. El-Serag, *Association between nonalcoholic fatty liver disease and risk for hepatocellular cancer, based on systematic review*. Clin Gastroenterol Hepatol, 2012. **10**(12): p. 1342-1359 e2.
25. Alberti, K.G.M.M. and P.Z. Zimmet, *Definition, diagnosis and classification of diabetes mellitus and its complications. Part 1: diagnosis and classification of diabetes mellitus. Provisional report of a WHO Consultation*. Diabetic Medicine, 1998. **15**(7): p. 539-553.
26. Garcia, G., T.S. Sunil, and P. Hinojosa, *The fast food and obesity link: consumption patterns and severity of obesity*. Obes Surg, 2012. **22**(5): p. 810-8.

27. Anderson, B., et al., *Fast-food consumption and obesity among Michigan adults*. *Prev Chronic Dis*, 2011. **8**(4): p. A71.
28. Owen, N., et al., *Sedentary behavior: emerging evidence for a new health risk*. *Mayo Clin Proc*, 2010. **85**(12): p. 1138-41.
29. Ruhl, C.E. and J.E. Everhart, *Determinants of the association of overweight with elevated serum alanine aminotransferase activity in the United States*. *Gastroenterology*, 2003. **124**(1): p. 71-9.
30. Angulo, P., *Nonalcoholic fatty liver disease*. *N Engl J Med*, 2002. **346**(16): p. 1221-31.
31. Sabir, N., et al., *Correlation of abdominal fat accumulation and liver steatosis: importance of ultrasonographic and anthropometric measurements*. *European Journal of Ultrasound*, 2001. **14**(2): p. 121-128.
32. Expert Panel on, D., Evaluation, and A. and Treatment of High Blood Cholesterol in, *Executive summary of the third report of the national cholesterol education program (ncep) expert panel on detection, evaluation, and treatment of high blood cholesterol in adults (adult treatment panel iii)*. *JAMA*, 2001. **285**(19): p. 2486-2497.
33. Bugianesi, E., et al., *Insulin resistance in nonalcoholic fatty liver disease*. *Curr Pharm Des*, 2010. **16**(17): p. 1941-51.
34. Sanyal, A.J., et al., *Nonalcoholic steatohepatitis: Association of insulin resistance and mitochondrial abnormalities*. *Gastroenterology*, 2001. **120**(5): p. 1183-1192.

35. Utzschneider, K.M. and S.E. Kahn, *The Role of Insulin Resistance in Nonalcoholic Fatty Liver Disease*. The Journal of Clinical Endocrinology & Metabolism, 2006. **91**(12): p. 4753-4761.
36. Samuel, V.T. and G.I. Shulman, *The pathogenesis of insulin resistance: integrating signaling pathways and substrate flux*. J Clin Invest, 2016. **126**(1): p. 12-22.
37. Altomare, D.A. and A.R. Khaled, *Homeostasis and the importance for a balance between AKT/mTOR activity and intracellular signaling*. Curr Med Chem, 2012. **19**(22): p. 3748-62.
38. Perry, R.J., et al., *Hepatic acetyl CoA links adipose tissue inflammation to hepatic insulin resistance and type 2 diabetes*. Cell, 2015. **160**(4): p. 745-758.
39. Perry, R.J., et al., *Leptin reverses diabetes by suppression of the hypothalamic-pituitary-adrenal axis*. Nat Med, 2014. **20**(7): p. 759-63.
40. Previs, S.F., G.W. Cline, and G.I. Shulman, *A critical evaluation of mass isotopomer distribution analysis of gluconeogenesis in vivo*. Am J Physiol, 1999. **277**(1 Pt 1): p. E154-60.
41. Weisberg, S.P., et al., *Obesity is associated with macrophage accumulation in adipose tissue*. J Clin Invest, 2003. **112**(12): p. 1796-808.
42. Xu, H., et al., *Chronic inflammation in fat plays a crucial role in the development of obesity-related insulin resistance*. J Clin Invest, 2003. **112**(12): p. 1821-30.
43. Laurencikiene, J., et al., *NF-kappaB is important for TNF-alpha-induced lipolysis in human adipocytes*. J Lipid Res, 2007. **48**(5): p. 1069-77.

44. Bezaire, V., et al., *Chronic TNF $\alpha$  and cAMP pre-treatment of human adipocytes alter HSL, ATGL and perilipin to regulate basal and stimulated lipolysis.* FEBS Lett, 2009. **583**(18): p. 3045-9.
45. Ranjit, S., et al., *Regulation of fat specific protein 27 by isoproterenol and TNF- $\alpha$  to control lipolysis in murine adipocytes.* J Lipid Res, 2011. **52**(2): p. 221-36.
46. Herman, M.A., et al., *A novel ChREBP isoform in adipose tissue regulates systemic glucose metabolism.* Nature, 2012. **484**(7394): p. 333-8.
47. Stefan, N., et al., *Circulating palmitoleate strongly and independently predicts insulin sensitivity in humans.* Diabetes Care, 2010. **33**(2): p. 405-7.
48. Cao, H., et al., *Identification of a lipokine, a lipid hormone linking adipose tissue to systemic metabolism.* Cell, 2008. **134**(6): p. 933-44.
49. Su, X., et al., *Adipose tissue monomethyl branched-chain fatty acids and insulin sensitivity: Effects of obesity and weight loss.* Obesity (Silver Spring), 2015. **23**(2): p. 329-34.
50. Yore, M.M., et al., *Discovery of a class of endogenous mammalian lipids with anti-diabetic and anti-inflammatory effects.* Cell, 2014. **159**(2): p. 318-32.
51. Bhatt, H.B. and R.J. Smith, *Fatty liver disease in diabetes mellitus.* Hepatobiliary Surg Nutr, 2015. **4**(2): p. 101-8.
52. Stefan, N. and H.U. Haring, *The metabolically benign and malignant fatty liver.* Diabetes, 2011. **60**(8): p. 2011-7.
53. Hebbard, L. and J. George, *Animal models of nonalcoholic fatty liver disease.* Nature Reviews Gastroenterology & Hepatology, 2010. **8**: p. 35.

54. Day, C.P. and O.F. James, *Steatohepatitis: a tale of two "hits"?* Gastroenterology, 1998. **114**(4): p. 842-5.
55. NIH, <https://ghr.nlm.nih.gov/condition/non-alcoholic-fatty-liver-disease>.
56. Marra, F. and S. Lotersztajn, *Pathophysiology of NASH: perspectives for a targeted treatment*. Curr Pharm Des, 2013. **19**(29): p. 5250-69.
57. Mansbach, C.M. and S.A. Siddiqi, *The biogenesis of chylomicrons*. Annu Rev Physiol, 2010. **72**: p. 315-33.
58. Garrido, G., M. Guzman, and J.M. Odriozola, *Effect of different types of high carbohydrate diets on glycogen metabolism in liver and skeletal muscle of endurance-trained rats*. Eur J Appl Physiol Occup Physiol, 1996. **74**(1-2): p. 91-9.
59. Masarone, M., et al., *Role of Oxidative Stress in Pathophysiology of Nonalcoholic Fatty Liver Disease*. Oxid Med Cell Longev, 2018. **2018**: p. 9547613.
60. Sumida, Y., et al., *Involvement of free radicals and oxidative stress in NAFLD/NASH*. Free Radic Res, 2013. **47**(11): p. 869-80.
61. Song, B., et al., *Chop deletion reduces oxidative stress, improves beta cell function, and promotes cell survival in multiple mouse models of diabetes*. J Clin Invest, 2008. **118**(10): p. 3378-89.
62. Syn, W.K., S.S. Choi, and A.M. Diehl, *Apoptosis and cytokines in non-alcoholic steatohepatitis*. Clin Liver Dis, 2009. **13**(4): p. 565-80.
63. Qin, J., et al., *A human gut microbial gene catalogue established by metagenomic sequencing*. Nature, 2010. **464**: p. 59.
64. Ley, R.E., D.A. Peterson, and J.I. Gordon, *Ecological and evolutionary forces shaping microbial diversity in the human intestine*. Cell, 2006. **124**(4): p. 837-48.

65. Backhed, F., et al., *Host-bacterial mutualism in the human intestine*. Science, 2005. **307**(5717): p. 1915-20.
66. Gill, S.R., et al., *Metagenomic Analysis of the Human Distal Gut Microbiome*. Science, 2006. **312**(5778): p. 1355-1359.
67. Wang, B., et al., *The Human Microbiota in Health and Disease*. Engineering, 2017. **3**(1): p. 71-82.
68. Roberfroid, M.B., et al., *Colonic microflora: nutrition and health. Summary and conclusions of an International Life Sciences Institute (ILSI) [Europe] workshop held in Barcelona, Spain*. Nutr Rev, 1995. **53**(5): p. 127-30.
69. Duncan, S.H., et al., *The role of pH in determining the species composition of the human colonic microbiota*. Environmental Microbiology, 2009. **11**(8): p. 2112-2122.
70. Cani, P.D., A. Everard, and T. Duparc, *Gut microbiota, enteroendocrine functions and metabolism*. Curr Opin Pharmacol, 2013. **13**(6): p. 935-40.
71. Flint, H.J., et al., *The role of the gut microbiota in nutrition and health*. Nature Reviews Gastroenterology & Hepatology, 2012. **9**: p. 577.
72. Cash, H.L., et al., *Symbiotic bacteria direct expression of an intestinal bactericidal lectin*. Science, 2006. **313**(5790): p. 1126-30.
73. Hooper, L.V., et al., *Angiogenins: a new class of microbicidal proteins involved in innate immunity*. Nature Immunology, 2003. **4**: p. 269.
74. Schauber, J., et al., *Expression of the cathelicidin LL-37 is modulated by short chain fatty acids in colonocytes: relevance of signalling pathways*. Gut, 2003. **52**(5): p. 735-741.

75. Macpherson, A.J. and N.L. Harris, *Interactions between commensal intestinal bacteria and the immune system*. Nature Reviews Immunology, 2004. **4**: p. 478.
76. Morgun, A., et al., *Uncovering effects of antibiotics on the host and microbiota using transkingdom gene networks*. Gut, 2015. **64**(11): p. 1732-43.
77. Turnbaugh, P.J., et al., *A core gut microbiome in obese and lean twins*. Nature, 2009. **457**(7228): p. 480-4.
78. Frank, D.N., et al., *Molecular-phylogenetic characterization of microbial community imbalances in human inflammatory bowel diseases*. Proc Natl Acad Sci U S A, 2007. **104**(34): p. 13780-5.
79. Larsen, N., et al., *Gut microbiota in human adults with type 2 diabetes differs from non-diabetic adults*. PLoS One, 2010. **5**(2): p. e9085.
80. Wang, F., et al., *Detecting Microbial Dysbiosis Associated with Pediatric Crohn Disease Despite the High Variability of the Gut Microbiota*. Cell Rep, 2016. **14**(4): p. 945-55.
81. Wang, Z., et al., *Gut flora metabolism of phosphatidylcholine promotes cardiovascular disease*. Nature, 2011. **472**(7341): p. 57-63.
82. Bashiardes, S., et al., *Non-alcoholic fatty liver and the gut microbiota*. Mol Metab, 2016. **5**(9): p. 782-94.
83. David, L.A., et al., *Diet rapidly and reproducibly alters the human gut microbiome*. Nature, 2014. **505**(7484): p. 559-63.
84. Rawls, J.F., et al., *Reciprocal gut microbiota transplants from zebrafish and mice to germ-free recipients reveal host habitat selection*. Cell, 2006. **127**(2): p. 423-33.

85. Backhed, F., et al., *Mechanisms underlying the resistance to diet-induced obesity in germ-free mice*. Proc Natl Acad Sci U S A, 2007. **104**(3): p. 979-84.
86. Turnbaugh, P.J., et al., *An obesity-associated gut microbiome with increased capacity for energy harvest*. Nature, 2006. **444**(7122): p. 1027-31.
87. Turnbaugh, P.J., et al., *Diet-induced obesity is linked to marked but reversible alterations in the mouse distal gut microbiome*. Cell Host Microbe, 2008. **3**(4): p. 213-23.
88. Backhed, F., et al., *The gut microbiota as an environmental factor that regulates fat storage*. Proc Natl Acad Sci U S A, 2004. **101**(44): p. 15718-23.
89. Ley, R.E., et al., *Microbial ecology: human gut microbes associated with obesity*. Nature, 2006. **444**(7122): p. 1022-3.
90. Volta, U., et al., *IgA antibodies to dietary antigens in liver cirrhosis*. Ric Clin Lab, 1987. **17**(3): p. 235-42.
91. Vajro, P., G. Paoletta, and A. Fasano, *Microbiota and gut-liver axis: their influences on obesity and obesity-related liver disease*. J Pediatr Gastroenterol Nutr, 2013. **56**(5): p. 461-8.
92. Valenzano, M.C., et al., *Remodeling of Tight Junctions and Enhancement of Barrier Integrity of the CACO-2 Intestinal Epithelial Cell Layer by Micronutrients*. PLOS ONE, 2015. **10**(7): p. e0133926.
93. Peng, L., et al., *Butyrate enhances the intestinal barrier by facilitating tight junction assembly via activation of AMP-activated protein kinase in Caco-2 cell monolayers*. J Nutr, 2009. **139**(9): p. 1619-25.

94. Elamin, E.E., et al., *Short-Chain Fatty Acids Activate AMP-Activated Protein Kinase and Ameliorate Ethanol-Induced Intestinal Barrier Dysfunction in Caco-2 Cell Monolayers*. The Journal of Nutrition, 2013. **143**(12): p. 1872-1881.
95. Ilan, Y., *Leaky gut and the liver: a role for bacterial translocation in nonalcoholic steatohepatitis*. World J Gastroenterol, 2012. **18**(21): p. 2609-18.
96. Ray, K., *Leaky guts: intestinal permeability and NASH*. Nature Reviews Gastroenterology & Hepatology, 2015. **12**: p. 123.
97. Marra, F. and G. Svegliati-Baroni, *Lipotoxicity and the gut-liver axis in NASH pathogenesis*. J Hepatol, 2018. **68**(2): p. 280-295.
98. Poeta, M., L. Pierri, and P. Vajro, *Gut-Liver Axis Derangement in Non-Alcoholic Fatty Liver Disease*. Children (Basel), 2017. **4**(8).
99. Hashimoto, C., K.L. Hudson, and K.V. Anderson, *The Toll gene of Drosophila, required for dorsal-ventral embryonic polarity, appears to encode a transmembrane protein*. Cell, 1988. **52**(2): p. 269-79.
100. Drexler, S.K. and B.M. Foxwell, *The role of Toll-like receptors in chronic inflammation*. The International Journal of Biochemistry & Cell Biology, 2010. **42**(4): p. 506-518.
101. Takeuchi, O. and S. Akira, *Toll-like receptors; their physiological role and signal transduction system*. International Immunopharmacology, 2001. **1**(4): p. 625-635.
102. Kawasaki, T. and T. Kawai, *Toll-like receptor signaling pathways*. Front Immunol, 2014. **5**: p. 461.
103. Akira, S. and K. Takeda, *Toll-like receptor signalling*. Nature Reviews Immunology, 2004. **4**: p. 499.

104. Deane, J.A. and S. Bolland, *Nucleic Acid-Sensing TLRs as Modifiers of Autoimmunity*. The Journal of Immunology, 2006. **177**(10): p. 6573-6578.
105. Ehlers, M. and J.V. Ravetch, *Opposing effects of Toll-like receptor stimulation induce autoimmunity or tolerance*. Trends Immunol, 2007. **28**(2): p. 74-9.
106. Marshak-Rothstein, A., *Toll-like receptors in systemic autoimmune disease*. Nature Reviews Immunology, 2006. **6**: p. 823.
107. Uematsu, S. and S. Akira, *Toll-Like receptors (TLRs) and their ligands*. Handb Exp Pharmacol, 2008(183): p. 1-20.
108. Barrat, F.J., et al., *Nucleic acids of mammalian origin can act as endogenous ligands for Toll-like receptors and may promote systemic lupus erythematosus*. The Journal of Experimental Medicine, 2005. **202**(8): p. 1131-1139.
109. Rhee, S.H., et al., *Pathophysiological role of Toll-like receptor 5 engagement by bacterial flagellin in colonic inflammation*. Proceedings of the National Academy of Sciences of the United States of America, 2005. **102**(38): p. 13610-13615.
110. Roep, B.O., *T-Cell Responses to Autoantigens in IDDM: The Search for the Holy Grail*. Diabetes, 1996. **45**(9): p. 1147-1156.
111. Lang, K.S., et al., *Toll-like receptor engagement converts T-cell autoreactivity into overt autoimmune disease*. Nature Medicine, 2005. **11**: p. 138.
112. Wen, L., et al., *The Effect of Innate Immunity on Autoimmune Diabetes and the Expression of Toll-Like Receptors on Pancreatic Islets*. The Journal of Immunology, 2004. **172**(5): p. 3173-3180.
113. Jandhyala, S.M., et al., *Role of the normal gut microbiota*. World J Gastroenterol, 2015. **21**(29): p. 8787-803.

114. Qin, J., et al., *A human gut microbial gene catalogue established by metagenomic sequencing*. Nature, 2010. **464**(7285): p. 59-65.
115. Guo, S., et al., *Lipopolysaccharide causes an increase in intestinal tight junction permeability in vitro and in vivo by inducing enterocyte membrane expression and localization of TLR-4 and CD14*. Am J Pathol, 2013. **182**(2): p. 375-87.
116. Moreira, A.P., et al., *Influence of a high-fat diet on gut microbiota, intestinal permeability and metabolic endotoxaemia*. Br J Nutr, 2012. **108**(5): p. 801-9.
117. Feingold, K.R. and C. Grunfeld, *The Effect of Inflammation and Infection on Lipids and Lipoproteins*, in *Endotext*, L.J. De Groot, et al., Editors. 2000: South Dartmouth (MA).
118. Osto, M., et al., *Subacute endotoxemia induces adipose inflammation and changes in lipid and lipoprotein metabolism in cats*. Endocrinology, 2011. **152**(3): p. 804-15.
119. Hardardottir, I., C. Grunfeld, and K.R. Feingold, *Effects of endotoxin on lipid metabolism*. Biochem Soc Trans, 1995. **23**(4): p. 1013-8.
120. Chung, K.W., et al., *The critical role played by endotoxin-induced liver autophagy in the maintenance of lipid metabolism during sepsis*. Autophagy, 2017. **13**(7): p. 1113-1129.
121. Zu, L., et al., *Bacterial Endotoxin Stimulates Adipose Lipolysis via Toll-Like Receptor 4 and Extracellular Signal-regulated Kinase Pathway*. Journal of Biological Chemistry, 2009. **284**(9): p. 5915-5926.
122. Cani, P.D., et al., *Metabolic endotoxemia initiates obesity and insulin resistance*. Diabetes, 2007. **56**(7): p. 1761-72.

123. Cani, P.D., et al., *Changes in gut microbiota control metabolic endotoxemia-induced inflammation in high-fat diet-induced obesity and diabetes in mice.* Diabetes, 2008. **57**(6): p. 1470-81.
124. Troseid, M., et al., *Plasma lipopolysaccharide is closely associated with glycemic control and abdominal obesity: evidence from bariatric surgery.* Diabetes Care, 2013. **36**(11): p. 3627-32.
125. Palsson-McDermott, E.M. and L.A. O'Neill, *Signal transduction by the lipopolysaccharide receptor, Toll-like receptor-4.* Immunology, 2004. **113**(2): p. 153-62.
126. Creely, S.J., et al., *Lipopolysaccharide activates an innate immune system response in human adipose tissue in obesity and type 2 diabetes.* Am J Physiol Endocrinol Metab, 2007. **292**(3): p. E740-7.
127. Schwabe, R.F., E. Seki, and D.A. Brenner, *Toll-like receptor signaling in the liver.* Gastroenterology, 2006. **130**(6): p. 1886-900.
128. Seki, E., et al., *Lipopolysaccharide-induced IL-18 secretion from murine Kupffer cells independently of myeloid differentiation factor 88 that is critically involved in induction of production of IL-12 and IL-1beta.* J Immunol, 2001. **166**(4): p. 2651-7.
129. Harte, A.L., et al., *Elevated endotoxin levels in non-alcoholic fatty liver disease.* J Inflamm (Lond), 2010. **7**: p. 15.
130. Volynets, V., et al., *Nutrition, intestinal permeability, and blood ethanol levels are altered in patients with nonalcoholic fatty liver disease (NAFLD).* Dig Dis Sci, 2012. **57**(7): p. 1932-41.

131. Thuy, S., et al., *Nonalcoholic fatty liver disease in humans is associated with increased plasma endotoxin and plasminogen activator inhibitor 1 concentrations and with fructose intake*. J Nutr, 2008. **138**(8): p. 1452-5.
132. Alisi, A., et al., *Endotoxin and plasminogen activator inhibitor-1 serum levels associated with nonalcoholic steatohepatitis in children*. J Pediatr Gastroenterol Nutr, 2010. **50**(6): p. 645-9.
133. Imajo, K., et al., *Hyperresponsivity to low-dose endotoxin during progression to nonalcoholic steatohepatitis is regulated by leptin-mediated signaling*. Cell Metab, 2012. **16**(1): p. 44-54.
134. Higgins GM, A.R., *Experimental pathology of the liver: I. Restoration of the liver of the white rat following partial surgical removal*, in Arch Pathol 1931. p. 186-202.
135. Yang, L., et al., *TRIF Differentially Regulates Hepatic Steatosis and Inflammation/Fibrosis in Mice*. Cell Mol Gastroenterol Hepatol, 2017. **3**(3): p. 469-483.
136. Thavasu, P.W., et al., *Measuring cytokine levels in blood. Importance of anticoagulants, processing, and storage conditions*. J Immunol Methods, 1992. **153**(1-2): p. 115-24.
137. Kim, K.-A., et al., *Gut microbiota lipopolysaccharide accelerates inflamm-aging in mice*. BMC Microbiology, 2016. **16**(1): p. 9.
138. Kleiner, D.E., et al., *Design and validation of a histological scoring system for nonalcoholic fatty liver disease*. Hepatology, 2005. **41**(6): p. 1313-21.

139. Brunt, E.M., et al., *Nonalcoholic fatty liver disease (NAFLD) activity score and the histopathologic diagnosis in NAFLD: distinct clinicopathologic meanings*. Hepatology, 2011. **53**(3): p. 810-20.
140. Imajo, K., et al., *Hyperresponsivity to Low-Dose Endotoxin during Progression to Nonalcoholic Steatohepatitis Is Regulated by Leptin-Mediated Signaling*. Cell Metabolism, 2012. **16**(1): p. 44-54.
141. Mehlem, A., et al., *Imaging of neutral lipids by oil red O for analyzing the metabolic status in health and disease*. Nat. Protocols, 2013. **8**(6): p. 1149-1154.
142. DeAngelis, R.A., et al., *A high-fat diet impairs liver regeneration in C57BL/6 mice through overexpression of the NF-kappaB inhibitor, IkappaBalpha*. Hepatology, 2005. **42**(5): p. 1148-57.
143. ThermoScientific, *T042-Technical Bulletin NanoDrop Spectrophotometers 260/280 and 260/230 Ratios* (<http://www.nhm.ac.uk/content/dam/nhmwww/our-science/dpts-facilities-staff/Coreresearchlabs/nanodrop.pdf>).
144. Livak, K.J. and T.D. Schmittgen, *Analysis of relative gene expression data using real-time quantitative PCR and the 2(-Delta Delta C(T)) Method*. Methods, 2001. **25**(4): p. 402-8.
145. Evans, Z.P., et al., *Mitochondrial uncoupling protein-2 deficiency protects steatotic mouse hepatocytes from hypoxia/reoxygenation*. Am J Physiol Gastrointest Liver Physiol, 2012. **302**(3): p. G336-42.
146. Li, Q., et al., *Resveratrol Sensitizes Carfilzomib-Induced Apoptosis via Promoting Oxidative Stress in Multiple Myeloma Cells*. Front Pharmacol, 2018. **9**: p. 334.

147. Yang, C.Y., et al., *CLEC4F is an inducible C-type lectin in F4/80-positive cells and is involved in alpha-galactosylceramide presentation in liver*. PLoS One, 2013. **8**(6): p. e65070.
148. Scott, C.L., et al., *Bone marrow-derived monocytes give rise to self-renewing and fully differentiated Kupffer cells*. Nat Commun, 2016. **7**: p. 10321.
149. Neuman, M.G., L.B. Cohen, and R.M. Nanau, *Biomarkers in nonalcoholic fatty liver disease*. Can J Gastroenterol Hepatol, 2014. **28**(11): p. 607-18.
150. Takahashi, Y., Y. Soejima, and T. Fukusato, *Animal models of nonalcoholic fatty liver disease/nonalcoholic steatohepatitis*. World J Gastroenterol, 2012. **18**(19): p. 2300-8.
151. Schattenberg, J.M. and P.R. Galle, *Animal models of non-alcoholic steatohepatitis: of mice and man*. Dig Dis, 2010. **28**(1): p. 247-54.
152. Sahai, A., et al., *Obese and diabetic db/db mice develop marked liver fibrosis in a model of nonalcoholic steatohepatitis: role of short-form leptin receptors and osteopontin*. Am J Physiol Gastrointest Liver Physiol, 2004. **287**(5): p. G1035-43.
153. Ip, E., et al., *Central role of PPARalpha-dependent hepatic lipid turnover in dietary steatohepatitis in mice*. Hepatology, 2003. **38**(1): p. 123-32.
154. Kashireddy, P.V. and M.S. Rao, *Lack of peroxisome proliferator-activated receptor alpha in mice enhances methionine and choline deficient diet-induced steatohepatitis*. Hepatol Res, 2004. **30**(2): p. 104-110.
155. Carmiel-Haggai, M., A.I. Cederbaum, and N. Nieto, *A high-fat diet leads to the progression of non-alcoholic fatty liver disease in obese rats*. FASEB J, 2005. **19**(1): p. 136-8.

156. Wouters, K., et al., *Dietary cholesterol, rather than liver steatosis, leads to hepatic inflammation in hyperlipidemic mouse models of nonalcoholic steatohepatitis*. *Hepatology*, 2008. **48**(2): p. 474-86.
157. NHANES, *Trends in intake of energy and macronutrients—United States 1971–2000* <http://www.cdc.gov/mmwr/preview/mmwrhtml/mm5304a3.htm>. 2004.
158. Cascio, G., G. Schiera, and I. Di Liegro, *Dietary fatty acids in metabolic syndrome, diabetes and cardiovascular diseases*. *Curr Diabetes Rev*, 2012. **8**(1): p. 2-17.
159. Devkota, S., et al., *Dietary-fat-induced taurocholic acid promotes pathobiont expansion and colitis in Il10<sup>-/-</sup> mice*. *Nature*, 2012. **487**: p. 104.
160. Wang, D., Y. Wei, and M.J. Pagliassotti, *Saturated fatty acids promote endoplasmic reticulum stress and liver injury in rats with hepatic steatosis*. *Endocrinology*, 2006. **147**(2): p. 943-51.
161. Wei, Y., et al., *Saturated fatty acids induce endoplasmic reticulum stress and apoptosis independently of ceramide in liver cells*. *Am J Physiol Endocrinol Metab*, 2006. **291**(2): p. E275-81.
162. van den Berg, S.A., et al., *High levels of dietary stearate promote adiposity and deteriorate hepatic insulin sensitivity*. *Nutr Metab (Lond)*, 2010. **7**: p. 24.
163. Sutter, A.G., et al., *Dietary Saturated Fat Promotes Development of Hepatic Inflammation Through Toll-Like Receptor 4 in Mice*. *J Cell Biochem*, 2016. **117**(7): p. 1613-21.
164. Leamy, A.K., R.A. Egnatchik, and J.D. Young, *Molecular mechanisms and the role of saturated fatty acids in the progression of non-alcoholic fatty liver disease*. *Prog Lipid Res*, 2013. **52**(1): p. 165-74.

165. Van Herck, M.A., L. Vonghia, and S.M. Francque, *Animal Models of Nonalcoholic Fatty Liver Disease-A Starter's Guide*. *Nutrients*, 2017. **9**(10).
166. Nakamura, A. and Y. Terauchi, *Lessons from mouse models of high-fat diet-induced NAFLD*. *Int J Mol Sci*, 2013. **14**(11): p. 21240-57.
167. Alkhouri, N. and A.J. McCullough, *Noninvasive Diagnosis of NASH and Liver Fibrosis Within the Spectrum of NAFLD*. *Gastroenterol Hepatol (N Y)*, 2012. **8**(10): p. 661-8.
168. Hansen, H.H., et al., *Mouse models of nonalcoholic steatohepatitis in preclinical drug development*. *Drug Discovery Today*, 2017. **22**(11): p. 1707-1718.
169. Alkhouri, N., L.J. Dixon, and A.E. Feldstein, *Lipotoxicity in nonalcoholic fatty liver disease: not all lipids are created equal*. *Expert Rev Gastroenterol Hepatol*, 2009. **3**(4): p. 445-51.
170. Kaufman, R.J., *Orchestrating the unfolded protein response in health and disease*. *J Clin Invest*, 2002. **110**(10): p. 1389-98.
171. Ron, D. and P. Walter, *Signal integration in the endoplasmic reticulum unfolded protein response*. *Nat Rev Mol Cell Biol*, 2007. **8**(7): p. 519-29.
172. Zhang, K. and R.J. Kaufman, *The unfolded protein response: a stress signaling pathway critical for health and disease*. *Neurology*, 2006. **66**(2 Suppl 1): p. S102-9.
173. Frangioudakis, G., et al., *Saturated- and n-6 polyunsaturated-fat diets each induce ceramide accumulation in mouse skeletal muscle: reversal and improvement of glucose tolerance by lipid metabolism inhibitors*. *Endocrinology*, 2010. **151**(9): p. 4187-96.

174. Turpin, S.M., et al., *Apoptosis in skeletal muscle myotubes is induced by ceramides and is positively related to insulin resistance*. Am J Physiol Endocrinol Metab, 2006. **291**(6): p. E1341-50.
175. Colombini, M., *Ceramide channels and their role in mitochondria-mediated apoptosis*. Biochim Biophys Acta, 2010. **1797**(6-7): p. 1239-44.
176. Woodcock, J., *Sphingosine and ceramide signalling in apoptosis*. IUBMB Life, 2006. **58**(8): p. 462-6.
177. Ohanian, J. and V. Ohanian, *Sphingolipids in mammalian cell signalling*. Cell Mol Life Sci, 2001. **58**(14): p. 2053-68.
178. Ruvolo, P.P., *Intracellular signal transduction pathways activated by ceramide and its metabolites*. Pharmacol Res, 2003. **47**(5): p. 383-92.
179. Dobrowsky, R.T., *Sphingolipid signalling domains floating on rafts or buried in caves?* Cell Signal, 2000. **12**(2): p. 81-90.
180. Pettus, B.J., C.E. Chalfant, and Y.A. Hannun, *Ceramide in apoptosis: an overview and current perspectives*. Biochim Biophys Acta, 2002. **1585**(2-3): p. 114-25.
181. Heinrich, M., et al., *Cathepsin D links TNF-induced acid sphingomyelinase to Bid-mediated caspase-9 and -3 activation*. Cell Death Differ, 2004. **11**(5): p. 550-63.
182. Hwang, D.H., J.A. Kim, and J.Y. Lee, *Mechanisms for the activation of Toll-like receptor 2/4 by saturated fatty acids and inhibition by docosahexaenoic acid*. Eur J Pharmacol, 2016. **785**: p. 24-35.
183. Lee, J.Y., et al., *Saturated fatty acids, but not unsaturated fatty acids, induce the expression of cyclooxygenase-2 mediated through Toll-like receptor 4*. J Biol Chem, 2001. **276**(20): p. 16683-9.

184. Rogero, M. and P. Calder, *Obesity, Inflammation, Toll-Like Receptor 4 and Fatty Acids*. *Nutrients*, 2018. **10**(4): p. 432.
185. Hoshino, K., et al., *Cutting edge: Toll-like receptor 4 (TLR4)-deficient mice are hyporesponsive to lipopolysaccharide: evidence for TLR4 as the Lps gene product*. *J Immunol*, 1999. **162**(7): p. 3749-52.
186. Calder, P.C., et al., *Dietary factors and low-grade inflammation in relation to overweight and obesity*. *Br J Nutr*, 2011. **106 Suppl 3**: p. S5-78.
187. Calder, P.C., *The role of marine omega-3 (n-3) fatty acids in inflammatory processes, atherosclerosis and plaque stability*. *Mol Nutr Food Res*, 2012. **56**(7): p. 1073-80.
188. Calder, P.C., *Marine omega-3 fatty acids and inflammatory processes: Effects, mechanisms and clinical relevance*. *Biochim Biophys Acta*, 2015. **1851**(4): p. 469-84.
189. Mansson, H.L., *Fatty acids in bovine milk fat*. *Food Nutr Res*, 2008. **52**.
190. Ahmad Fadzillah, N., et al., *Differentiation of fatty acid composition of butter adulterated with lard using gas chromatography mass spectrometry combined with principal component analysis*. Vol. 78. 2016.
191. *Milk and Dairy Products*, in *Ullmann's Encyclopedia of Industrial Chemistry*.
192. Forbes, S.J. and N. Rosenthal, *Preparing the ground for tissue regeneration: from mechanism to therapy*. *Nature Medicine*, 2014. **20**: p. 857.
193. Duncan, A.W. and A. Soto-Gutierrez, *Liver repopulation and regeneration: new approaches to old questions*. *Curr Opin Organ Transplant*, 2013. **18**(2): p. 197-202.

194. Koniaris, L.G., et al., *Liver regeneration*. Journal of the American College of Surgeons. **197**(4): p. 634-659.
195. Poon, R.T. and S.T. Fan, *Hepatectomy for hepatocellular carcinoma: patient selection and postoperative outcome*. Liver Transpl, 2004. **10**(2 Suppl 1): p. S39-45.
196. Hackl, C., et al., *Liver surgery in cirrhosis and portal hypertension*. World J Gastroenterol, 2016. **22**(9): p. 2725-35.
197. DeAngelis, R.A., et al., *Normal liver regeneration in p50/nuclear factor kappaB1 knockout mice*. Hepatology, 2001. **33**(4): p. 915-24.
198. Cholankeril, G., et al., *Hepatocellular carcinoma in non-alcoholic steatohepatitis: Current knowledge and implications for management*. World J Hepatol, 2017. **9**(11): p. 533-543.
199. Poon, R.T., *Optimal initial treatment for early hepatocellular carcinoma in patients with preserved liver function: transplantation or resection?* Ann Surg Oncol, 2007. **14**(2): p. 541-7.
200. El-Serag, H.B. and K.L. Rudolph, *Hepatocellular carcinoma: epidemiology and molecular carcinogenesis*. Gastroenterology, 2007. **132**(7): p. 2557-76.
201. Elcioglu, Z.C. and H.L. Reeves, *NAFLD-which patients should have hepatocellular carcinoma surveillance?* Hepatobiliary Surg Nutr, 2017. **6**(5): p. 353-355.
202. Chassaing, B., L. Etienne-Mesmin, and A.T. Gewirtz, *Microbiota-liver axis in hepatic disease*. Hepatology, 2014. **59**(1): p. 328-39.

203. Hooper, L.V., T. Midtvedt, and J.I. Gordon, *How host-microbial interactions shape the nutrient environment of the mammalian intestine*. *Annu Rev Nutr*, 2002. **22**: p. 283-307.
204. Ley, R.E., et al., *Obesity alters gut microbial ecology*. *Proc Natl Acad Sci U S A*, 2005. **102**(31): p. 11070-5.
205. Ferreira, C.M., et al., *The central role of the gut microbiota in chronic inflammatory diseases*. *J Immunol Res*, 2014. **2014**: p. 689492.
206. Musso, G., R. Gambino, and M. Cassader, *Gut microbiota as a regulator of energy homeostasis and ectopic fat deposition: mechanisms and implications for metabolic disorders*. *Curr Opin Lipidol*, 2010. **21**(1): p. 76-83.
207. Kessler, J.I., et al., *Alterations of hepatic triglyceride in patients before and after jejunoileal bypass for morbid obesity*. *Gastroenterology*, 1979. **76**(1): p. 159-65.
208. Beymer, C., et al., *Prevalence and predictors of asymptomatic liver disease in patients undergoing gastric bypass surgery*. *Arch Surg*, 2003. **138**(11): p. 1240-4.
209. Bures, J., et al., *Small intestinal bacterial overgrowth syndrome*. *World J Gastroenterol*, 2010. **16**(24): p. 2978-90.
210. Nazim, M., G. Stamp, and H.J. Hodgson, *Non-alcoholic steatohepatitis associated with small intestinal diverticulosis and bacterial overgrowth*. *Hepatogastroenterology*, 1989. **36**(5): p. 349-51.
211. Rabot, S., et al., *Germ-free C57BL/6J mice are resistant to high-fat-diet-induced insulin resistance and have altered cholesterol metabolism*. *FASEB J*, 2010. **24**(12): p. 4948-59.

212. Le Roy, T., et al., *Intestinal microbiota determines development of non-alcoholic fatty liver disease in mice*. Gut, 2013. **62**(12): p. 1787-94.
213. Solga, S.F. and A.M. Diehl, *Non-alcoholic fatty liver disease: lumen-liver interactions and possible role for probiotics*. J Hepatol, 2003. **38**(5): p. 681-7.
214. Cassiman, D. and T. Roskams, *Beauty is in the eye of the beholder: emerging concepts and pitfalls in hepatic stellate cell research*. Journal of Hepatology, 2002. **37**(4): p. 527-535.
215. Wang, P.-p., et al., *HGF and Direct Mesenchymal Stem Cells Contact Synergize to Inhibit Hepatic Stellate Cells Activation through TLR4/NF- $\kappa$ B Pathway*. PLOS ONE, 2012. **7**(8): p. e43408.
216. Modi, S.R., J.J. Collins, and D.A. Relman, *Antibiotics and the gut microbiota*. J Clin Invest, 2014. **124**(10): p. 4212-8.
217. Nash, M.J., D.N. Frank, and J.E. Friedman, *Early Microbes Modify Immune System Development and Metabolic Homeostasis-The "Restaurant" Hypothesis Revisited*. Front Endocrinol (Lausanne), 2017. **8**: p. 349.
218. Xiao, E., et al., *Microbiota regulates bone marrow mesenchymal stem cell lineage differentiation and immunomodulation*. Stem Cell Res Ther, 2017. **8**(1): p. 213.
219. Onishi, J.C., et al., *Bacterial communities in the small intestine respond differently to those in the caecum and colon in mice fed low- and high-fat diets*. Microbiology, 2017. **163**(8): p. 1189-1197.
220. Uchida, D., et al., *Beneficial and Paradoxical Roles of Anti-Oxidative Nutritional Support for Non-Alcoholic Fatty Liver Disease*. Nutrients, 2018. **10**(8).

221. Radilla-Vazquez, R.B., et al., *Gut Microbiota and Metabolic Endotoxemia in Young Obese Mexican Subjects*. *Obes Facts*, 2016. **9**(1): p. 1-11.
222. Hawkesworth, S., et al., *Evidence for metabolic endotoxemia in obese and diabetic Gambian women*. *Nutrition & Diabetes*, 2013. **3**: p. e83.
223. Mogensen, T.H., *Pathogen recognition and inflammatory signaling in innate immune defenses*. *Clin Microbiol Rev*, 2009. **22**(2): p. 240-73, Table of Contents.
224. Patten, D.A. and A. Collett, *Exploring the immunomodulatory potential of microbial-associated molecular patterns derived from the enteric bacterial microbiota*. *Microbiology*, 2013. **159**(Pt 8): p. 1535-44.
225. *Pathogen-associated molecular pattern*. *Immunology for Pharmacy*, 2012.
226. Matsunaga, N., et al., *TAK-242 (resatorvid), a small-molecule inhibitor of Toll-like receptor (TLR) 4 signaling, binds selectively to TLR4 and interferes with interactions between TLR4 and its adaptor molecules*. *Mol Pharmacol*, 2011. **79**(1): p. 34-41.
227. Takashima, K., et al., *Analysis of binding site for the novel small-molecule TLR4 signal transduction inhibitor TAK-242 and its therapeutic effect on mouse sepsis model*. *Br J Pharmacol*, 2009. **157**(7): p. 1250-62.
228. Sha, T., et al., *Therapeutic effects of TAK-242, a novel selective Toll-like receptor 4 signal transduction inhibitor, in mouse endotoxin shock model*. *Eur J Pharmacol*, 2007. **571**(2-3): p. 231-9.
229. Rice, T.W., et al., *A randomized, double-blind, placebo-controlled trial of TAK-242 for the treatment of severe sepsis*. *Crit Care Med*, 2010. **38**(8): p. 1685-94.

230. Liu, S., et al., *Role of toll-like receptors in changes in gene expression and NF-kappa B activation in mouse hepatocytes stimulated with lipopolysaccharide*. Infect Immun, 2002. **70**(7): p. 3433-42.
231. Su, G.L., et al., *Kupffer cell activation by lipopolysaccharide in rats: role for lipopolysaccharide binding protein and toll-like receptor 4*. Hepatology, 2000. **31**(4): p. 932-6.
232. Singh, I., A.K. Singh, and M.A. Contreras, *Peroxisomal dysfunction in inflammatory childhood white matter disorders: an unexpected contributor to neuropathology*. J Child Neurol, 2009. **24**(9): p. 1147-57.
233. Singh, I., *Biochemistry of peroxisomes in health and disease*. Mol Cell Biochem, 1997. **167**(1-2): p. 1-29.
234. Wanders, R.J. and H.R. Waterham, *Biochemistry of mammalian peroxisomes revisited*. Annu Rev Biochem, 2006. **75**: p. 295-332.
235. Terlecky, S.R., L.J. Terlecky, and C.R. Giordano, *Peroxisomes, oxidative stress, and inflammation*. World J Biol Chem, 2012. **3**(5): p. 93-7.
236. Fransen, M., C. Lismont, and P. Walton, *The Peroxisome-Mitochondria Connection: How and Why?* Int J Mol Sci, 2017. **18**(6).
237. Smyth, E.M. and G.A. FitzGerald, *The Eicosanoids: Prostaglandins, Thromboxanes, Leukotrienes, & Related Compounds*, in *Basic & Clinical Pharmacology, 13e*, B.G. Katzung and A.J. Trevor, Editors. 2015, McGraw-Hill Medical: New York, NY.
238. Rogero, M.M. and P.C. Calder, *Obesity, Inflammation, Toll-Like Receptor 4 and Fatty Acids*. Nutrients, 2018. **10**(4).

239. Ariel, A. and C.N. Serhan, *Resolvins and protectins in the termination program of acute inflammation*. Trends Immunol, 2007. **28**(4): p. 176-83.
240. Serhan, C.N., et al., *Maresins: novel macrophage mediators with potent antiinflammatory and proresolving actions*. J Exp Med, 2009. **206**(1): p. 15-23.
241. Narasimha Das, U., *Lipoxins, resolvins, protectins, maresins and nitrolipids, and their clinical implications with specific reference to diabetes mellitus and other diseases: part II*. Clinical Lipidology, 2013. **8**(4): p. 465-480.
242. Schrader, M. and H.D. Fahimi, *Peroxisomes and oxidative stress*. Biochimica et Biophysica Acta (BBA) - Molecular Cell Research, 2006. **1763**(12): p. 1755-1766.
243. Boveris, A., N. Oshino, and B. Chance, *The cellular production of hydrogen peroxide*. Biochem J, 1972. **128**(3): p. 617-30.
244. Rui, L., *Energy metabolism in the liver*. Compr Physiol, 2014. **4**(1): p. 177-97.
245. Lodish, H.F. and National Center for Biotechnology Information (U.S.), *Molecular cell biology*. 2000, W.H. Freeman: New York. p. xxxix, 1084 p.
246. Kakimoto, P.A., et al., *H<sub>2</sub>O<sub>2</sub> release from the very long chain acyl-CoA dehydrogenase*. Redox Biol, 2015. **4**: p. 375-80.
247. Kersten, S., et al., *Peroxisome proliferator-activated receptor alpha mediates the adaptive response to fasting*. J Clin Invest, 1999. **103**(11): p. 1489-98.
248. Cook, W.S., et al., *Peroxisome proliferator-activated receptor alpha-responsive genes induced in the newborn but not prenatal liver of peroxisomal fatty acyl-CoA oxidase null mice*. Exp Cell Res, 2001. **268**(1): p. 70-6.

249. Contreras, M.A., et al., *Endotoxin induces structure-function alterations of rat liver peroxisomes: Kupffer cells released factors as possible modulators*. Hepatology, 2000. **31**(2): p. 446-55.
250. Khan, M., M. Contreras, and I. Singh, *Endotoxin-induced alterations of lipid and fatty acid compositions in rat liver peroxisomes*. J Endotoxin Res, 2000. **6**(1): p. 41-50.
251. Soares, J.B., et al., *The role of lipopolysaccharide/toll-like receptor 4 signaling in chronic liver diseases*. Hepatol Int, 2010. **4**(4): p. 659-72.
252. Yang, S.Q., et al., *Obesity increases sensitivity to endotoxin liver injury: implications for the pathogenesis of steatohepatitis*. Proc Natl Acad Sci U S A, 1997. **94**(6): p. 2557-62.
253. Imanaka, T., et al., *Characterization of the 70-kDa peroxisomal membrane protein, an ATP binding cassette transporter*. J Biol Chem, 1999. **274**(17): p. 11968-76.
254. Starkov, A.A., *The role of mitochondria in reactive oxygen species metabolism and signaling*. Ann N Y Acad Sci, 2008. **1147**: p. 37-52.
255. Sandalio, L.M., et al., *Role of peroxisomes as a source of reactive oxygen species (ROS) signaling molecules*. Subcell Biochem, 2013. **69**: p. 231-55.
256. Ray, P.D., B.W. Huang, and Y. Tsuji, *Reactive oxygen species (ROS) homeostasis and redox regulation in cellular signaling*. Cell Signal, 2012. **24**(5): p. 981-90.
257. Reuter, S., et al., *Oxidative stress, inflammation, and cancer: how are they linked?* Free Radic Biol Med, 2010. **49**(11): p. 1603-16.
258. Hussain, T., et al., *Oxidative Stress and Inflammation: What Polyphenols Can Do for Us?* Oxid Med Cell Longev, 2016. **2016**: p. 7432797.

259. Fransen, M., et al., *Role of peroxisomes in ROS/RNS-metabolism: Implications for human disease*. Biochimica et Biophysica Acta (BBA) - Molecular Basis of Disease, 2012. **1822**(9): p. 1363-1373.
260. Braverman, N.E. and A.B. Moser, *Functions of plasmalogen lipids in health and disease*. Biochimica et Biophysica Acta (BBA) - Molecular Basis of Disease, 2012. **1822**(9): p. 1442-1452.
261. Cardoso, A.R., P.A. Kakimoto, and A.J. Kowaltowski, *Diet-sensitive sources of reactive oxygen species in liver mitochondria: role of very long chain acyl-CoA dehydrogenases*. PLoS One, 2013. **8**(10): p. e77088.
262. Caligiuri, A., A. Gentilini, and F. Marra, *Molecular Pathogenesis of NASH*. Int J Mol Sci, 2016. **17**(9).
263. Gentile, C.L., M.A. Frye, and M.J. Pagliassotti, *Fatty acids and the endoplasmic reticulum in nonalcoholic fatty liver disease*. Biofactors, 2011. **37**(1): p. 8-16.
264. Simões, I.C.M., et al., *Mitochondria in non-alcoholic fatty liver disease*. The International Journal of Biochemistry & Cell Biology, 2018. **95**: p. 93-99.
265. Harlan-Teklad, *Custom Research Diets* (<http://www.onlyscience.com.tw/downloads/reagent/Harlan%20Reserch%20Diet.pdf>).
266. ENVIGO, <https://www.envigo.com/products-services/teklad/laboratory-animal-diets/custom-research/diet-induced-obesity/>.
267. dela Peña, A., et al., *NF- $\kappa$ B Activation, Rather Than TNF, Mediates Hepatic Inflammation in a Murine Dietary Model of Steatohepatitis*. Gastroenterology, 2005. **129**(5): p. 1663-1674.

268. Sanyal, A.J., *AGA technical review on nonalcoholic fatty liver disease*. Gastroenterology, 2002. **123**(5): p. 1705-1725.
269. Joseph, A.E., et al., *Comparison of liver histology with ultrasonography in assessing diffuse parenchymal liver disease*. Clin Radiol, 1991. **43**(1): p. 26-31.
270. Hultcrantz, R. and N. Gabrielsson, *Patients with persistent elevation of aminotransferases: investigation with ultrasonography, radionuclide imaging and liver biopsy*. J Intern Med, 1993. **233**(1): p. 7-12.
271. Saadeh, S., et al., *The utility of radiological imaging in nonalcoholic fatty liver disease*. Gastroenterology, 2002. **123**(3): p. 745-50.
272. Bayard, M., J. Holt, and E. Boroughs, *Nonalcoholic fatty liver disease*. Am Fam Physician, 2006. **73**(11): p. 1961-8.
273. Ludwig, J., et al., *Nonalcoholic steatohepatitis. Mayo Clinic experiences with a hitherto unnamed disease*. Mayo Clinic Proceedings, 1980. **55**(7): p. 434-438.
274. Sanyal, A.J. and A. American Gastroenterological, *AGA technical review on nonalcoholic fatty liver disease*. Gastroenterology, 2002. **123**(5): p. 1705-25.
275. Zhu, L., et al., *Characterization of gut microbiomes in nonalcoholic steatohepatitis (NASH) patients: a connection between endogenous alcohol and NASH*. Hepatology, 2013. **57**(2): p. 601-9.
276. Baker, S.S., et al., *Role of alcohol metabolism in non-alcoholic steatohepatitis*. PLoS One, 2010. **5**(3): p. e9570.
277. Wang, Y., et al., *Modulation of Gut Microbiota in Pathological States*. Engineering, 2017. **3**(1): p. 83-89.

278. Joyce, S.A., et al., *Regulation of host weight gain and lipid metabolism by bacterial bile acid modification in the gut*. Proc Natl Acad Sci U S A, 2014. **111**(20): p. 7421-6.
279. Hakansson, A. and G. Molin, *Gut microbiota and inflammation*. Nutrients, 2011. **3**(6): p. 637-82.
280. Fei, N. and L. Zhao, *An opportunistic pathogen isolated from the gut of an obese human causes obesity in germfree mice*. The Isme Journal, 2012. **7**: p. 880.
281. Gibiino, G., et al., *Exploring Bacteroidetes: Metabolic key points and immunological tricks of our gut commensals*. Digestive and Liver Disease, 2018. **50**(7): p. 635-639.
282. Shin, N.R., T.W. Whon, and J.W. Bae, *Proteobacteria: microbial signature of dysbiosis in gut microbiota*. Trends Biotechnol, 2015. **33**(9): p. 496-503.
283. Ruiz, A.G., et al., *Lipopolysaccharide-binding protein plasma levels and liver TNF- $\alpha$  gene expression in obese patients: evidence for the potential role of endotoxin in the pathogenesis of non-alcoholic steatohepatitis*. Obes Surg, 2007. **17**(10): p. 1374-80.
284. Luther, J., et al., *Hepatic Injury in Nonalcoholic Steatohepatitis Contributes to Altered Intestinal Permeability*. Cell Mol Gastroenterol Hepatol, 2015. **1**(2): p. 222-232.
285. Pendyala, S., et al., *Diet-induced weight loss reduces colorectal inflammation: implications for colorectal carcinogenesis*. Am J Clin Nutr, 2011. **93**(2): p. 234-42.

286. Rao, R.K., A. Seth, and P. Sheth, *Recent Advances in Alcoholic Liver Disease I. Role of intestinal permeability and endotoxemia in alcoholic liver disease*. Am J Physiol Gastrointest Liver Physiol, 2004. **286**(6): p. G881-4.
287. Lieber, C.S., *Microsomal ethanol-oxidizing system (MEOS): the first 30 years (1968-1998)--a review*. Alcohol Clin Exp Res, 1999. **23**(6): p. 991-1007.
288. Guo, J. and S.L. Friedman, *Toll-like receptor 4 signaling in liver injury and hepatic fibrogenesis*. Fibrogenesis Tissue Repair, 2010. **3**: p. 21.
289. Munford, R.S., *Sensing gram-negative bacterial lipopolysaccharides: a human disease determinant?* Infect Immun, 2008. **76**(2): p. 454-65.
290. Miller, S.I., R.K. Ernst, and M.W. Bader, *LPS, TLR4 and infectious disease diversity*. Nat Rev Microbiol, 2005. **3**(1): p. 36-46.
291. Munford, R.S. and A.W. Varley, *Shield as signal: lipopolysaccharides and the evolution of immunity to gram-negative bacteria*. PLoS Pathog, 2006. **2**(6): p. e67.
292. Matsunaga, N., et al., *TAK-242 (Resatorvid), a Small-Molecule Inhibitor of Toll-Like Receptor (TLR) 4 Signaling, Binds Selectively to TLR4 and Interferes with Interactions between TLR4 and Its Adaptor Molecules*. Molecular Pharmacology, 2011. **79**(1): p. 34-41.
293. li, M., et al., *A novel cyclohexene derivative, ethyl (6R)-6-[N-(2-Chloro-4-fluorophenyl)sulfamoyl]cyclohex-1-ene-1-carboxylate (TAK-242), selectively inhibits toll-like receptor 4-mediated cytokine production through suppression of intracellular signaling*. Mol Pharmacol, 2006. **69**(4): p. 1288-95.
294. Kawamoto, T., et al., *TAK-242 selectively suppresses Toll-like receptor 4-signaling mediated by the intracellular domain*. Eur J Pharmacol, 2008. **584**(1): p. 40-8.

295. Tsoulfas, G., et al., *Activation of the lipopolysaccharide signaling pathway in hepatic transplantation preservation injury*. *Transplantation*, 2002. **74**(1): p. 7-13.
296. Ellett, J.D., et al., *Toll-like receptor 4 is a key mediator of murine steatotic liver warm ischemia/reperfusion injury*. *Liver Transpl*, 2009. **15**(9): p. 1101-9.
297. Fiorini, R.N., et al., *Anti-Endotoxin Monoclonal Antibodies are Protective against Hepatic Ischemia/Reperfusion Injury in Steatotic Mice*. *American Journal of Transplantation*, 2004. **4**(10): p. 1567-1573.
298. Fiorini, R.N., et al., *Anti-endotoxin monoclonal antibodies are protective against hepatic ischemia/reperfusion injury in steatotic mice*. *Am J Transplant*, 2004. **4**(10): p. 1567-73.
299. Alberts, B. and National Center for Biotechnology Information (U.S.), *Molecular biology of the cell*. 2002, Garland Science: New York. p. xxxiv, 1463, 86 p.
300. Poirier, Y., et al., *Peroxisomal  $\beta$ -oxidation—A metabolic pathway with multiple functions*. *Biochimica et Biophysica Acta (BBA) - Molecular Cell Research*, 2006. **1763**(12): p. 1413-1426.
301. Hall, D., et al., *Peroxisomal and microsomal lipid pathways associated with resistance to hepatic steatosis and reduced pro-inflammatory state*. *J Biol Chem*, 2010. **285**(40): p. 31011-23.
302. Peeters, A., et al., *Hepatosteatosis in peroxisome deficient liver despite increased  $\beta$ -oxidation capacity and impaired lipogenesis*. *Biochimie*, 2011. **93**(10): p. 1828-1838.

303. Park, H.S., et al., *Statins Increase Mitochondrial and Peroxisomal Fatty Acid Oxidation in the Liver and Prevent Non-Alcoholic Steatohepatitis in Mice*. *Diabetes Metab J*, 2016. **40**(5): p. 376-385.
304. Necela, B.M., W. Su, and E.A. Thompson, *Toll-like receptor 4 mediates cross-talk between peroxisome proliferator-activated receptor gamma and nuclear factor-kappaB in macrophages*. *Immunology*, 2008. **125**(3): p. 344-58.
305. Grygiel-Górniak, B., *Peroxisome proliferator-activated receptors and their ligands: nutritional and clinical implications - a review*. *Nutrition Journal*, 2014. **13**(1): p. 17.